Non-canonical β-Catenin interactions promote leukemia-initiating activity in early T-cell acute lymphoblastic leukemia

Patrizio Panelli[1], Elisabetta De Santis[1], Mattia Colucci[1], Francesco Tamiro[1], Francesca Sansico[1], Mattia Miroballo[1], Emanuele Murgo[1], Costanzo Padovano[1], Sam Gusscott[3], Michele Ciavarella[1], Elizabeth A Chavez[4], Fabrizio Bianchi[1], Giovanni Rossi[2], Angelo M. Carella[2], Christian Steidl[4], Andrew P. Weng[3], Vincenzo Giambra[1*]

[1]Institute for Stem Cell Biology, Regenerative Medicine and Innovative Therapies (ISBReMIT), Fondazione IRCCS Casa Sollievo della Sofferenza; 71013, San Giovanni Rotondo (FG), Italy.

[2]Department of Hematology and Stem Cell Transplant Unit, IRCCS Casa Sollievo della Sofferenza; 71013, San Giovanni Rotondo (FG), Italy.

[3]Terry Fox Laboratory, BC Cancer Agency; Vancouver, BC, V5Z 1L3, Canada.

[4]Centre for Lymphoid Cancer, BC Cancer Agency; Vancouver, BC, V5Z 1L3, Canada.

Supplemental Information including:

Materials and Methods

Mice

All NOTCH1 leukemia transplant donors were C57BL/6 background. All transplant recipients were C57BL/6, B6.SJL-Ptprc^{a}Pepc^{b}/BoyJ (Ly5.1) or NOD/Scid/*Il2rg*$^{-/-}$ (NSG) mice. The animals were housed in specific pathogen-free facilities at the BC Cancer Center (BCCA, Vancouver, Canada) and Plaisant s.r.l. (Rome, Italy). The animal experiments were performed after the protocols had been approved by the Institutional Review Boards of the BCCA/UBC (University of British Columbia) and the Casa Sollievo della Sofferenza Research Hospital (CSS; San Giovanni Rotondo, Italy), according to the Canadian Council on Animal Care (CCAC) guidelines and the Italian Regulation for Animal Health and Animal Welfare. Syngeneic (C57BL/6; RRID:IMSR- JAX:000664) transplant recipient mice were 8-13 weeks of age. Immunodeficient (NOD.Cg-Prkdcscid Il2rgtm1Wjl/SzJ, or NSG; RRID: IMSR_JAX:005557) xenograft recipient mice were 7-17 weeks of age. Male and female animals were represented in balanced proportion when in-house colony stock availability necessitated using mixed sex recipients.

Human samples

Primary human T-ALL samples were obtained under appropriate institutional approvals (CSS and UBC/BCCA Research Ethics Boards), and the informed consent was obtained in compliance with the guidelines established by the Declaration of Helsinki. Patient-derived xenografts were established by injection of primary patient biopsy material into irradiated NOD-Scid/IL2Rγc$^{-/-}$ (NSG) mice as described previously [1].

Generation of primary mouse leukemias

Bone marrow cells from 5-fluorouracil treated mice were transduced with NOTCH1-ΔE/NGFR retrovirus by spinoculation as described [2]. Three days later, 10,000-40,000 NGFR+ cells (including at least 1 x 10^5 normal bone marrow cells) were injected by tail vein into lethally irradiated (810 rad) syngeneic C57BL/6 recipient mice. Animals typically develop clinically morbid disease within 8-12 weeks following transplantation.

Plasmids

The TOPflash and lentiviral 7TGC reporter constructs have previously been described [3,4]. The FOPflash luciferase reporter with mutant TCF/LEF binding sites was derived from Merck Millipore (cod. # 21-169). The pGL-3xDBE and pGL-3xDBE mut luciferase FOXO reporters [5] were kindly provided by Dr. Wolfgang Link (CSIC-UAM, Madrid, Spain) and cloned into lentiviral vectors with 3xDBE-tNGFR or 3xDBE-hCD8 and SV40-mCherry or SV40-mTagBFP2 cassettes for tagging human or mouse transduced cells, respectively. A cDNA encoding the human FOXO3 T32A/S253A/S315A triple mutant (FOXO3_TM)[6], derived from the Addgene construct cod. #1788, was subcloned with a HA epitope tag into a pRRL-based lentivector with mouse CD8 (mCD8) marker (PGK/mCD8). A cDNA encoding the human *β*-Catenin S33A/S37A/T41A/S45A mutant (*β*-Catenin_ΔGSK)[3], derived from the Addgene construct cod. #24313, was subcloned into a lentivector with Cherry fluorescent marker (PGK/mCherry). The lentivector encoding the human CDK4 R24L mutant (CDK4_R24L)[7] with GFP fluorescent marker was derived from Addgene (cod. #116217). The RNAi Consortium (TRC) shRNAs targeting CTNNB1 (shCTNNB1_21, TRCN0000314921; shCTNNB1_91, TRCN0000314991), FOXO3 (shFOXO3_98, TRCN0000040098; shFOXO3_102, TRCN0000040102) or CDK4 (shCDK4_363, TRCN0000000363; shCDK4_520, TRCN0000010520) were cloned into a derivative of pLKO.1 vector (Addgene #8453) with the GFP or tNGFR selection marker. All constructs were verified by sequencing.

Genome editing

CRISPR/Cas9-mediated genome editing was performed by direct electroporation of recombinant Cas9-sgRNA ribonucleoprotein (RNP) complexes. Chemically synthesized AltR-crRNA 0.11ul and tracrRNA 0.11ul from 200uM stock solution were mixed with 0.6ul nuclease-free IDT water for 5 min at room temperature and subsequently with Alt-R S.p Cas9 Nuclease 3NLS (Integrated DNA Technologies, Inc) 0.66ul from stock solution for 20 min at room temperature, according to the manufacturer's specifications. RNP electroporation was performed in 5×10^5 cells using 4 μM (1:1.2:1.2, Cas9:crRNA:tracrRNA) Alt-R S.p Cas9 RNP complex and 4 μM Alt-R S.p Cas9 Electroporation Enhancer (Integrated DNA Technologies, Inc), (Neon Transfection System, ThermoFisher) as previously described [8]. In order to insert the hPGK/GFP and hPGK/NGFR DNA fragments into the exon 1 of FOXO3 human gene (chr6:108561762-

108561829) and exon 3 of CTNNB1 human gene (chr3:41224526-41224753) respectively, vectors including the marker gene under the constitutive hPGK-1 promoter were generated with the following flanked homologous arms: 5' FOXO3 arm (chr6:108561210-108561730); 3' FOXO3 arm (chr6:108561754-108562300); 5' CTNNB1 arm (chr3:41224070-41224582) and 3' CTNNB1 arm (chr3: 41224614-41225175). For the CRISPR/Cas9-mediated insertion, RNP electroporation was performed using the Alt-R S.p.Cas9 D10A nickase V3 (Cat #1081062, Integrated DNA Technologies) and 1 μg of vector at the same condition as above. Treated cells were then cultured in RPMI 1640 medium supplemented with 20% fetal bovine serum (FBS), 1 mM sodium pyruvate, 2 mM L-glutamine (Invitrogen) without antibiotics for two days and then transferred at limiting dilution into a 96-well plate. Each expanded clone was validated by DNA sequencing of targeted regions and Western blot for protein expression. The sequences of Cas9 crRNAs were: crCTNNB1exo2 5′-GCGTGGACAATGGCTACTCAGTTTTAGAGCTATGCT-3′ and crCTNNB1-ex 5'-AAGGTTATGCAAGGTCCCAGGTTTTAGAGCTATGCT-3' for targeting *β*-Catenin and Foxo3-exo2 5'-CCACGGCTGACTGATATGGCG-3' for targeting FOXO3. For the CRISPR/Cas9-mediated insertion, the sequences of Cas9 crRNAs were: CTNNB1-crRNA sense 5'-GCTCCTTCTCTGAGTGGTAAAGG-3; CTNNB1-crRNA antisense 5'-CTAACAGCCGCTTTTCTGTCTGG-3'; FOXO3-crRNA sense 5'-CTCTGTCCCAGATCTACGAGTGG-3; FOXO3A-crRNA antisense 5'-CCGGGGAGCTCTCGATGGCGCGG-3'. The level of CRISPR/Cas9-mediated insertion was assessed using the QX200 ddPCR EvaGreen Supermix (Bio-Rad, #1864033) on QX200 Droplet Digital PCR system (Bio-Rad). Genomic DNA was purified from CRISPR/Cas9-treated cells after 3 days of *in vitro* growth. The grade of CRISPR/Cas9-mediated insertion was reported as fraction of PCR-amplified region in the targeted exon over an internal untreated region located in the GAPDH locus (chr12:6534373-6534538). The primer sequences used for amplification were CTNNB1-Fwd 5'TTTGATGGAGTTGGACATGG-3'; CTNNB1-Rev 5'-CAGGACTTGGGAGGTATCCA-3'; FOXO3-Fwd 5'-CTGAGCGGGGGTACACAG-3'; FOXO3-Rev 5'-CTGTCGCCCTTATCCTTGAA-3'; GAPDH-Fwd 5'-TACTAGCGGTTTTACGGGCG-3' and GAPDH-Rev 5'-TCGAACAGGAGGAGCAGAGAGCGA-3'.

Liquid-chromatography mass spectrometry (LC/MS^2)

Protein separation and fractionation were performed by SDS-PAGE as previously reported [9]. Peptides were extracted adding and sequentially collecting the following solutions: 0.5% (v/v) formic acid, 30% (v/v) acetonitrile, 0.1% (v/v) formic acid, 80% (v/v) acetonitrile and 100% (v/v) acetonitrile. The dry vacuum centrifugation step was used to remove the solvent portion and the peptides resuspended in 0.5% (v/v) formic acid. The resulting peptides were purified by STAGE (STop And Go Extraction) TIPS Desalting Procedure using high-capacity C18 resin (ThermoFisher). Each fraction was analyzed in tandem by LC-MS/MS on a Thermo Fisher Scientific Q-Exactive coupled to an nUPLC Easy nLC 1000 of the Proxeon Biosystems. The samples were resolved on 60 min. gradient column 15 cm, ID = 75 µm; OD = 360 µm, packed with resin 1.9 µm Reprosil-Pur C18-AQ 120 Angstrom, of Dr. Maisch. Solvent used: A= 0.1% formic acid in water; B= 0.1% formic acid in ACN; flux= 300 nl/min. After 5 min. of 2% B, the phase B rose up to 40% in 83 minutes followed by a washing step of 90% of B solvent. Lock mass option was utilized. The resolution is 70000 per MS with a mass range of m/z 300 a 2000. The method is a top 10, for Ion containing 2 and 3 charges. Centroided fragment peak lists were processed to Mascot generic format using Proteome Discoverer (PD, 2.2) largely configurated with default parameters. Fragment spectra were searched using the Mascot server against the databases *Homo sapiens* (SwissProt TaxID=9606). Protein N-terminal acetylation, methionine oxidation and asparagine and glutamine deamination were included as variable modifications with trypsin as the protease (K/R cleavage specificity), allowing a maximum of two missed cleavages and carbamidomethyl cysteine as a fixed modification. We allowed for a 1% false discovery rate at both the peptide and protein level and also removed all proteins identified by fewer than two peptides. The results were further filtered by removing the duplicated entries from amino acid sequences with identical accession numbers, as reported in the databases used for the search. The Kyoto Encyclopedia of Genes and Genome (KEGG) pathway analysis [10] was conducted to identify LC/MS2 proteins identified at the biologically functional level. The Database for Annotation, Visualization, and Integrated Discovery (DAVID; david.abcc.ncifcrf.gov) [11] was used for functional interpretation of protein annotations. Biological process with $P<0.05$ was considered to indicate a statistically significant.

Western blot

Whole cell lysates were generated after washing in ice-cold phosphate-buffered saline and then lysis in ice-cold 50 mM Tris-HCl (pH 7.4), 1% Nonidet P-40, 0.25% sodium deoxycholate, 150 mM sodium chloride, 1 mM sodium orthovanadate, 1 mM sodium fluoride, 2.5 mM sodium pyrophosphate, 1 mM EDTA, 1 mM phenylmethylsulphonyl fluoride, and protease inhibitor cocktail (cat #539134, Calbiochem). Nuclear and cytoplasmic fractions of soluble proteins were obtained using the NE-PER Nuclear and Cytoplasmic Extraction Kit (Cat. 78833, ThermoFisher Scientific) and following the manufacturer's instructions. Cell lysates or immunoprecipitated complexes were incubated at 95°C for 10 minutes, loaded on SDS-PAGE gels and then transferred to Hybond-ECL membranes (Amersham). The membranes were blocked with 5% milk/0.3% TBS-Tween20 at 4°C for 1 hour and then probed with primary antibodies against β-Catenin (1:1,000 dilution; Cat. #9582, Cell Signaling Technology), Non-phospho (Active) β-Catenin (1:1,000 dilution; Cat. #8814, Cell Signaling Technology), FOXO3 (1:1,000 dilution; Cat. #12829, Cell Signaling Technology), Lamin B1 (1:1,000 dilution; Cat. #15068, Cell Signaling Technology), HA-Tag (1:1,000 dilution; Cat. #3724, Cell Signaling Technology), Myc-Tag (1:1,000 dilution; Cat. #2278, Cell Signaling Technology), or β-Actin (1:6,000 dilution; Cat. #A1978, Sigma). HRP-conjugated secondary antibodies (Cat. NEF812001EA, Perkin Elmer) were used at 1:10 000 dilution. The chemiluminescent signal was detected with enhanced chemiluminescence (ECL) (cat. 32106, Pierce) and subsequently with autoradiography. Band intensity was quantified using the ImageJ software[12].

Expression Profiling by RNA-Sequencing (RNA-Seq)

Total RNA was isolated from cell lines using the RNeasy Kit (Qiagen) and following the manufacturer's instructions. Library preparation and sequencing of ribodepleted total RNA was performed in service at the Applied Biological Materials Inc. (abm) (Vancouver), reaching about 25 million reads for sample. The quality of the RNA was assessed by Quibit RNA assay and Agilent Bioanalyzer. The RNA-seq data were aligned to human genome reference assembly GRCh37/hg19 using STAR 2.7.5a for gene expression counts. Differential gene expression analyses, gene set variation analysis (GSVA)[13] and Gene Set Enrichment Analysis (GSEA) [14,15] were performed using normalized mRNA counts with DESeq2 v1.26.0 in RStudio (R Version 1.2.5033).

RT-PCR

Total RNA from lysed cells was extracted using the RNeasy Kit (Qiagen). We generated first strand cDNA by reverse transcription with SuperScript III/VILO master mix (Invitrogen) including a combination of random 15-mer and anchored oligo(dT) primers. We then amplified the product by Taqman probe-based droplet digital PCR (ddPCR) with a QX200 instrument (Bio-Rad). Absolute quantification analysis was performed using a Poisson algorithm with QuantaSoft software (Bio-Rad) and included normalization to B2M control. We used the following TaqMan probe-based assays: CDK4 (qHsaCEP0024768; FAM) (Bio-Rad) and B2M (Hs99999907_m1; VIC, primer limited) (Applied Biosystems/ThermoFisher).

ChIP-Sequencing

We performed chromatin immunoprecipitation (ChIP) as described previously[1] with validated antibodies against H3K27me3 (Cat. C15410069-50, Diagenode) and H3K27Ac (Cat. Ab4729, Abcam). ChIP-Seq libraries were prepared according to Accel-NGS 2S Plus DNA Library preparation kit (Cat. 21024, Swift Biosciences). ChIP DNA was quantified using a Qubit dsDNA HS Assay Kit (Cat. Q32851, ThermoFisher Scientific) and the quality was assessed by the 4200 TapeStation System using High Sensitivity D1000 Reagents (Cat. 5067-5585, Agilent Technologies). DNA sequencing was performed on NextSeq550 Illumina System using a Mid Output Kit v2.5 - 150 cycles flow cell (Cat. 20024904, Illumina) for reaching about 10 million reads/sample. Chromatin immunoprecipitation (ChIP) with validated antibodies against β-Catenin (Cat. 71-2700, ThermoFisher Scientific) and FOXO3 (Cat. NBP2-16521, Novus Biologicals) and ChIP-Seq libraries were performed in service by Active Motif Enabling Epigenetics Research Biotechnology (Carlsbad, USA). The ChIP-Seq data were aligned against human genome hg38 using STAR v2.7.0f with default parameters and filtered for removing reads aligning to ENCODE blacklist regions using sub-commands from the BedTools suit, the bedtools intersect. Peaks were called with Model-based Analysis for ChIP-seq (MACS2)[16] version 2.1.2 using default parameters after normalization with input as control. The peaks with p-value <0.05 were retained. The ChIP-seq data were visualized using the Integrative Genomics Viewer (IGV). The peak overlaps between different ChIP-seq datasets were determined with the BedTools suit bedtools intersect. Peak annotation and genomic features (transcription starting sites TSS and genes associated with peaks) were found using the R Bioconductor package ChIPseeker [17]. The BAMM tool [18] was used

to find β-Catenin and FOXO3 shared consensus motives, 500bp centered on each peak position. The deeptools software was used to convert BAM alignment files to bigwig (bamCoverage). To visualize the enrichment of genomic signal on specific target region (TSS) was used the R package Enriched Heatmap[19].

ChIP-PCR.

Chromatin immumoprecipitation (ChIP) was performed as described previously [1] using the following antibodies against: FOXO3 (Cat. Ab12162, Abcam), β-Catenin (Cat. 610153, BD Biosciences) and rabbit IgG (Cat. 2729, Cell Signaling Technology). DNA enrichment was assessed using the QX200 ddPCR EvaGreen Supermix (Bio-Rad, #1864033) on QX200 Droplet Digital PCR system (Bio-Rad). The ddPCR data were analyzed with QuantaSoft Software. The primer sequences used for amplification are listed in **Table S1**.

Single cell RNA-sequencing (scRNA-Seq) and Ab-sequencing (AbSeq)

Whole transcriptome analyses at single cell level and profiling of oligoconjugated antibodies were performed on FACS-sorted primary T-ALL cells using the BD Rhapsody Single-Cell Analysis System (BD, Biosciences). Specifically, leukemia cells from cryopreserved bone marrow samples of T-ALL patients were isolated as CD45+CD3-CD99+CD7+ cell fraction by FACS-sorting as previously reported[20]. Isolated cells from each sample were labeled with the BD Single-Cell Multiplexing Kit (cat. 633781, BD Biosciences) and the BD AbSeq Ab-Oligos for 1 hour (**Table S9**), following the manufacturer's protocol. The cell viability and concentration were determined with the BD Rhapsody Scanner system after staining with viability dyes, Calcein AM (1:200 dilution; cat. #C1430, ThermoFisher) and DRAQ7™ (1:200 dilution; cat. #564904, BD Biosciences), and incubation for 5 min at 37°C. Cells were counted using the Improved Neubauer Hemocytometer (INCYTO). Afterward, leukemia cells for each sample at d0 and d30 were pooled equally in 650ml cold BD Sample Buffer and three BD Rhapsody cartridges were loaded with 10,000 pooled cells for single cell separation. Single cells were isolated using Single-Cell Capture and cDNA Synthesis with the BD Rhapsody Express Single-Cell Analysis System according to the manufacturer's recommendations (BD Biosciences). Based on the number of viable cells revealed and captured on the beads, the final resuspension volume was calculated to subsample and sequence about 4,000 cells. Whole transcriptome, Sample Tag, and BD™ AbSeq

amplification was performed with the BD Rhapsody Whole Transcriptome and AbSeq Amplification Kit (cat. #633774), following the manufacturer's instructions. Unwanted PCR products and other small molecules were excluded performing a side cleanup using the AMPure XP Beckman magnetic beads (cat. #A63880, Beckman Coulter). DNA quantity and quality control were performed using the Qubit™ dsDNA HS Assay Kit (cat. # Q32851, ThermoFisher Scientific) and the electrophoresis system Agilent 2200 TapeStation, cartridge (cat. #5067-5584). Sequencing was performed in paired-end mode (2*75 cycles) on NextSeq 500 System (Illumina) with the NextSeq 500/550 High Output Kit v2.5 (150 Cycles) chemistry to reach a depth of 75,000 reads for WTA, 21,500 reads for AbSeq and 500 reads for SMK per cell for a total of 97,000 reads per cell on average. Sequencing data were processed on the Seven Bridges Platform (https://www.sevenbridges.com/) for sample demultiplexing and generation of expression sparse matrixes. Briefly, a quality sequencing step was performed to filter out reads with a Phred quality score below 20, reads with a single type of nucleotide and short reads (less than 60 bases for R1 and less then 42 for R2). AbSeq reference generator was used to create the Ab-seq oligo FASTA file required for the 'AbSeq Reference' input for the BD Rhapsody WTA Analysis Pipeline of SevenBridges (http://abseq-ref-gen.genomics.bd.com). For Abseq data, UMI counting was done including two types of algorithms used for PCR and sequencing reads correction, recursive substation error correction (RSEC) and distribution-based error correction (DBEC). Accepted reads were aligned to the reference genome (GRCh38) for identification and quantification, and consequently the count genes matrix was generated. Highly dimensional Sc-RNA-Seq data were analyzed using the SeqGeq software (Becton Dickinson) for visualization, clustering by Phenograph algorithm[21] and differential expression analysis. The workflow based on the package Seurat (Version 3.2.2(DOI: 10.1016/j.cell.2019.05.031)) was also applied. Only cells with mitochondrial read rate ≤ 30%, detectable genes ≥ 200 and genes expressed in 10 or more cells were considered passing the QC and further analyzed using functions provided with the Seurat library. In the end, we counted 2,064 cells (d0=385; d30=1,679) for CSS15501; 4,258 cells (d0=441; d30=3,817) for CSS13693 and 2,175 cells (d0=1,767; d30=408) for CSS20705. Data were log normalized regressing out both the number of counts and percentage of reads aligning to mitochondrial genes. Clusters were allocated to cell populations based on gene markers using uncentered correlation and centroid linkage. Identification of differential expressed genes was performed using the Wilcox test implemented by Seurat's FindMarker.

Data set availability

The data generated by liquid-chromatography mass spectrometry (LC/MS^2) for the identification of interacting proteins of β-Catenin can be found in **Table S12**. The normalized (rLog) data for mRNA expression can be found in **Table S13** and are also accessible at NCBI SRA PRJNA785416. The scRNA-Seq and ChIP-Seq data are accessible at NCBI SRA PRJNA784728 and PRJNA785422, respectively.

Supplementary References

1. Giambra V, Gusscott S, Gracias D, et al. Epigenetic Restoration of Fetal-like IGF1 Signaling Inhibits Leukemia Stem Cell Activity. *Cell Stem Cell*. 2018.
2. Giambra V, Jenkins CR, Wang H, et al. NOTCH1 promotes T cell leukemia-initiating activity by RUNX-mediated regulation of PKC-theta and reactive oxygen species. *Nat Med*. 2012;18(11):1693-1698.
3. Fuerer C, Nusse R. Lentiviral vectors to probe and manipulate the Wnt signaling pathway. *PLoS One*. 2010;5(2):e9370.
4. Giambra V, Jenkins CE, Lam SH, et al. Leukemia stem cells in T-ALL require active Hif1alpha and Wnt signaling. *Blood*. 2015;125(25):3917-3927.
5. Zanella F, Rosado A, Garcia B, Carnero A, Link W. Using multiplexed regulation of luciferase activity and GFP translocation to screen for FOXO modulators. *BMC Cell Biol*. 2009;10:14.
6. Brunet A, Bonni A, Zigmond MJ, et al. Akt promotes cell survival by phosphorylating and inhibiting a Forkhead transcription factor. *Cell*. 1999;96(6):857-868.
7. Ng PK, Li J, Jeong KJ, et al. Systematic Functional Annotation of Somatic Mutations in Cancer. *Cancer Cell*. 2018;33(3):450-462 e410.
8. Gundry MC, Brunetti L, Lin A, et al. Highly Efficient Genome Editing of Murine and Human Hematopoietic Progenitor Cells by CRISPR/Cas9. *Cell Rep*. 2016;17(5):1453-1461.
9. Shevchenko A, Wilm M, Vorm O, Mann M. Mass spectrometric sequencing of proteins silver-stained polyacrylamide gels. *Anal Chem*. 1996;68(5):850-858.
10. Kanehisa M, Goto S. KEGG: kyoto encyclopedia of genes and genomes. *Nucleic Acids Res*. 2000;28(1):27-30.
11. Jiao X, Sherman BT, Huang da W, et al. DAVID-WS: a stateful web service to facilitate gene/protein list analysis. *Bioinformatics*. 2012;28(13):1805-1806.
12. Schneider CA, Rasband WS, Eliceiri KW. NIH Image to ImageJ: 25 years of image analysis. *Nat Methods*. 2012;9(7):671-675.
13. Hanzelmann S, Castelo R, Guinney J. GSVA: gene set variation analysis for microarray and RNA-seq data. *BMC Bioinformatics*. 2013;14:7.

14. Subramanian A, Tamayo P, Mootha VK, et al. Gene set enrichment analysis: a knowledge-based approach for interpreting genome-wide expression profiles. *Proc Natl Acad Sci U S A*. 2005;102(43):15545-15550.
15. Mootha VK, Lindgren CM, Eriksson KF, et al. PGC-1alpha-responsive genes involved in oxidative phosphorylation are coordinately downregulated in human diabetes. *Nat Genet*. 2003;34(3):267-273.
16. Zhang Y, Liu T, Meyer CA, et al. Model-based analysis of ChIP-Seq (MACS). *Genome Biol*. 2008;9(9):R137.
17. Yu G, Wang LG, He QY. ChIPseeker: an R/Bioconductor package for ChIP peak annotation, comparison and visualization. *Bioinformatics*. 2015;31(14):2382-2383.
18. Kiesel A, Roth C, Ge W, Wess M, Meier M, Soding J. The BaMM web server for de-novo motif discovery and regulatory sequence analysis. *Nucleic Acids Res*. 2018;46(W1):W215-W220.
19. Gu Z, Eils R, Schlesner M, Ishaque N. EnrichedHeatmap: an R/Bioconductor package for comprehensive visualization of genomic signal associations. *BMC Genomics*. 2018;19(1):234.
20. Dworzak MN, Froschl G, Printz D, et al. CD99 expression in T-lineage ALL: implications for flow cytometric detection of minimal residual disease. *Leukemia*. 2004;18(4):703-708.
21. Levine JH, Simonds EF, Bendall SC, et al. Data-Driven Phenotypic Dissection of AML Reveals Progenitor-like Cells that Correlate with Prognosis. *Cell*. 2015;162(1):184-197.
22. Coustan-Smith E, Mullighan CG, Onciu M, et al. Early T-cell precursor leukaemia: a subtype of very high-risk acute lymphoblastic leukaemia. *Lancet Oncol*. 2009;10(2):147-156.
23. Basso G, Veltroni M, Valsecchi MG, et al. Risk of relapse of childhood acute lymphoblastic leukemia is predicted by flow cytometric measurement of residual disease on day 15 bone marrow. *J Clin Oncol*. 2009;27(31):5168-5174.
24. Sulis ML, Williams O, Palomero T, et al. NOTCH1 extracellular juxtamembrane expansion mutations in T-ALL. *Blood*. 2008;112(3):733-740.
25. Kuzilkova D, Bugarin C, Rejlova K, et al. Either IL-7 activation of JAK-STAT or BEZ inhibition of PI3K-AKT-mTOR pathways dominates the single-cell phosphosignature of ex vivo treated pediatric T-cell acute lymphoblastic leukemia cells. *Haematologica*. 2022;107(6):1293-1310.
26. Kucukcankurt F, Erbilgin Y, Firtina S, et al. PTEN and AKT1 Variations in Childhood T-Cell Acute Lymphoblastic Leukemia. *Turk J Haematol*. 2020;37(2):98-103.
27. Diccianni MB, Yu J, Hsiao M, Mukherjee S, Shao LE, Yu AL. Clinical significance of p53 mutations in relapsed T-cell acute lymphoblastic leukemia. *Blood*. 1994;84(9):3105-3112.
28. Asnafi V, Buzyn A, Le Noir S, et al. NOTCH1/FBXW7 mutation identifies a large subgroup with favorable outcome in adult T-cell acute lymphoblastic leukemia (T-ALL): a Group for Research on Adult Acute Lymphoblastic Leukemia (GRAALL) study. *Blood*. 2009;113(17):3918-3924.
29. Yost AJ, Shevchuk OO, Gooch R, et al. Defined, serum-free conditions for in vitro culture of primary human T-ALL blasts. *Leukemia*. 2013;27(6):1437-1440.
30. Greer EL, Oskoui PR, Banko MR, et al. The energy sensor AMP-activated protein kinase directly regulates the mammalian FOXO3 transcription factor. *J Biol Chem*. 2007;282(41):30107-30119.
31. Hu MC, Lee DF, Xia W, et al. IkappaB kinase promotes tumorigenesis through inhibition of forkhead FOXO3a. *Cell*. 2004;117(2):225-237.

32. Liberzon A, Birger C, Thorvaldsdottir H, Ghandi M, Mesirov JP, Tamayo P. The Molecular Signatures Database (MSigDB) hallmark gene set collection. *Cell Syst*. 2015;1(6):417-425.

Supplementary Tables

Table S1.

CDK4 Amplicon	Forward primer	Reverse Primer
CDK4_#1	GCCACACCTCTGCTCCTCAGAG	GAGGGCTGGGCGAACGCCGGAC
CDK4_#2	GGAGCCCGAGGCGGTGCCAT	AACTCCCACCCCCTCCCCAAT
CDK4_#3	GTGACAGCATCACCTCTGGTACC	ACCCAGAGCCCAACTCCCGGCT
CDK4_#4	TTGCACATGTGCAATCCTGTATC	GCAGGAGACAGGAATACTTGAC
CDK4_#5	CTGTTTTCCTTAACCATCTG	GGAGGGGCCCAGGGCTACAA

Table S1. Primer sequences used for amplification of CDK4 promoter regions described in Fig. S22.

Table S2.

Donor (clone)	Donor Type	Recipient ID (Strain)	Injected Cells after Sorting (% purity)	Injected Cell Dose	Clinical Outcome	Latency (days)	% CD45+ Cherry+ mCD8+ Spleen Cells at Necropsy	% GFP+ NGFR+ Leukemic Spleen Cells at Necropsy
M71-10	Secondary Leukemia (PDX)	1 (NSG)	$CD45^+Cherry^+mCD8^+$ **GFP+ NGFR+** (92)	100,000	Leukemia	40	93	3.2
M71-10	Secondary Leukemia (PDX)	2 (NSG)	$CD45^+Cherry^+mCD8^+$ **GFP+ NGFR+** (92)	100,000	Leukemia	40	76	1.43
M71-10	Secondary Leukemia (PDX)	3 (NSG)	$CD45^+Cherry^+mCD8^+$ **GFP+ NGFR+** (92)	100,000	Leukemia	40	88.2	4.3
M71-10	Secondary Leukemia (PDX)	4 (NSG)	$CD45^+Cherry^+mCD8^+$ **GFP+ NGFR+** (92)	100,000	Leukemia	41	ND	ND
M71-10	Secondary Leukemia (PDX)	1 (NSG)	$CD45^+Cherry^+mCD8^+$ **GFP+ NGFR+** (92)	10,000	Leukemia	45	78	5.3
M71-10	Secondary Leukemia (PDX)	2 (NSG)	$CD45^+Cherry^+mCD8^+$ **GFP+ NGFR+** (92)	10,000	NED (d100)			
M71-10	Secondary Leukemia (PDX)	3 (NSG)	$CD45^+Cherry^+mCD8^+$ **GFP+ NGFR+** (92)	10,000	NED (d100)			
M71-10	Secondary Leukemia (PDX)	4 (NSG)	$CD45^+Cherry^+mCD8^+$ **GFP+ NGFR+** (92)	10,000	Leukemia	46	82.3	4.5
M71-10	Secondary Leukemia (PDX)	1 (NSG)	$CD45^+Cherry^+mCD8^+$ **GFP+ NGFR-** (97.3)	100,000	Leukemia	56	75.4	2.1 (GFP+ only)
M71-10	Secondary Leukemia (PDX)	2 (NSG)	$CD45^+Cherry^+mCD8^+$ **GFP+ NGFR-** (97.3)	100,000	NED (d100)			
M71-10	Secondary Leukemia (PDX)	3 (NSG)	$CD45^+Cherry^+mCD8^+$ **GFP+ NGFR-** (97.3)	100,000	NED (d100)			
M71-10	Secondary Leukemia (PDX)	4 (NSG)	$CD45^+Cherry^+mCD8^+$ **GFP+ NGFR-** (97.3)	100,000	NED (d100)			
M71-10	Secondary Leukemia (PDX)	1 (NSG)	$CD45^+Cherry^+mCD8^+$ **GFP+ NGFR-** (97.3)	10,000	NED (d100)			
M71-10	Secondary Leukemia (PDX)	2 (NSG)	$CD45^+Cherry^+mCD8^+$ **GFP+ NGFR-** (97.3)	10,000	NED (d100)			
M71-10	Secondary Leukemia (PDX)	3 (NSG)	$CD45^+Cherry^+mCD8^+$ **GFP+ NGFR-** (97.3)	10,000	NED (d100)			
M71-10	Secondary Leukemia (PDX)	4 (NSG)	$CD45^+Cherry^+mCD8^+$ **GFP+ NGFR-** (97.3)	10,000	NED (d100)			
M71-10	Secondary Leukemia (PDX)	1 (NSG)	$CD45^+Cherry^+mCD8^+$ **GFP- NGFR+** (86.5)	100,000	NED (d100)			
M71-10	Secondary Leukemia (PDX)	2 (NSG)	$CD45^+Cherry^+mCD8^+$ **GFP- NGFR+** (86.5)	100,000	NED (d100)			
M71-10	Secondary Leukemia (PDX)	3 (NSG)	$CD45^+Cherry^+mCD8^+$ **GFP- NGFR+** (86.5)	100,000	NED (d100)			
M71-10	Secondary Leukemia (PDX)	4 (NSG)	$CD45^+Cherry^+mCD8^+$ **GFP- NGFR+** (86.5)	100,000	NED (d100)			
M71-10	Secondary Leukemia (PDX)	1 (NSG)	$CD45^+Cherry^+mCD8^+$ **GFP- NGFR-** (96.2)	100,000	NED (d100)			
M71-10	Secondary Leukemia (PDX)	2 (NSG)	$CD45^+Cherry^+mCD8^+$ **GFP- NGFR-** (96.2)	100,000	NED (d100)			
M71-10	Secondary Leukemia (PDX)	3 (NSG)	$CD45^+Cherry^+mCD8^+$ **GFP- NGFR-** (96.2)	100,000	NED (d100)			
M71-10	Secondary Leukemia (PDX)	4 (NSG)	$CD45^+Cherry^+mCD8^+$ **GFP- NGFR-** (96.2)	100,000	NED (d100)			
M71-10	Secondary Leukemia (PDX)	1 (NSG)	$CD45^+Cherry^+mCD8^+$ **GFP- NGFR-** (96.2)	10,000	NED (d100)			
M71-10	Secondary Leukemia (PDX)	2 (NSG)	$CD45^+Cherry^+mCD8^+$ **GFP- NGFR-** (96.2)	10,000	NED (d100)			
M71-10	Secondary Leukemia (PDX)	3 (NSG)	$CD45^+Cherry^+mCD8^+$ **GFP- NGFR-** (96.2)	10,000	NED (d100)			
M71-10	Secondary Leukemia (PDX)	4 (NSG)	$CD45^+Cherry^+mCD8^+$ **GFP- NGFR-** (96.2)	10,000	NED (d100)			

Table S2.

Donor (clone)	Donor Type	Recipient ID (Strain)	Injected Cells after Sorting (% purity)	Injected Cell Dose	Clinical Outcome	Latency (days)	% CD45+ Cherry+ mCD8+ Spleen Cells at Necropsy	% GFP+ NGFR+ Leukemic Spleen Cells at Necropsy
H3255-1	Secondary Leukemia (PDX)	1 (NSG)	$CD45^+Cherry^+mCD8^+$ **GFP+ NGFR+** (91)	50,000	Leukemia	38	82	3.75
H3255-1	Secondary Leukemia (PDX)	2 (NSG)	$CD45^+Cherry^+mCD8^+$ **GFP+ NGFR+** (91)	50,000	NED (d100)			
H3255-1	Secondary Leukemia (PDX)	3 (NSG)	$CD45^+Cherry^+mCD8^+$ **GFP+ NGFR+** (91)	50,000	Leukemia	38	85	1.2
H3255-1	Secondary Leukemia (PDX)	4 (NSG)	$CD45^+Cherry^+mCD8^+$ **GFP+ NGFR+** (91)	50,000	Leukemia	38	87	4.5
H3255-1	Secondary Leukemia (PDX)	1 (NSG)	$CD45^+Cherry^+mCD8^+$ **GFP+ NGFR-** (87.1)	50,000	NED (d100)			
H3255-1	Secondary Leukemia (PDX)	2 (NSG)	$CD45^+Cherry^+mCD8^+$ **GFP+ NGFR-** (87.1)	50,000	NED (d100)			
H3255-1	Secondary Leukemia (PDX)	3 (NSG)	$CD45^+Cherry^+mCD8^+$ **GFP+ NGFR-** (87.1)	50,000	NED (d100)			
H3255-1	Secondary Leukemia (PDX)	4 (NSG)	$CD45^+Cherry^+mCD8^+$ **GFP+ NGFR-** (87.1)	50,000	NED (d100)			
H3255-1	Secondary Leukemia (PDX)	1 (NSG)	$CD45^+Cherry^+mCD8^+$ **GFP- NGFR+** (96)	50,000	NED (d100)			
H3255-1	Secondary Leukemia (PDX)	2 (NSG)	$CD45^+Cherry^+mCD8^+$ **GFP- NGFR+** (96)	50,000	NED (d100)			
H3255-1	Secondary Leukemia (PDX)	3 (NSG)	$CD45^+Cherry^+mCD8^+$ **GFP- NGFR+** (96)	50,000	NED (d100)			
H3255-1	Secondary Leukemia (PDX)	4 (NSG)	$CD45^+Cherry^+mCD8^+$ **GFP- NGFR+** (96)	50,000	NED (d100)			
H3255-1	Secondary Leukemia (PDX)	1 (NSG)	$CD45^+Cherry^+mCD8^+$ **GFP- NGFR-** (98)	50,000	NED (d100)			
H3255-1	Secondary Leukemia (PDX)	2 (NSG)	$CD45^+Cherry^+mCD8^+$ **GFP- NGFR-** (98)	50,000	NED (d100)			
H3255-1	Secondary Leukemia (PDX)	3 (NSG)	$CD45^+Cherry^+mCD8^+$ **GFP- NGFR-** (98)	50,000	NED (d100)			
H3255-1	Secondary Leukemia (PDX)	4 (NSG)	$CD45^+Cherry^+mCD8^+$ **GFP- NGFR-** (98)	50,000	NED (d100)			

Table S2, related to Figure 2F. Summary of transplant experiments with M71-10 and H3255-1, human 7TGC_3DNm8 transduced PDXs.

% CD45+ Cherry+ mCD8+ cell fraction is among gated viable spleen cells; % GFP+NGFR+ is among gated viable human CD45+ Cherry+ mCD8+ cells.

NED (dX), no evidence of disease as of X days post-transplant; ND, not determined.

Table S3.

Donor (clone)	Donor Type	Recipient ID (Strain)	Injected Cells after Sorting (% purity)	Injected Cell Dose	Clinical Outcome	Latency (days)	% Cherry+ mTagBFP2+ Spleen Cells at Necropsy	% GFP+ hCD8+ Leukemic Spleen Cells at Necropsy
V12-1	Secondary Notch1-induced mouse leukemia	1 (C57BL/6)	$Cherry^+mTagBFP2^+$ **GFP+ hCD8+** (88.2)	7,000	Leukemia	42	87	1.4
V12-1	Secondary Notch1-induced mouse leukemia	2 (C57BL/6)	$Cherry^+mTagBFP2^+$ **GFP+ hCD8+** (88.2)	7,000	Leukemia	42	98	5.2
V12-1	Secondary Notch1-induced mouse leukemia	3 (C57BL/6)	$Cherry^+mTagBFP2^+$ **GFP+ hCD8+** (88.2)	7,000	Leukemia	43	76.3	4.3
V12-1	Secondary Notch1-induced mouse leukemia	4 (C57BL/6)	$Cherry^+mTagBFP2^+$ **GFP+ hCD8+** (88.2)	7,000	Leukemia	43	ND	ND
V12-1	Secondary Notch1-induced mouse leukemia	1 (C57BL/6)	$Cherry^+mTagBFP2^+$ **GFP+ hCD8-** (83.9)	7,000	Leukemia	50	76.7	2.3 (GFP+ only)
V12-1	Secondary Notch1-induced mouse leukemia	2 (C57BL/6)	$Cherry^+mTagBFP2^+$ **GFP+ hCD8-** (83.9)	7,000	NED (d100)			
V12-1	Secondary Notch1-induced mouse leukemia	3 (C57BL/6)	$Cherry^+mTagBFP2^+$ **GFP+ hCD8-** (83.9)	7,000	NED (d100)			
V12-1	Secondary Notch1-induced mouse leukemia	4 (C57BL/6)	$Cherry^+mTagBFP2^+$ **GFP+ hCD8-** (83.9)	7,000	NED (d100)			
V12-1	Secondary Notch1-induced mouse leukemia	1 (C57BL/6)	$Cherry^+mTagBFP2^+$ **GFP- hCD8-** (100)	7,000	Leukemia	84	79.8	ND
V12-1	Secondary Notch1-induced mouse leukemia	2 (C57BL/6)	$Cherry^+mTagBFP2^+$ **GFP- hCD8-** (100)	7,000	NED (d100)			
V12-1	Secondary Notch1-induced mouse leukemia	3 (C57BL/6)	$Cherry^+mTagBFP2^+$ **GFP- hCD8-** (100)	7,000	NED (d100)			
V12-1	Secondary Notch1-induced mouse leukemia	4 (C57BL/6)	$Cherry^+mTagBFP2^+$ **GFP- hCD8-** (100)	7,000	NED (d100)			

Table S3. related to Figure S14C. Summary of transplant experiments with "7TGC" and "3DB8" transduced Notch1-induced mouse leukemia.

% Cherry+ mTagBFP2+ cell fraction is among gated viable spleen cells; % GFP+hCD8+ is among gated viable mouse Cherry+ mTagBFP2+ cells.

NED (dX), no evidence of disease as of X days post-transplant; ND, not determined.

Table S4.

Donor (clone)	Donor Type	Recipient ID (Strain)	Injected Cells after Sorting (% purity)	Injected Cell Dose	Clinical Outcome	Latency (days)	% CD45+ Spleen Cells at Necropsy	% GFP+ or NGFR+ Leukemic Spleen Cells at Necropsy
M71-10	in vitro CRISPR/Cas9-treated PDX	1 (NSG)	CD45+ **GFP+ NGFR+** (88.8)	80,000	NED (d90)			
M71-10	in vitro CRISPR/Cas9-treated PDX	2 (NSG)	CD45+ **GFP+ NGFR+** (88.8)	80,000	NED (d90)			
M71-10	in vitro CRISPR/Cas9-treated PDX	3 (NSG)	CD45+ **GFP+ NGFR+** (88.8)	80,000	NED (d90)			
M71-10	in vitro CRISPR/Cas9-treated PDX	4 (NSG)	CD45+ **GFP+ NGFR+** (88.8)	80,000	NED (d90)			
M71-10	in vitro CRISPR/Cas9-treated PDX	5 (NSG)	CD45+ **GFP+ NGFR+** (88.8)	80,000	NED (d90)			
M71-10	in vitro CRISPR/Cas9-treated PDX	1 (NSG)	CD45+ **GFP- NGFR+** (84)	80,000	NED (d90)			
M71-10	in vitro CRISPR/Cas9-treated PDX	2 (NSG)	CD45+ **GFP- NGFR+** (84)	80,000	NED (d90)			
M71-10	in vitro CRISPR/Cas9-treated PDX	3 (NSG)	CD45+ **GFP- NGFR+** (84)	80,000	NED (d90)			
M71-10	in vitro CRISPR/Cas9-treated PDX	4 (NSG)	CD45+ **GFP- NGFR+** (84)	80,000	NED (d90)			
M71-10	in vitro CRISPR/Cas9-treated PDX	5 (NSG)	CD45+ **GFP- NGFR+** (84)	80,000	NED (d90)			
M71-10	in vitro CRISPR/Cas9-treated PDX	1 (NSG)	CD45+ **GFP+ NGFR-** (95.4)	80,000	NED (d90)			
M71-10	in vitro CRISPR/Cas9-treated PDX	2 (NSG)	CD45+ **GFP+ NGFR-** (95.4)	80,000	NED (d90)			
M71-10	in vitro CRISPR/Cas9-treated PDX	3 (NSG)	CD45+ **GFP+ NGFR-** (95.4)	80,000	NED (d90)			
M71-10	in vitro CRISPR/Cas9-treated PDX	4 (NSG)	CD45+ **GFP+ NGFR-** (95.4)	80,000	NED (d90)			
M71-10	in vitro CRISPR/Cas9-treated PDX	5 (NSG)	CD45+ **GFP+ NGFR-** (95.4)	80,000	Leukemia	44	76.5	73
M71-10	in vitro CRISPR/Cas9-treated PDX	1 (NSG)	CD45+ **GFP- NGFR-** (100)	80,000	NED (d90)			
M71-10	in vitro CRISPR/Cas9-treated PDX	2 (NSG)	CD45+ **GFP- NGFR-** (100)	80,000	Leukemia	26	78	ND
M71-10	in vitro CRISPR/Cas9-treated PDX	3 (NSG)	CD45+ **GFP- NGFR-** (100)	80,000	Leukemia	28	82	ND
M71-10	in vitro CRISPR/Cas9-treated PDX	4 (NSG)	CD45+ **GFP- NGFR-** (100)	80,000	Leukemia	30	92	ND
M71-10	in vitro CRISPR/Cas9-treated PDX	5 (NSG)	CD45+ **GFP- NGFR-** (100)	80,000	Leukemia	41	ND	ND

Table S4.

Donor (clone)	Donor Type	Recipient ID (Strain)	Injected Cells after Sorting (% purity)	Injected Cell Dose	Clinical Outcome	Latency (days)	% CD45+ Spleen Cells at Necropsy	% GFP+ or NGFR+ Leukemic Spleen Cells at Necropsy
H3255-1	in vitro CRISPR/Cas9-treated PDX	1 (NSG)	CD45+ **GFP+ NGFR+** (86.2)	100,000	NED (d90)			
H3255-1	in vitro CRISPR/Cas9-treated PDX	2 (NSG)	CD45+ **GFP+ NGFR+** (86.2)	100,000	NED (d90)			
H3255-1	in vitro CRISPR/Cas9-treated PDX	3 (NSG)	CD45+ **GFP+ NGFR+** (86.2)	100,000	NED (d90)			
H3255-1	in vitro CRISPR/Cas9-treated PDX	4 (NSG)	CD45+ **GFP+ NGFR+** (86.2)	100,000	NED (d90)			
H3255-1	in vitro CRISPR/Cas9-treated PDX	5 (NSG)	CD45+ **GFP+ NGFR+** (86.2)	100,000	NED (d90)			
H3255-1	in vitro CRISPR/Cas9-treated PDX	1 (NSG)	CD45+ **GFP- NGFR+** (81.3)	100,000	NED (d90)			
H3255-1	in vitro CRISPR/Cas9-treated PDX	2 (NSG)	CD45+ **GFP- NGFR+** (81.3)	100,000	NED (d90)			
H3255-1	in vitro CRISPR/Cas9-treated PDX	3 (NSG)	CD45+ **GFP- NGFR+** (81.3)	100,000	Leukemia	50	76	65
H3255-1	in vitro CRISPR/Cas9-treated PDX	4 (NSG)	CD45+ **GFP- NGFR+** (81.3)	100,000	NED (d90)			
H3255-1	in vitro CRISPR/Cas9-treated PDX	5 (NSG)	CD45+ **GFP- NGFR+** (81.3)	100,000	NED (d90)			
H3255-1	in vitro CRISPR/Cas9-treated PDX	1 (NSG)	CD45+ **GFP+ NGFR-** (92)	100,000	Leukemia	28	ND	ND
H3255-1	in vitro CRISPR/Cas9-treated PDX	2 (NSG)	CD45+ **GFP+ NGFR-** (92)	100,000	Leukemia	48	77	61
H3255-1	in vitro CRISPR/Cas9-treated PDX	3 (NSG)	CD45+ **GFP+ NGFR-** (92)	100,000	NED (d90)			
H3255-1	in vitro CRISPR/Cas9-treated PDX	4 (NSG)	CD45+ **GFP+ NGFR-** (92)	100,000	NED (d90)			
H3255-1	in vitro CRISPR/Cas9-treated PDX	5 (NSG)	CD45+ **GFP+ NGFR-** (92)	100,000	Leukemia			
H3255-1	in vitro CRISPR/Cas9-treated PDX	1 (NSG)	CD45+ **GFP- NGFR-** (100)	100,000	NED (d90)	28	ND	ND
H3255-1	in vitro CRISPR/Cas9-treated PDX	2 (NSG)	CD45+ **GFP- NGFR-** (100)	100,000	Leukemia	40	83	ND
H3255-1	in vitro CRISPR/Cas9-treated PDX	3 (NSG)	CD45+ **GFP- NGFR-** (100)	100,000	Leukemia	41	77	ND
H3255-1	in vitro CRISPR/Cas9-treated PDX	4 (NSG)	CD45+ **GFP- NGFR-** (100)	100,000	Leukemia	41	ND	ND
H3255-1	in vitro CRISPR/Cas9-treated PDX	5 (NSG)	CD45+ **GFP- NGFR-** (100)	100,000	Leukemia	41	79	ND

Table S4, related to Figure S15E. Summary of transplant experiments with M71-10 and H3255-1, in vitro CRISPR/Cas9-treated PDXs.
% CD45+ cell fraction is among gated viable spleen cells; % GFP+ or NGFR+ is among gated viable human CD45+ cells.
NED (dX), no evidence of disease as of X days post-transplant; ND, not determined.

Table S5.

Donor (clone)	Donor Type	Recipient ID (Strain)	Injected Cells after Sorting (% purity)	Injected Cell Dose	Clinical Outcome	Latency (days)	% CD45+ Spleen Cells at Necropsy	% mCD8+ /Cherry+ Leukemic Spleen Cells at Necropsy
M22-7	FOXO3(TM) and β-Cat. (ΔGSK) transduced PDX	1 (NSG)	CD45+ **mCD8+ mCherry+** (87)	80,000	Leukemia	30	80	69
M22-7	FOXO3(TM) and β-Cat. (ΔGSK) transduced PDX	2 (NSG)	CD45+ **mCD8+ mCherry+** (87)	80,000	Leukemia	50	49	57
M22-7	FOXO3(TM) and β-Cat. (ΔGSK) transduced PDX	3 (NSG)	CD45+ **mCD8+ mCherry+** (87)	80,000	Leukemia	50	78	86
M22-7	FOXO3(TM) and β-Cat. (ΔGSK) transduced PDX	4 (NSG)	CD45+ **mCD8+ mCherry+** (87)	80,000	Leukemia	50	nd	nd
M22-7	FOXO3(TM) and β-Cat. (ΔGSK) transduced PDX	5 (NSG)	CD45+ **mCD8+ mCherry+** (87)	8,000	Leukemia	50	nd	nd
M22-7	FOXO3(TM) and β-Cat. (ΔGSK) transduced PDX	6 (NSG)	CD45+ **mCD8+ mCherry+** (87)	8,000	NED (d71)			
M22-7	FOXO3(TM) and β-Cat. (ΔGSK) transduced PDX	7 (NSG)	CD45+ **mCD8+ mCherry+** (87)	8,000	NED (d71)			
M22-7	FOXO3(TM) and β-Cat. (ΔGSK) transduced PDX	8 (NSG)	CD45+ **mCD8+ mCherry+** (87)	8,000	NED (d71)			
M22-7	β-Cat. (ΔGSK) transduced PDX	1 (NSG)	CD45+ **mCherry+** (88)	80,000	Leukemia	34	88	57
M22-7	β-Cat. (ΔGSK) transduced PDX	2 (NSG)	CD45+ **mCherry+** (88)	80,000	NED (d71)			
M22-7	β-Cat. (ΔGSK) transduced PDX	3 (NSG)	CD45+ **mCherry+** (88)	80,000	NED (d71)			
M22-7	β-Cat. (ΔGSK) transduced PDX	4 (NSG)	CD45+ **mCherry+** (88)	80,000	NED (d71)			
M22-7	β-Cat. (ΔGSK) transduced PDX	5 (NSG)	CD45+ **mCherry+** (88)	8,000	NED (d71)			
M22-7	β-Cat. (ΔGSK) transduced PDX	6 (NSG)	CD45+ **mCherry+** (88)	8,000	NED (d71)			
M22-7	β-Cat. (ΔGSK) transduced PDX	7 (NSG)	CD45+ **mCherry+** (88)	8,000	NED (d71)			
M22-7	β-Cat. (ΔGSK) transduced PDX	8 (NSG)	CD45+ **mCherry+** (88)	8,000	NED (d71)			
M22-7	FOXO3(TM) transduced PDX	1 (NSG)	CD45+ **mCD8+** (100)	80,000	NED (d71)			
M22-7	FOXO3(TM) transduced PDX	2 (NSG)	CD45+ **mCD8+** (100)	80,000	NED (d71)			
M22-7	FOXO3(TM) transduced PDX	3 (NSG)	CD45+ **mCD8+** (100)	80,000	Leukemia	47	77	23
M22-7	FOXO3(TM) transduced PDX	4 (NSG)	CD45+ **mCD8+** (100)	80,000	NED (d71)			
M22-7	FOXO3(TM) transduced PDX	5 (NSG)	CD45+ **mCD8+** (100)	8,000	NED (d71)			
M22-7	FOXO3(TM) transduced PDX	6 (NSG)	CD45+ **mCD8+** (100)	8,000	NED (d71)			
M22-7	FOXO3(TM) transduced PDX	7 (NSG)	CD45+ **mCD8+** (100)	8,000	NED (d71)			
M22-7	FOXO3(TM) transduced PDX	8 (NSG)	CD45+ **mCD8+** (100)	8,000	NED (d71)			
M22-7	Empty Vector transduced PDX	1 (NSG)	CD45+ **mCherry** (100)	80,000	NED (d71)			
M22-7	Empty Vector transduced PDX	2 (NSG)	CD45+ **mCherry** (100)	80,000	Leukemia	34	nd	nd
M22-7	Empty Vector transduced PDX	3 (NSG)	CD45+ **mCherry** (100)	80,000	NED (d71)			
M22-7	Empty Vector transduced PDX	4 (NSG)	CD45+ **mCherry** (100)	80,000	NED (d71)			

M22-7	Empty Vector transduced PDX	5 (NSG)	CD45+ **mCherry** (100)	8,000	NED (d71)			
M22-7	Empty Vector transduced PDX	6 (NSG)	CD45+ **mCherry** (100)	8,000	NED (d71)			
M22-7	Empty Vector transduced PDX	7 (NSG)	CD45+ **mCherry** (100)	8,000	NED (d71)			
M22-7	Empty Vector transduced PDX	8 (NSG)	CD45+ **mCherry** (100)	8,000	NED (d71)			

Donor (clone)	Donor Type	Recipient ID (Strain)	Injected Cells after Sorting (% purity)	Injected Cell Dose	Clinical Outcome	Latency (days)	% CD45+ Spleen Cells at Necropsy	% mCD8+ Cherry+ Leukemic Spleen Cells at Necropsy
M69-12	FOXO3(TM) and β-Cat. (ΔGSK) transduced PDX	1 (NSG)	CD45+ **mCD8+ mCherry+** (90)	100,000	Leukemia	28	60	79
M69-12	FOXO3(TM) and β-Cat. (ΔGSK) transduced PDX	2 (NSG)	CD45+ **mCD8+ mCherry+** (90)	100,000	Leukemia	30	57	80
M69-12	FOXO3(TM) and β-Cat. (ΔGSK) transduced PDX	3 (NSG)	CD45+ **mCD8+ mCherry+** (90)	100,000	NED (d71)			
M69-12	FOXO3(TM) and β-Cat. (ΔGSK) transduced PDX	4 (NSG)	CD45+ **mCD8+ mCherry+** (90)	100,000	NED (d71)			
M69-12	β-Cat. (ΔGSK) transduced PDX	1 (NSG)	CD45+ **mCherry+** (96)	100,000	NED (d71)			
M69-12	β-Cat. (ΔGSK) transduced PDX	2 (NSG)	CD45+ **mCherry+** (96)	100,000	NED (d71)			
M69-12	β-Cat. (ΔGSK) transduced PDX	3 (NSG)	CD45+ **mCherry+** (96)	100,000	NED (d71)			
M69-12	β-Cat. (ΔGSK) transduced PDX	4 (NSG)	CD45+ **mCherry+** (96)	100,000	NED (d71)			
M69-12	FOXO3(TM) transduced PDX	1 (NSG)	CD45+ **mCD8+** (100)	100,000	NED (d71)			
M69-12	FOXO3(TM) transduced PDX	2 (NSG)	CD45+ **mCD8+** (100)	100,000	NED (d71)			
M69-12	FOXO3(TM) transduced PDX	3 (NSG)	CD45+ **mCD8+** (100)	100,000	NED (d71)			
M69-12	FOXO3(TM) transduced PDX	4 (NSG)	CD45+ **mCD8+** (100)	100,000	NED (d71)			
M69-12	Empty Vector transduced PDX	1 (NSG)	CD45+ **mCherry** (99)	100,000	NED (d71)			
M69-12	Empty Vector transduced PDX	2 (NSG)	CD45+ **mCherry** (99)	100,000	NED (d71)			
M69-12	Empty Vector transduced PDX	3 (NSG)	CD45+ **mCherry** (99)	100,000	NED (d71)			
M69-12	Empty Vector transduced PDX	4 (NSG)	CD45+ **mCherry** (99)	100,000	NED (d71)			

Table S5, related to Figure S16. Summary of transplant experiments with M22-7 and M69-12, after transduction of FOXO3_TM/mCD8 alone or in combination with β-Catenin_ΔGSK/mCherry.

% CD45+ cell fraction is among gated viable spleen cells; % mCD8+ or mCherry+ is among gated viable human CD45+ cells.

NED (dX), no evidence of disease as of X days post-transplant; ND, not determined.

Table S6.

Donor (clone)	Donor Type	Recipient ID (Strain)	Injected Cells after Sorting (% purity)	Injected Cell Dose	Clinical Outcome	Latency (days)	% CD45+ Spleen Cells at Necropsy
CSS13693	Primary human T-ALL at **diagnosis (d0)**	1 (NSG)	CD45+ CD3-CD99+CD7+(96)	100,000	NED (d100)		
CSS13693	Primary human T-ALL at **diagnosis (d0)**	2 (NSG)	CD45+ CD3-CD99+CD7+(96)	100,000	NED (d100)		
CSS13693	Primary human T-ALL at **diagnosis (d0)**	3 (NSG)	CD45+ CD3-CD99+CD7+(96)	100,000	NED (d100)		
CSS13693	Primary human T-ALL at **diagnosis (d0)**	4 (NSG)	CD45+ CD3-CD99+CD7+(96)	100,000	NED (d100)		
CSS13693	Primary human T-ALL at **diagnosis (d0)**	5 (NSG)	CD45+ CD3-CD99+CD7+(96)	100,000	NED (d100)		
CSS13693	Primary human T-ALL at **MRD (d30)**	1 (NSG)	CD45+ CD3-CD99+CD7+(98)	100,000	NED (d100)		
CSS13693	Primary human T-ALL at **MRD (d30)**	2 (NSG)	CD45+ CD3-CD99+CD7+(98)	100,000	Leukemia	51	75
CSS13693	Primary human T-ALL at **MRD (d30)**	3 (NSG)	CD45+ CD3-CD99+CD7+(98)	100,000	NED (d100)		
CSS13693	Primary human T-ALL at **MRD (d30)**	4 (NSG)	CD45+ CD3-CD99+CD7+(98)	100,000	Leukemia	52	88
CSS13693	Primary human T-ALL at **MRD (d30)**	5 (NSG)	CD45+ CD3-CD99+CD7+(98)	100,000	NED (d100)		

Donor (clone)	Donor Type	Recipient ID (Strain)	Injected Cells after Sorting (% purity)	Injected Cell Dose	Clinical Outcome	Latency (days)	% CD45+ Spleen Cells at Necropsy
CSS20705	Primary human T-ALL at **diagnosis (d0)**	1 (NSG)	CD45+ CD3-CD99+CD7+(nd)	100,000	NED (d100)		
CSS20705	Primary human T-ALL at **diagnosis (d0)**	2 (NSG)	CD45+ CD3-CD99+CD7+(nd)	100,000	NED (d100)		
CSS20705	Primary human T-ALL at **diagnosis (d0)**	3 (NSG)	CD45+ CD3-CD99+CD7+(nd)	100,000	NED (d100)		
CSS20705	Primary human T-ALL at **diagnosis (d0)**	4 (NSG)	CD45+ CD3-CD99+CD7+(nd)	100,000	NED (d100)		
CSS20705	Primary human T-ALL at **diagnosis (d0)**	5 (NSG)	CD45+ CD3-CD99+CD7+(nd)	100,000	Leukemia	47	77
CSS20705	Primary human T-ALL at **MRD (d30)**	1 (NSG)	CD45+ CD3-CD99+CD7+(nd)	100,000	Leukemia	42	
CSS20705	Primary human T-ALL at **MRD (d30)**	2 (NSG)	CD45+ CD3-CD99+CD7+(nd)	100,000	Leukemia	43	
CSS20705	Primary human T-ALL at **MRD (d30)**	3 (NSG)	CD45+ CD3-CD99+CD7+(nd)	100,000	Leukemia	44	
CSS20705	Primary human T-ALL at **MRD (d30)**	4 (NSG)	CD45+ CD3-CD99+CD7+(nd)	100,000	Leukemia	52	
CSS20705	Primary human T-ALL at **MRD (d30)**	5 (NSG)	CD45+ CD3-CD99+CD7+(nd)	100,000	NED (d100)		

Table S6, related to Figure S26B. Summary of transplant experiments CSS13693 and CSS20705 primary samples at the diagnosis (d0) and MRD (d30).
% CD45+ cell fraction is among gated viable spleen cells.
NED (dX), no evidence of disease as of X days post-transplant; ND, not determined.

Table S7.

Donor (clone)	Donor Type	Recipient ID (Strain)	Injected Cells after Sorting (% purity)	Injected Cell Dose	Clinical Outcome	Latency (days)	% CD45+ Spleen Cells at Necropsy	% CD117+ CD82+ Leukemic Spleen Cells at Necropsy
CSS13693	Primary human T-ALL	1 (NSG)	CD45+ **CD117+ CD82+** (92)	100,000	Leukemia	48	88	7.5
CSS13693	Primary human T-ALL	2 (NSG)	CD45+ **CD117+ CD82+** (92)	100,000	Leukemia	50	76	8.2
CSS13693	Primary human T-ALL	3 (NSG)	CD45+ **CD117+ CD82+** (92)	100,000	Leukemia	50	ND	ND
CSS13693	Primary human T-ALL	4 (NSG)	CD45+ **CD117+ CD82+** (92)	100,000	NED (d120)			
CSS13693	Primary human T-ALL	1 (NSG)	CD45+ **CD117+ CD82+** (92)	10,000	NED (d120)			
CSS13693	Primary human T-ALL	2 (NSG)	CD45+ **CD117+ CD82+** (92)	10,000	NED (d120)			
CSS13693	Primary human T-ALL	3 (NSG)	CD45+ **CD117+ CD82+** (92)	10,000	NED (d120)			
CSS13693	Primary human T-ALL	4 (NSG)	CD45+ **CD117+ CD82+** (92)	10,000	NED (d120)			
CSS13693	Primary human T-ALL	1 (NSG)	CD45+ **NOT CD117+ CD82+** (100)	100,000	NED (d120)			
CSS13693	Primary human T-ALL	2 (NSG)	CD45+ **NOT CD117+ CD82+** (100)	100,000	NED (d120)			
CSS13693	Primary human T-ALL	3 (NSG)	CD45+ **NOT CD117+ CD82+** (100)	100,000	NED (d120)			
CSS13693	Primary human T-ALL	4 (NSG)	CD45+ **NOT CD117+ CD82+** (100)	100,000	NED (d120)			
CSS13693	Primary human T-ALL	1 (NSG)	CD45+ **NOT CD117+ CD82+** (100)	10,000	NED (d120)			
CSS13693	Primary human T-ALL	2 (NSG)	CD45+ **NOT CD117+ CD82+** (100)	10,000	NED (d120)			
CSS13693	Primary human T-ALL	3 (NSG)	CD45+ **NOT CD117+ CD82+** (100)	10,000	NED (d120)			
CSS13693	Primary human T-ALL	4 (NSG)	CD45+ **NOT CD117+ CD82+** (100)	10,000	NED (d120)			
CSS13693	Primary human T-ALL	1 (NSG)	CD45+ **CD117+ CD82-** (93.4)	100,000	NED (d120)	54	68	5.4
CSS13693	Primary human T-ALL	2 (NSG)	CD45+ **CD117+ CD82-** (93.4)	100,000	NED (d120)			
CSS13693	Primary human T-ALL	3 (NSG)	CD45+ **CD117+ CD82-** (93.4)	100,000	NED (d120)			
CSS13693	Primary human T-ALL	4 (NSG)	CD45+ **CD117+ CD82-** (93.4)	100,000	NED (d120)			
CSS13693	Primary human T-ALL	5 (NSG)	CD45+ **CD117+ CD82-** (93.4)	100,000	NED (d120)			
CSS13693	Primary human T-ALL	1 (NSG)	CD45+ **CD117+ CD82-** (93.4)	10,000	NED (d120)			
CSS13693	Primary human T-ALL	2 (NSG)	CD45+ **CD117+ CD82-** (93.4)	10,000	NED (d120)			
CSS13693	Primary human T-ALL	3 (NSG)	CD45+ **CD117+ CD82-** (93.4)	10,000	NED (d120)			
CSS13693	Primary human T-ALL	4 (NSG)	CD45+ **CD117+ CD82-** (93.4)	10,000	NED (d120)			
CSS13693	Primary human T-ALL	5 (NSG)	CD45+ **CD117+ CD82-** (93.4)	10,000	NED (d120)			
CSS13693	Primary human T-ALL	1 (NSG)	CD45+ **CD117- CD82-** (100)	100,000	NED (d120)			
CSS13693	Primary human T-ALL	2 (NSG)	CD45+ **CD117- CD82-** (100)	100,000	NED (d120)			
CSS13693	Primary human T-ALL	3 (NSG)	CD45+ **CD117- CD82-** (100)	100,000	NED (d120)			
CSS13693	Primary human T-ALL	4 (NSG)	CD45+ **CD117- CD82-** (100)	100,000	NED (d120)			
CSS13693	Primary human T-ALL	5 (NSG)	CD45+ **CD117- CD82-** (100)	100,000	NED (d120)			

Table S7.

Donor (clone)	Donor Type	Recipient ID (Strain)	Injected Cells after Sorting (% purity)	Injected Cell Dose	Clinical Outcome	Latency (days)	% CD45+ Spleen Cells at Necropsy	% CD117+ CD82+ Leukemic Spleen Cells at Necropsy
CSS15501	Primary human T-ALL	1 (NSG)	CD45+ **CD117+ CD82+** (89)	100,000	Leukemia	54	83	7.3
CSS15501	Primary human T-ALL	2 (NSG)	CD45+ **CD117+ CD82+** (89)	100,000	Leukemia	58	79	8.2
CSS15501	Primary human T-ALL	3 (NSG)	CD45+ **CD117+ CD82+** (89)	100,000	Leukemia	60	57	4.5
CSS15501	Primary human T-ALL	4 (NSG)	CD45+ **CD117+ CD82+** (89)	100,000	Leukemia	60	77	5.2
CSS15501	Primary human T-ALL	1 (NSG)	CD45+ **CD117+ CD82+** (89)	10,000	Leukemia	75	ND	ND
CSS15501	Primary human T-ALL	2 (NSG)	CD45+ **CD117+ CD82+** (89)	10,000	NED (d120)			
CSS15501	Primary human T-ALL	3 (NSG)	CD45+ **CD117+ CD82+** (89)	10,000	NED (d120)			
CSS15501	Primary human T-ALL	4 (NSG)	CD45+ **CD117+ CD82+** (89)	10,000	NED (d120)			
CSS15501	Primary human T-ALL	1 (NSG)	CD45+ **NOT CD117+ CD82+** (100)	100,000	NED (d120)			
CSS15501	Primary human T-ALL	2 (NSG)	CD45+ **NOT CD117+ CD82+** (100)	100,000	NED (d120)			
CSS15501	Primary human T-ALL	3 (NSG)	CD45+ **NOT CD117+ CD82+** (100)	100,000	NED (d120)			
CSS15501	Primary human T-ALL	4 (NSG)	CD45+ **NOT CD117+ CD82+** (100)	100,000	NED (d120)			
CSS15501	Primary human T-ALL	1 (NSG)	CD45+ **NOT CD117+ CD82+** (100)	10,000	NED (d120)			
CSS15501	Primary human T-ALL	2 (NSG)	CD45+ **NOT CD117+ CD82+** (100)	10,000	NED (d120)			
CSS15501	Primary human T-ALL	3 (NSG)	CD45+ **NOT CD117+ CD82+** (100)	10,000	NED (d120)			
CSS15501	Primary human T-ALL	4 (NSG)	CD45+ **NOT CD117+ CD82+** (100)	10,000	NED (d120)			
CSS15501	Primary human T-ALL	1 (NSG)	CD45+ **CD117+ CD82-** (83)	100,000	NED (d120)	54	72	6.2
CSS15501	Primary human T-ALL	2 (NSG)	CD45+ **CD117+ CD82-** (83)	100,000	NED (d120)	57	ND	ND
CSS15501	Primary human T-ALL	3 (NSG)	CD45+ **CD117+ CD82-** (83)	100,000	NED (d120)			
CSS15501	Primary human T-ALL	4 (NSG)	CD45+ **CD117+ CD82-** (83)	100,000	NED (d120)			
CSS15501	Primary human T-ALL	5 (NSG)	CD45+ **CD117+ CD82-** (83)	100,000	NED (d120)			
CSS15501	Primary human T-ALL	1 (NSG)	CD45+ **CD117+ CD82-** (83)	10,000	NED (d120)			
CSS15501	Primary human T-ALL	2 (NSG)	CD45+ **CD117+ CD82-** (83)	10,000	NED (d120)			
CSS15501	Primary human T-ALL	3 (NSG)	CD45+ **CD117+ CD82-** (83)	10,000	NED (d120)			
CSS15501	Primary human T-ALL	4 (NSG)	CD45+ **CD117+ CD82-** (83)	10,000	NED (d120)			
CSS15501	Primary human T-ALL	5 (NSG)	CD45+ **CD117+ CD82-** (83)	10,000	NED (d120)			
CSS15501	Primary human T-ALL	1 (NSG)	CD45+ **CD117- CD82-** (98)	100,000	NED (d120)			
CSS15501	Primary human T-ALL	2 (NSG)	CD45+ **CD117- CD82-** (98)	100,000	NED (d120)			
CSS15501	Primary human T-ALL	3 (NSG)	CD45+ **CD117- CD82-** (98)	100,000	NED (d120)			
CSS15501	Primary human T-ALL	4 (NSG)	CD45+ **CD117- CD82-** (98)	100,000	NED (d120)			
CSS15501	Primary human T-ALL	5 (NSG)	CD45+ **CD117- CD82-** (98)	100,000	NED (d120)			

Table S7, related to Figure 4H. Summary of transplant experiments with CSS13693 and CSS15501, primary T-ALL samples of MRD at d30.

% CD45+ cell fraction is among gated viable spleen cells; % CD117+ CD82+ is among gated viable human CD45+ cells.

NED (dX), no evidence of disease as of X days post-transplant; ND, not determined.

Table S8.

Hallmark gene set	Size	ES	NES	NOM. p-value	FDR q-value	FWER p-value	Rank at Max	Leading Edge
G2/M Checkpoint	41	0.23	1.73	0.014	0.159	0.194	1261	tags=85%, list=63%, signal=225%
Oxidative Phosphorylation	38	0.24	1.71	0.029	0.193	0.310	535	tags=50%, list=27%, signal=67%
MTORC1 Signaling	43	0.21	1.64	0.051	0.191	0.429	1399	tags=91%, list=70%, signal=293%
DNA Repair	27	0.25	1.52	0.062	0.252	0.620	623	tags=56%, list=31%, signal=79%
P53 Pathway	21	0.26	1.47	0.078	0.250	0.697	725	tags=62%, list=36%, signal=96%
IL2 STAT5 Signaling	22	0.25	1.40	0.099	0.286	0.803	1150	tags=82%, list=57%, signal=190%
Xenobiotic Metabolism	15	0.30	1.37	0.126	0.273	0.832	1283	tags=93%, list=64%, signal=257%
E2F Targets	36	0.18	1.26	0.196	0.372	0.951	1378	tags=86%, list=69%, signal=270%
Protein Secretion	15	0.26	1.21	0.218	0.395	0.975	1218	tags=87%, list=61%, signal=219%
Fatty Acid Metabolism	18	0.22	1.12	0.304	0.481	0.993	459	tags=44%, list=23%, signal=57%
Unfolded Protein Response	18	0.19	0.97	0.482	0.700	1.000	1625	tags=100%, list=81%, signal=522%
Adipogenesis	28	0.14	0.87	0.629	0.820	1.000	1515	tags=89%, list=76%, signal=360%
Hypoxia	21	0.14	0.77	0.782	0.925	1.000	1442	tags=86%, list=72%, signal=302%
UV Response DN	17	0.14	0.70	0.863	0.967	1.000	1254	tags=76%, list=63%, signal=202%
Allograft Rejection	27	0.10	0.58	0.948	1.000	1.000	630	tags=41%, list=31%, signal=59%
Glycolysis	28	0.08	0.49	0.987	0.992	1.000	275	tags=21%, list=14%, signal=24%

Table S8 related to Figure 3C. List of hallmark gene sets determined in FOXO3^{null} CTNNB1^{null} PF382 cells, doubly transduced with *β*-Catenin(ΔGSK) and FOXO3(TM) with respect to other cell conditions by Gene Set Enrichment Analysis (GSEA) of RNA-Seq data. ES, enrichment score; NES, normalized enrichment score; NOM, nominal p-value; FDR, false discovery rate q-value; FWER, family-wise error rate p-value.

Table S9.

Marker	Ab Clone	BD Code
CD10	HI10A	940045
CD103	BER-ACT8	940067
CD110	1.6.1	940302
CD117 (c-KIT)	104D2	940250
CD123 (IL-3RA)	TG3	940020
CD127 (IL-7R)	HIL-7R-M21	940012
CD13	WM15	940044
CD132 (IL2RG)	TUGh4	940230
CD14	MPHIP9	940005
CD154 (CD40L)	TRAP1	940053
CD183 (CXCR3)	1C6/CXCR3	940030
CD184 (CXCR4)	12G5	940056
CD185 (CXCR5)	RF8B2	940042
CD194 (CCR4)	1G1	940047
CD197 (CCR7)	L1-A	940394
CD1a	HI149	940063
CD2	RPA-2.10	940046
CD25 (IL-2R)	2A3	940009
CD278 (ICOS)	DX29	940043
CD279 PD1	EH12.1	940015
CD3	UCHT1	940307
CD33	P67.6	940255
CD34	581	940021
CD366 (TIM-3)	7D3	940066
CD371	50C1	940212
CD38	HIT2	940013
CD4	RPA-T4	940304
CD43	1G10	940278
CD44	515	940364
CD45	HI30	940002
CD45RA	HI100	940011
CD47 (IAP)	B6H12	940082
CD5	UCHT2	940038
CD54 (ICAM1)	HA58	940072
CD56	NCAM16.2	940007
CD69	FN50	940019
CD7	M-T701	940029
CD8	RPA-T8	940003
CD99	TU12	940214
HLA-DR	G46.6	940010
TCRαβ	IP26	940074
TCRγδ	B1	940057

Table S9. Panel of cell surface markers, recognized by the oligo-conjugated antibodies in the Abseq assay.

Table S10.

	CSS15501	CSS13693	CSS20705	M71-10 (PDX)	H3255-1 (PDX)
Gender	M	M	F		M
Age at diagnosis (years)	30	36	55	<18	26
NOTCH1 (exons 26-27-34)	wt	TAD mut	TAD mut	HD mut	PEST mut
FBXW7 (exons 9-12)	wt	mut	wt	wt	mut
PTEN (exon 7)	wt	wt	wt	wt	wt
P53 (exons 4-5)	wt	wt	wt	wt	wt
IL7R (exon 6)	mut	wt	wt	nd	nd
Year of diagnosis	2019	2020	2020		
WBC/mm^3 at diagnosis	3,800	65,000	64,000		
EGIL score	5	5	5		
ETP immunophenotype	no	no	yes		
MRD at day 30	1.78%	2.64%	4.17%		
Therapy	prot GIMEMA LAL1913	prot GIMEMA LAL1913	prot GIMEMA LAL1913		
vital status	alive	alive	alive		
Year of last follow-up	2022	2022	2022		
Karyotype		46,XY	46,XX,del(12)(q24::qter)[9]		

Table S10. Demographic, clinical and genetic features of considered T-ALL patients and patient-derived xenografts (PDXs).
Early T-cell (ETP) phenotype was assessed according to Coustan-Smith E. et al.[22] The percentage of minimal residual disease (MRD) in the bone marrow at day 30 was determined by flow cytometry according to Basso G. et al.[23] Mutations on the exons of indicated genes were determined as previously reported[24-28]. The characteristics of patient-derived xenografts (PDXs) were previously reported in Yost A. et al.[29] TAD, Transactivation domain; HD, Heterodimerization domain; nd, not determined.

Table S11.

A

	$CD117^{high}$ $CD82^{low}$	Other
ETP-ALL	3	16
Other	39	207

p-value >0.999

	$CD117^{low}$ $CD82^{high}$	Other
ETP-ALL	4	14
Other	40	194

p-value = 0.643

B

	$CD117^{high}$ $CD82^{low}$	Other
Pre-cortical	5	35
Other	37	175

p-value = 0.529

	$CD117^{low}$ $CD82^{high}$	Other
Pre-cortical	11	29
Other	33	179

p-value = 0.109

Table S11. Correlation between CD117/CD82 subgroups and ETP-ALL (A) and pre-cortical stage (B) among 252 T-ALL patients.
Statistical p-values were calculated by the Fisher's exact test, corrected for multiple comparisons by false discovery rate (FDR) using a two-stage linear step-up procedure of Benjamini, Krieger and Yekutieli.

Table S12. related to Figure 1. List of interacting proteins of *β*-Catenin as determined by liquid-chromatography mass spectrometry (LC/MS^2)

Table S13. related to Figure 3B. Normalized (rLog) data for for mRNA expression of $FOXO3^{null}$ $CTNNB1^{null}$ PF382 cells, transduced with an active FOXO3 triple mutant (FOXO3_TM) alone or in combination with a stable isoform of *β*-Catenin (ΔGSK).

Table S14. related to Figure 5F. List of differentially expressed and co-bound genes by both FOXO3 /βCatenin in PF382 cell line.

Supplementary Figures

Fig. S1.

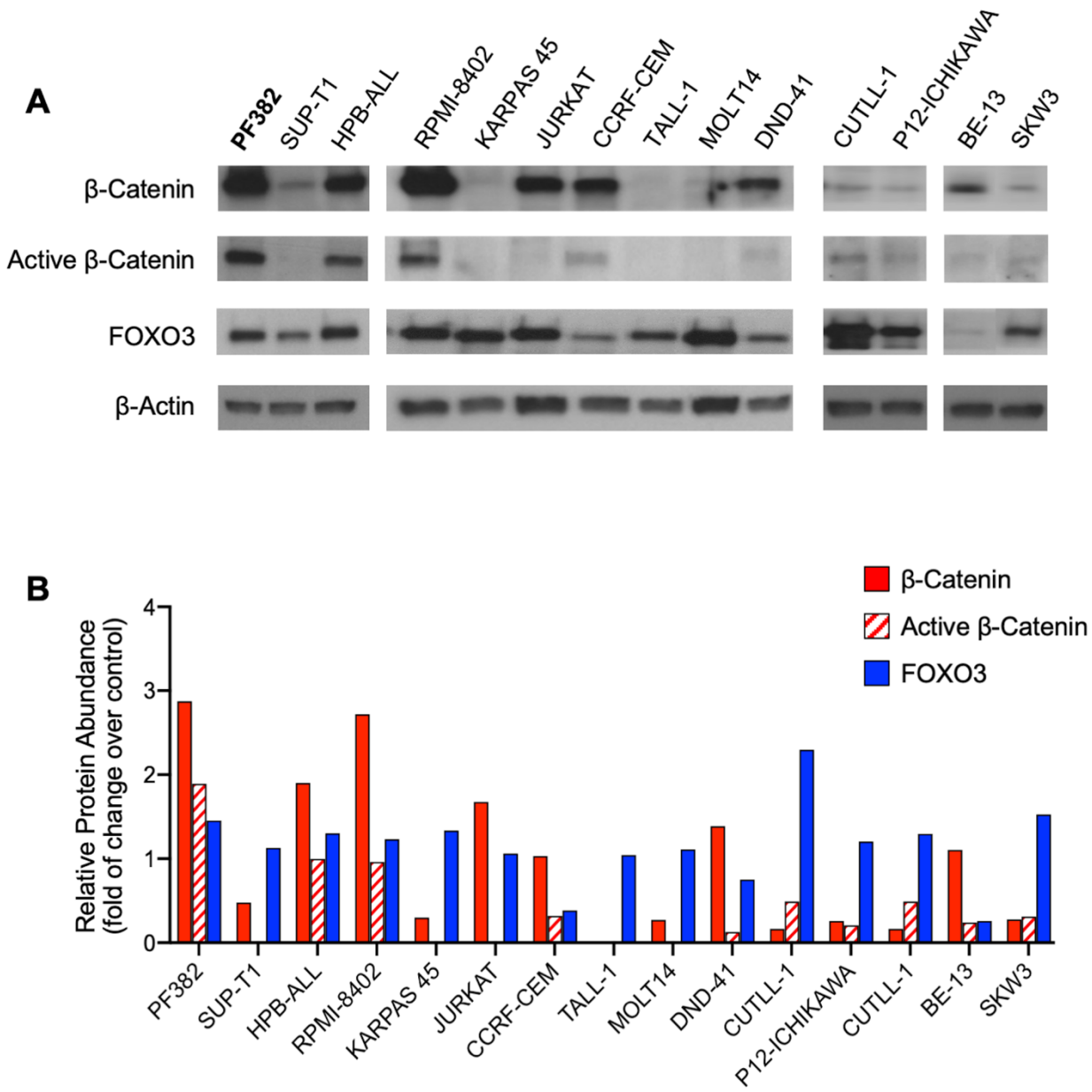

Figure S1. Active *β*-Catenin and FOXO3 proteins are highly expressed in PF382, HPB-ALL and RPMI-8402 T-ALL cell lines.
(**A**) Western blot analysis of total *β*-Catenin, non-phospho (active) *β*-Catenin and FOXO3 in human T-ALL cell lines.
(**B**) Densitometric analysis for quantification of Western blot signals. The numbers in vertical axis indicate relative band intensities after normalization to the β-Actin loading control.

Fig. S2

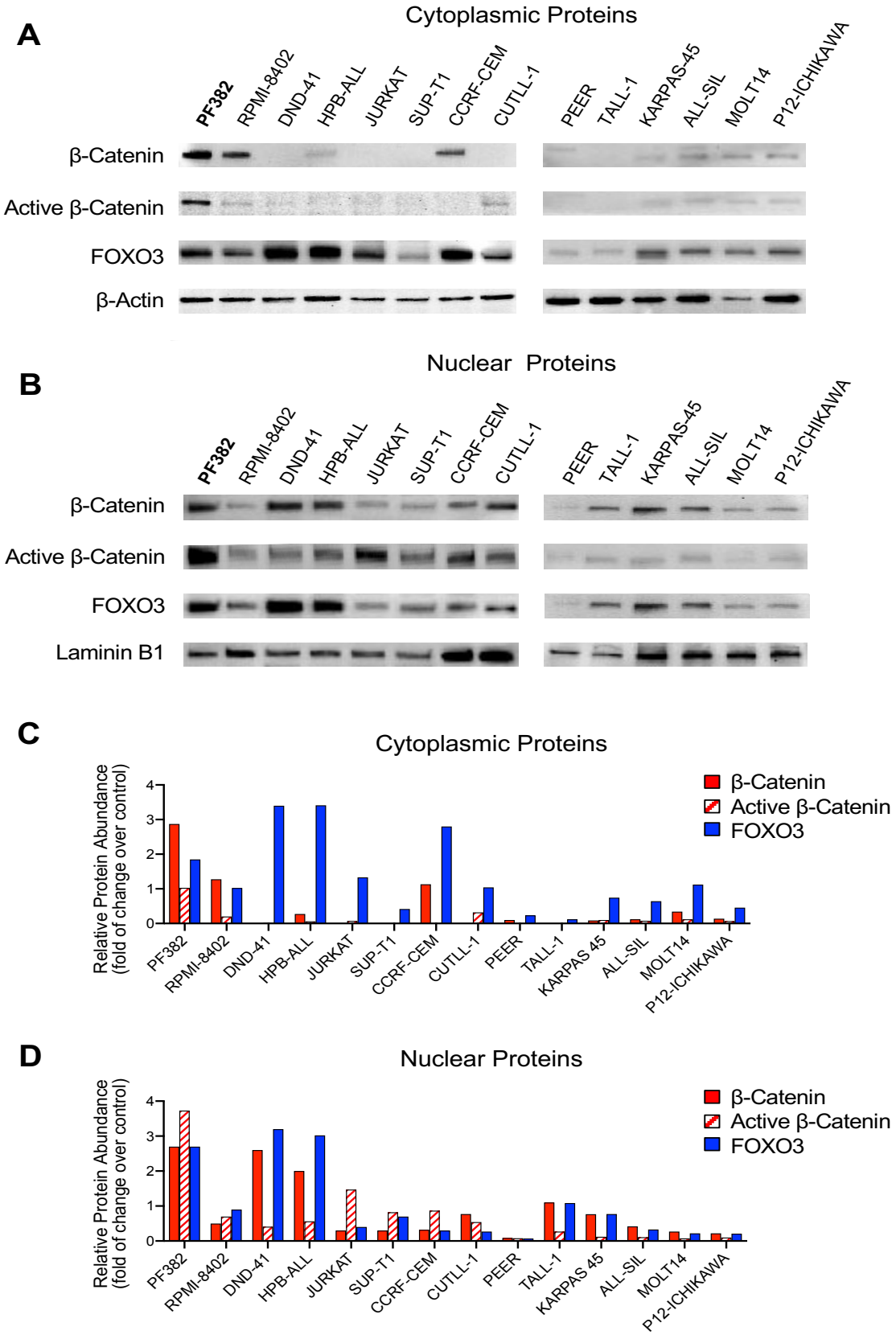
A
Cytoplasmic Proteins
PF382
RPMI-8402
DND-41
HPB-ALL
JURKAT
SUP-T1
CCRF-CEM
CUTLL-1
PEER
TALL-1
KARPAS-45
ALL-SIL
MOLT14
P12-ICHIKAWA
β-Catenin
Active β-Catenin
FOXO3
β-Actin
B
Nuclear Proteins
β-Catenin
Active β-Catenin
FOXO3
Laminin B1
C
Cytoplasmic Proteins
Relative Protein Abundance (fold of change over control)
β-Catenin
Active β-Catenin
FOXO3
D
Nuclear Proteins

Figure S2. Expression of total *β*-Catenin, non-phospho (active) *β*-Catenin and FOXO3 proteins in the cytoplasmic and nuclear fractions, separated from human T-ALL cell lines.
(**A-B**) Western blot analysis of total *β*-Catenin, non-phospho (active) *β*-Catenin and FOXO3 in the cytoplasmic (A) and nuclear (B) fractions, separated from fourteen human T-ALL cell lines.
(**C-D**) Densitometric analysis for quantification of Western blot signals. The numbers in vertical axis indicate relative band intensities after normalization to the *β*-Actin loading control for the cytoplasmic proteins (C) and Lamini B1 for the nuclear fraction (D).

Fig. S3.

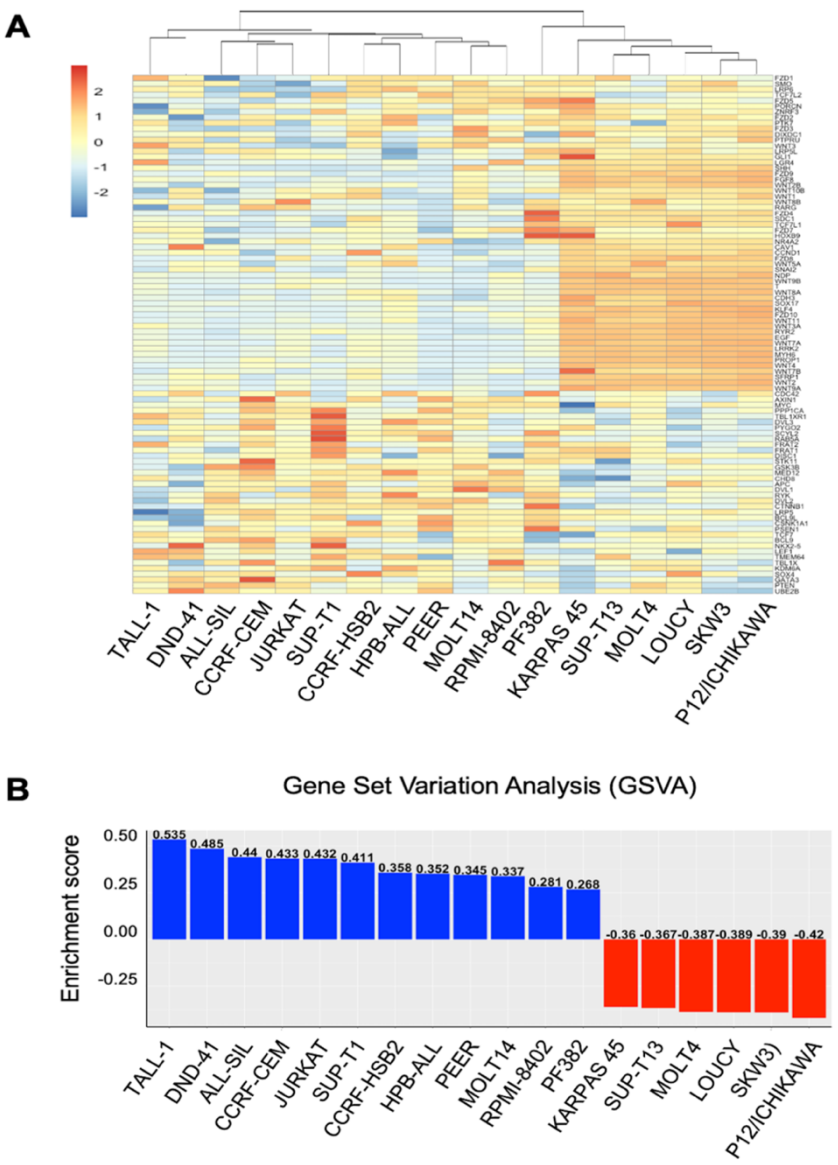

Figure S3. Variations of the Wnt/*β*-Catenin pathway activity in established human T-ALL cell lines by gene set variation analysis (GSVA).

(**A**) Hierarchical clustering and mRNA expression heatmap of canonical Wnt/*β*-Catenin signaling pathway genes (GO0060070) in 18 T-ALL cell lines. Rlog values were calculated from RNA-seq data using DESeq2. Heatmap is scaled by gene (=row) with mean=0 and SD=1. Data are reanalyzed from EGA accession EGAD00001008493.

(B) The GSVA enrichment score of reported T-ALL cell across the genes (GO0060070), using a non-parametric and unsupervised approach. The bar above zero (blue color) represent cells lines with gene enrichment.

Fig. S4.

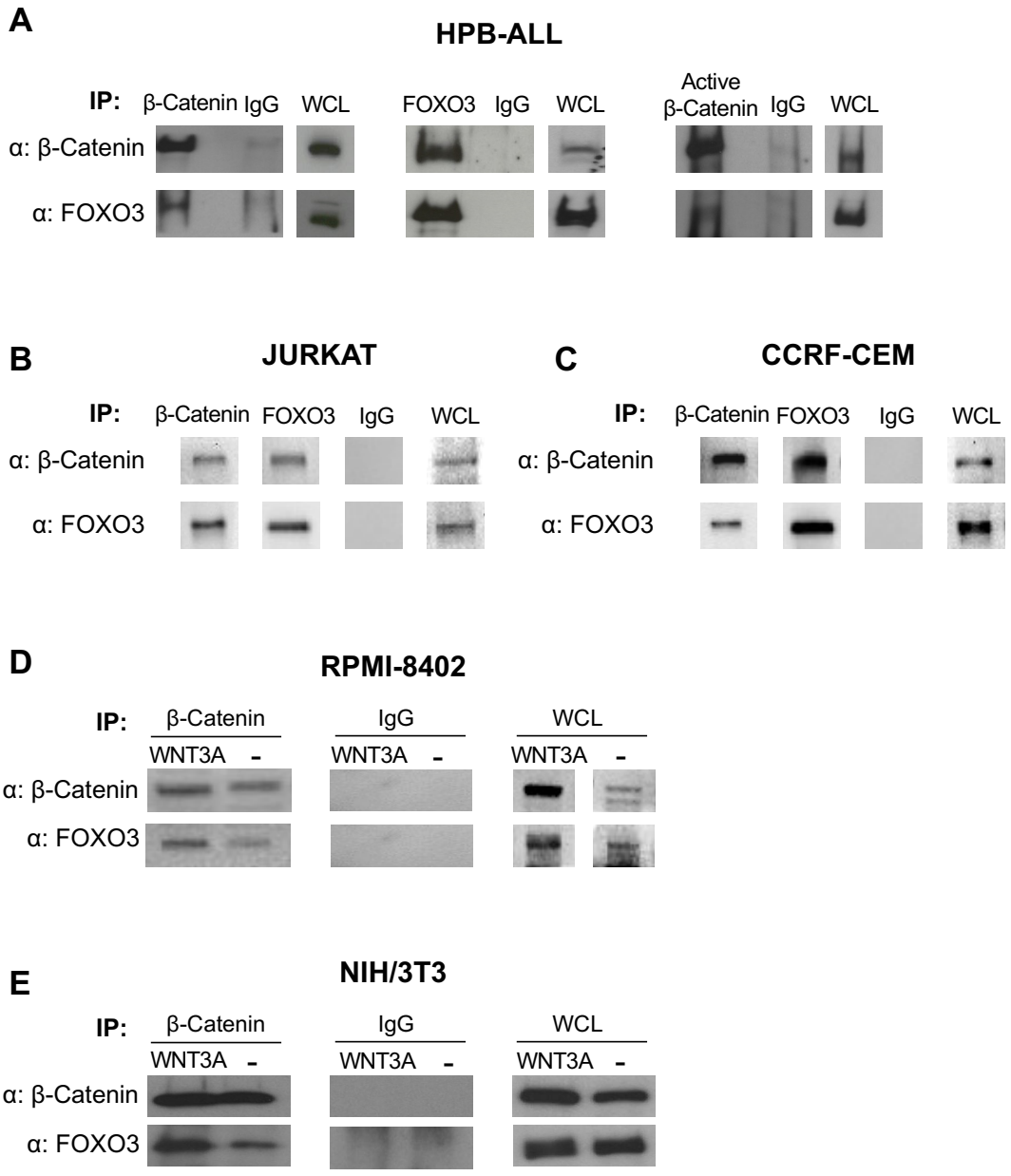

Figure S4. Binding of *β*-Catenin to FOXO3 transcription factor in human cell lines.
(**A-C**) Co-Immunoprecipitation (Co-IP) between β-Catenin, non-phospho (active) β-Catenin and FOXO3 in HPB-ALL cell line (**A**) as well as between β-Catenin and FOXO3 in JURKAT (**B**) and CCRF-CEM (**C**) cell lines, followed by immunoblot analysis using the indicated antibodies.
(**D-E**) Co-Immunoprecipitation (co-IP) between β-Catenin and FOXO3 in RPMI-8402 (**D**) and NIH/3T3 (**E**) cell lines after in vitro growth into L-Wnt3A-conditioned medium or control conditioned medium for 48 and 24 hours respectively. Protein lysate were immunoprecipitated with indicated antibodies followed by immunoblot analysis.

Fig. S5.

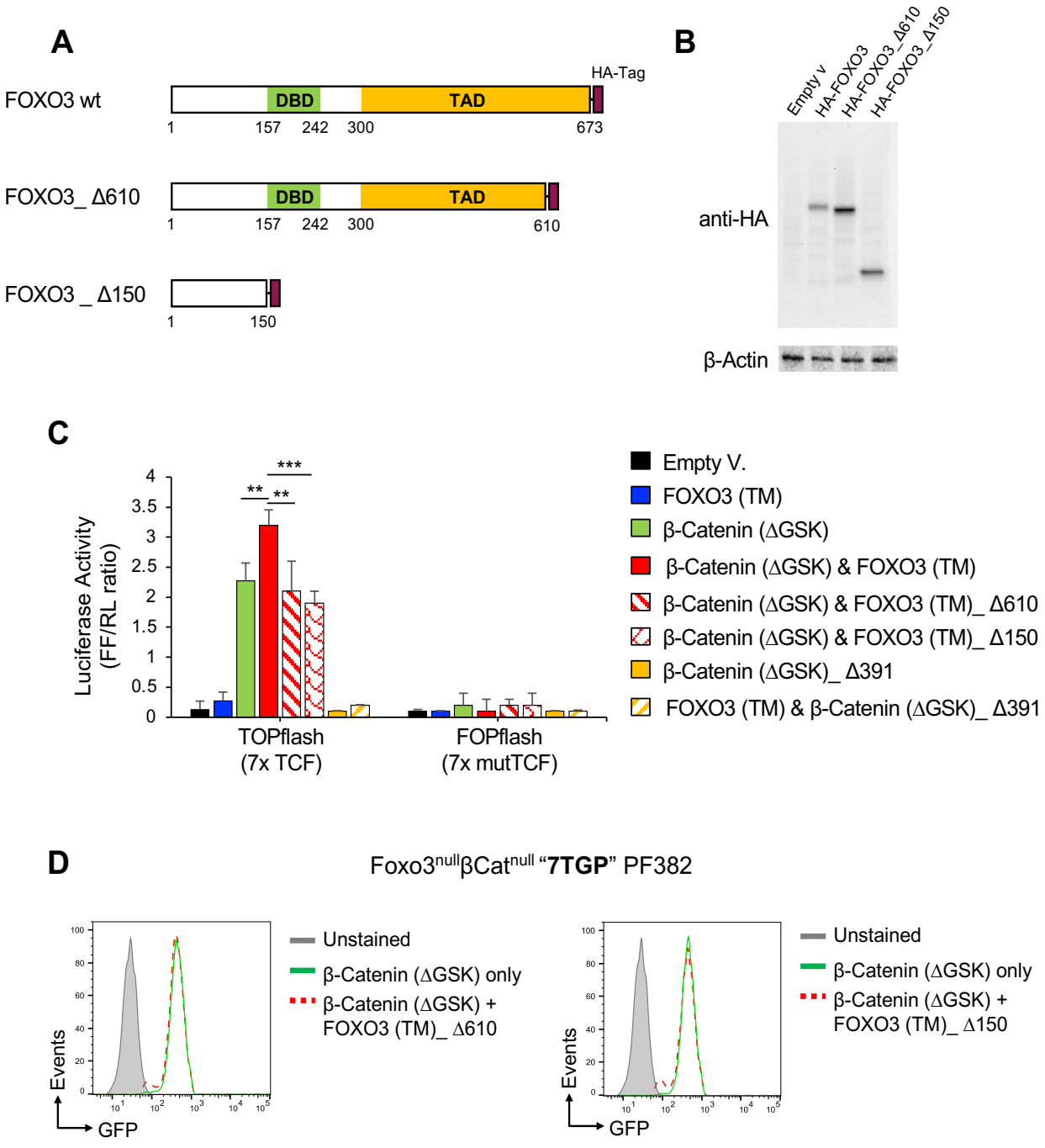
A
FOXO3 wt
HA-Tag
DBD
TAD
1
157
242
300
673
FOXO3_ Δ610
610
FOXO3 _ Δ150
150
B
Empty v
HA-FOXO3
HA-FOXO3_Δ610
HA-FOXO3_Δ150
anti-HA
β-Actin
C
Luciferase Activity
(FF/RL ratio)
TOPflash
(7x TCF)
FOPflash
(7x mutTCF)
Empty V.
FOXO3 (TM)
β-Catenin (ΔGSK)
β-Catenin (ΔGSK) & FOXO3 (TM)
β-Catenin (ΔGSK) & FOXO3 (TM)_ Δ610
β-Catenin (ΔGSK) & FOXO3 (TM)_ Δ150
β-Catenin (ΔGSK)_ Δ391
FOXO3 (TM) & β-Catenin (ΔGSK)_ Δ391
D
Foxo3nullβCatnull "7TGP" PF382
Events
GFP
Unstained
β-Catenin (ΔGSK) only
β-Catenin (ΔGSK) +
FOXO3 (TM)_ Δ610
β-Catenin (ΔGSK) +
FOXO3 (TM)_ Δ150

Figure S5. The synergistic activity of FOXO3 on TCF/*β*-Catenin reporter is compromised by the Δ610 and Δ150 deletions.

(**A**) Schematic map of Δ610 and Δ150 deletion mutants and wild type FOXO3 protein. The Δ610 deletion affects the activity of transactivation domain (TAD) by removing phosphoserines involved in the physical interaction with AMP-activated protein kinase (AMPK)[30] and IkappaB kinase (IKK)[31]. Each of the different human FOXO3 isoforms was expressed using a pRRL-based lentivector with mouse CD8 (mCD8) marker and subcloned with the hemagglutinin (HA) epitope tag at C-terminal domain.

(**B**) Western blot analysis of Δ610 and Δ150 mutant isoforms and wild type FOXO3 in HEK/293T cell line following transduction with the indicated lentivectors or empty vector as negative control.

(**C**) The TCF/*β*-Catenin transcriptional activity was evaluated by the TOPFlash luciferase and FOPFlash reporter in FOXO3^{null} CTNNB1^{null} PF382 cells (Fig. 3), co-transfected with the wild type stable isoform of *β*-Catenin (ΔGSK) alone or in combination with the active FOXO3 triple mutant (FOXO3_TM) wild type or deletion mutant isoforms as indicated. Data were normalized to the Renilla luciferase reporter vector and given as mean and SD. The graphs report the result of three independent experiments performed in triplicate. *** $p<0.01$, *** $p<0.001$, by the Student's t-test.*

(**D**) Flow cytometric analysis of GFP+ cell abundance in FOXO3^{null} CTNNB1^{null} PF382 cell line, transduced with TCF/*β*-Catenin (7TGP) reporter[4]. After puromycin selection *in vitro*, the FOXO3^{null} CTNNB1^{null} PF382 cell lines were transduced with *β*-Catenin (ΔGSK) alone or in combination with the mutant of FOXO3_TM as indicated. Cells transduced with empty vector were also analyzed as control.

Fig. S6.

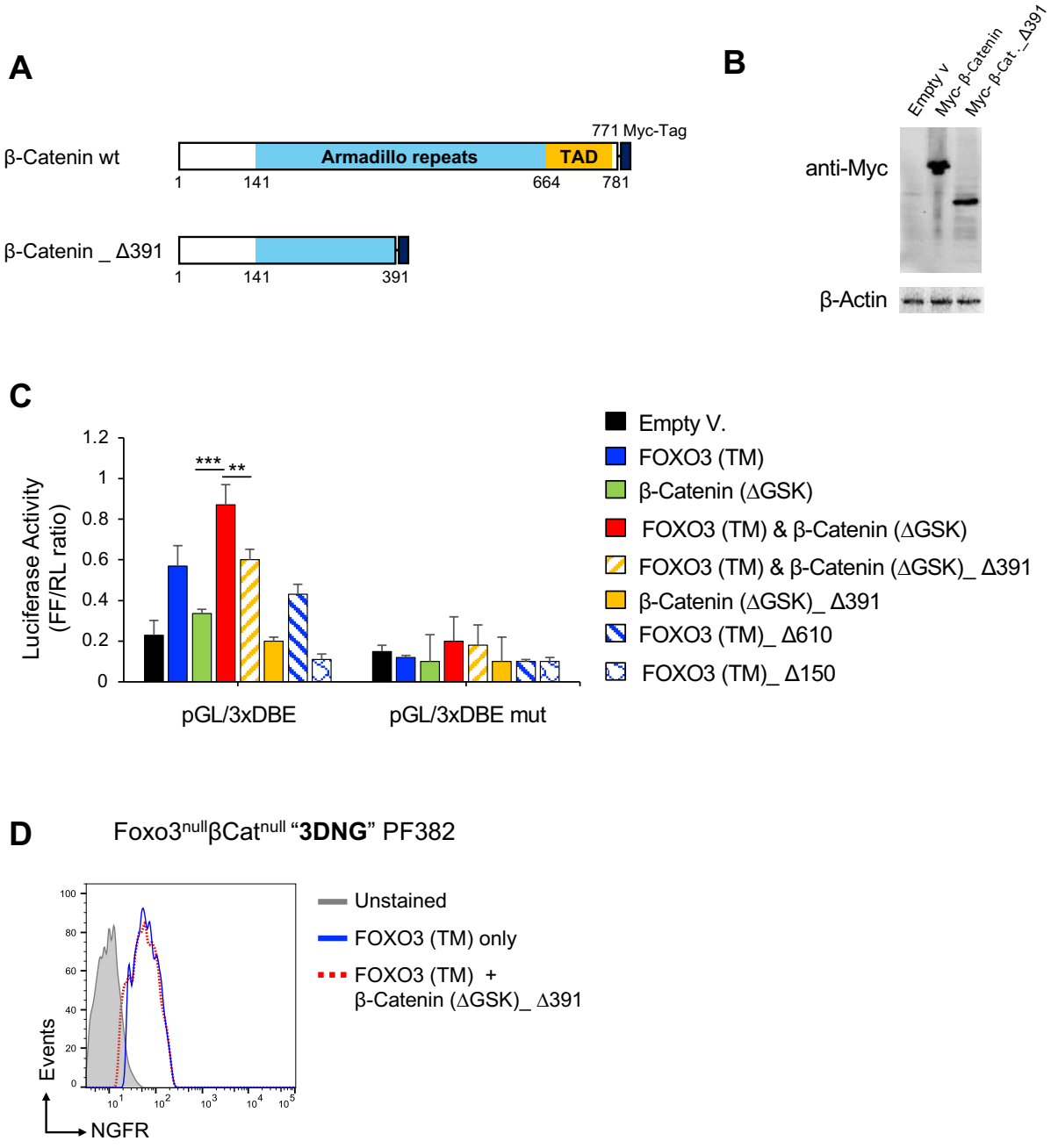
A
β-Catenin wt
771 Myc-Tag
Armadillo repeats
TAD
1
141
664
781
β-Catenin _ Δ391
1
141
391
B
Empty v
Myc-β-Catenin
Myc-β-Cat._Δ391
anti-Myc
β-Actin
C
Luciferase Activity (FF/RL ratio)
1.2
1
0.8
0.6
0.4
0.2
0
***
**
pGL/3xDBE
pGL/3xDBE mut
Empty V.
FOXO3 (TM)
β-Catenin (ΔGSK)
FOXO3 (TM) & β-Catenin (ΔGSK)
FOXO3 (TM) & β-Catenin (ΔGSK)_ Δ391
β-Catenin (ΔGSK)_ Δ391
FOXO3 (TM)_ Δ610
FOXO3 (TM)_ Δ150
D
Foxo3nullβCatnull "3DNG" PF382
Events
NGFR
Unstained
FOXO3 (TM) only
FOXO3 (TM) + β-Catenin (ΔGSK)_ Δ391

Figure S6. The synergistic activity of *β*-Catenin on FOXO reporter is impaired by the Δ391 deletion.

(**A**) Schematic map of wild type *β*-Catenin protein and Δ391 deletion mutant, which fully removes the protein transactivation domain (TAD) and part of Armadillo repeats. Both *β*-Catenin isoforms were expressed using a pRRL-based lentivector with mCherry marker and subcloned with the Myc epitope tag at C-terminal domain.

(**B**) Western blot analysis of Δ391 mutant isoform and wild type *β*-Catenin in HEK/293T cell line following transduction with the indicated lentivectors or empty vector as negative control.

(**C**) The FOXO transcriptional activity was evaluated by the pGL-3xDBE luciferase and the pGL-3xDBE mutant reporter as control in FOXO3^{null} CTNNB1^{null} PF382 cells (Fig. 3), co-transfected with the wild type active FOXO3 triple mutant (FOXO3_TM) alone or in combination with the stable isoform of *β*-Catenin (ΔGSK) wild type or deletion mutant as indicated. Data were normalized to the Renilla luciferase reporter vector and given as mean and SD. The graphs report the results of three independent experiments performed in triplicate. *** $p<0.01$, *** $p<0.001$, by the Student's t-test.*

(**D**) Flow cytometric analysis of NGFR+ cell abundance in FOXO3^{null} CTNNB1^{null} PF382 cell line, transduced with FOXO "3DNG" reporter. The FOXO3^{null} CTNNB1^{null} PF382 cell lines were also transduced with FOXO3_TM alone or in combination with the mutant of *β*-Catenin (ΔGSK) as indicated. Cells transduced with empty vector were also analyzed as control.

Fig. S7.

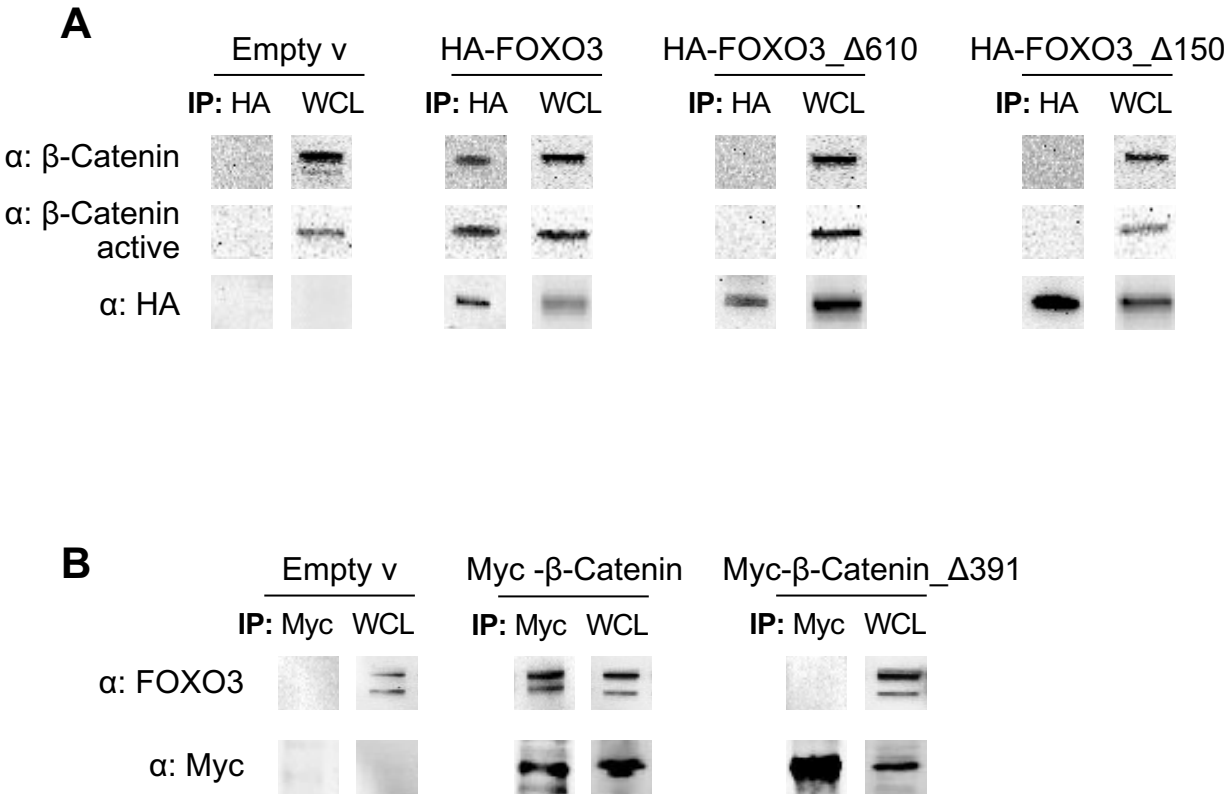

Figure S7. Deletion mutants of FOXO3 and *β*-Catenin proteins negatively affect their physical interactions.
(**A**) Co-Immunoprecipitation (Co-IP) between endogenous *β*-Catenin, non-phospho (active) *β*-Catenin and HA-tagged FOXO3 isoforms in HEK/293T cells, after transduction with the wild type or deletion mutants of active FOXO3 triple mutant (FOXO3_TM). Protein lysates were immunoprecipitated with indicated antibodies followed by immunoblot analysis.

(**B**) Co-Immunoprecipitation (Co-IP) between endogenous FOXO3 and Myc-tagged *β*-Catenin isoforms in HEK/293T cells, after transduction with the wild type or deletion mutant of the stable isoform of *β*-Catenin (ΔGSK). Protein lysates were immunoprecipitated with indicated antibodies followed by immunoblot analysis.

Fig. S8.

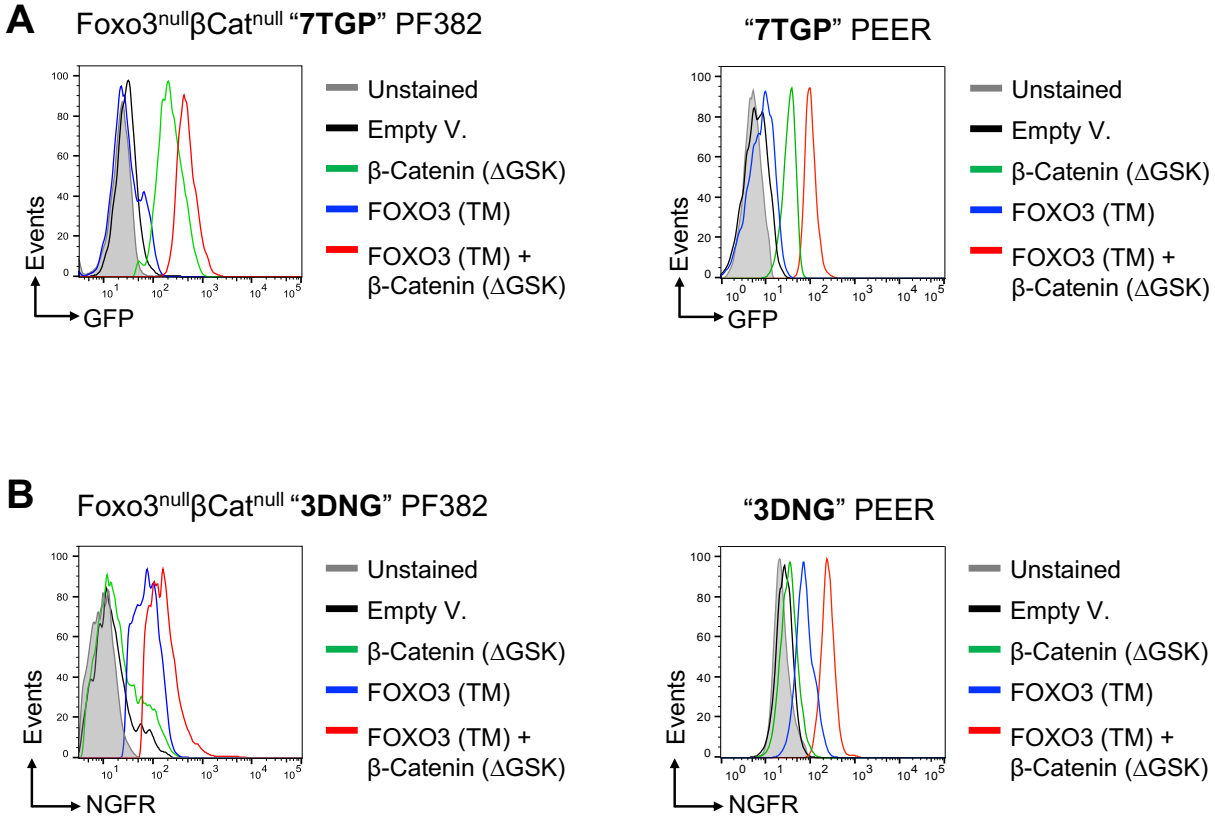

Figure S8. β-Catenin and FOXO together modulate the transcriptional activity in FOXO3^{null}CTNNB1^{null} PF382 and wild type PEER cell lines.
(**A**) Flow cytometric analysis of GFP+ cell abundance in FOXO3^{null} CTNNB1^{null} PF382 and wild type PEER cell lines, transduced with TCF/*β*-Catenin (7TGP) reporter[4]. After puromycin selection *in vitro*, both cell lines were transduced with the stable isoform of *β*-Catenin (ΔGSK) alone or in combination with the active FOXO3 triple mutant (FOXO3_TM) as indicated. GFP+ alive cells were measured after three days of *in vitro* growth by flow cytometry. Cells transduced with empty vector were also analyzed as control.

(**B**) Flow cytometric analysis of NGFR+ cell abundance in FOXO3^{null} CTNNB1^{null} PF382 and wild type PEER cells, transduced with FOXO "3DNG" reporter. Both cell lines were also transduced with FOXO3_TM alone or in combination with *β*-Catenin (ΔGSK) as indicated. NGFR+ alive cells were measured after three days of *in vitro* growth by flow cytometry. Cells transduced with empty vector were also analyzed as control.

Fig. S9.

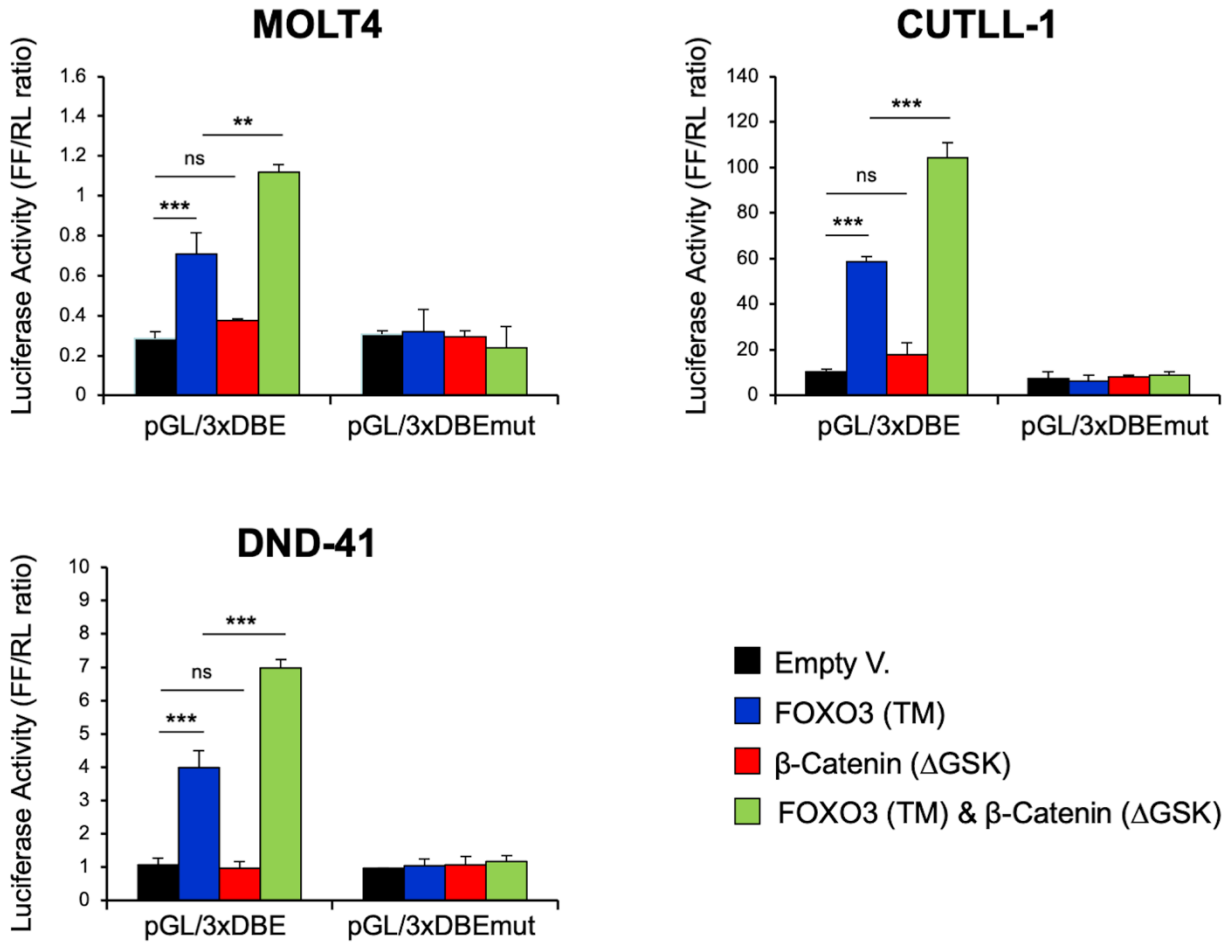

Figure S9. *β*-Catenin enhances the FOXO transcriptional activity in T-ALL cell lines. FOXO3 transcriptional activity was evaluated using the reporter pGL-3xDBE-luciferase, which contains three canonical DAF-16 binding elements (DBE) for FOXO binding. A reporter with three mutated DBEs (DBEmut) was used as control. In the MOLT-4, DND-41 and CUTLL1 cell lines, the luciferase FOXO reporter construct or control was co-transfected with an active FOXO3 triple mutant (FOXO3_TM) alone or in combination with a stable isoform of *β*-Catenin (ΔGSK) and Renilla luciferase. Data were normalized to the Renilla luciferase reporter vector and given as mean and SD. The graphs report the result of three independent experiments performed in triplicate. * $p<0.05$, ** $p<0.01$, *** $p<0.001$, by the Student's t-test.

Fig. S10.

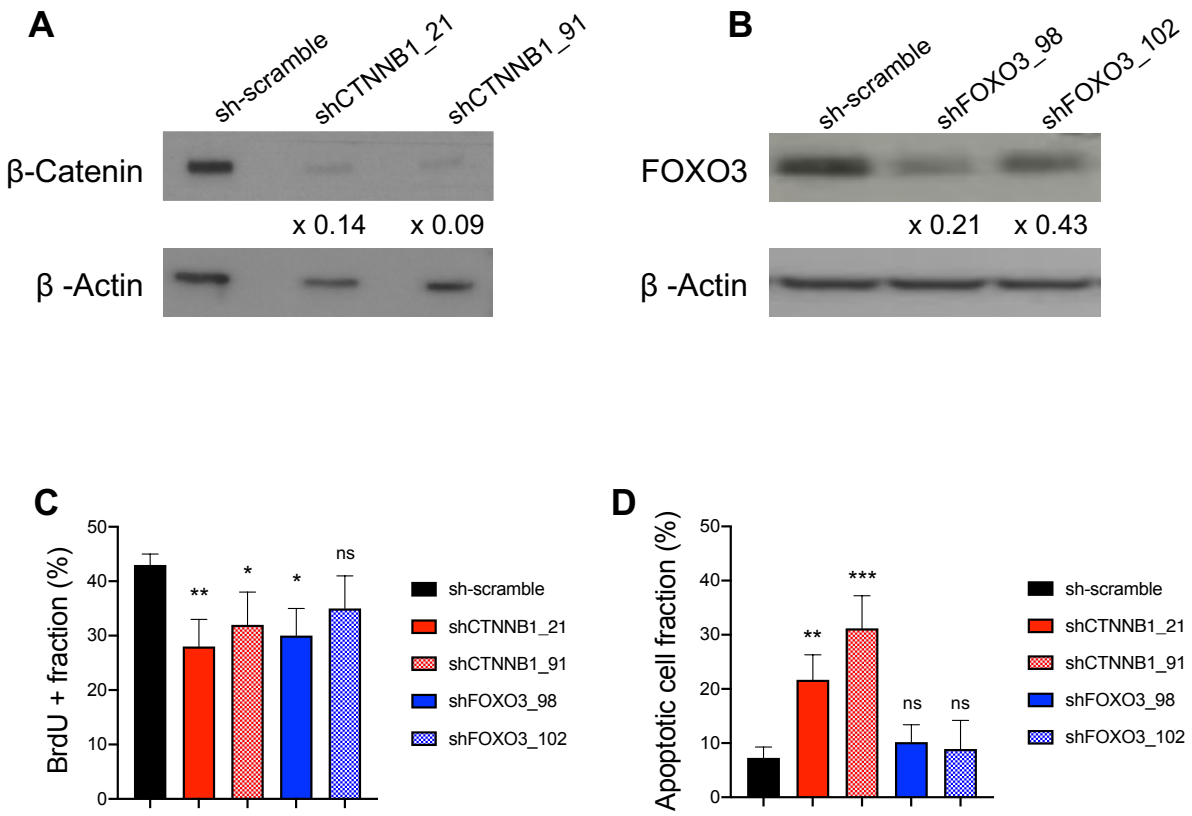

Figure S10. Expression level of *β*-Catenin and FOXO3 proteins, cell proliferation and apoptotic level in PF382 cells, transduced with shScramble, shCTNNB1 or shFOXO3 lentivectors.

(**A**) Western blot analyses of total *β*-Catenin (**A**) and FOXO3 (**B**) protein levels in the human T-ALL cell line PF382 following knock-down of *β*-Catenin or FOXO3 by transduction with lentiviral shRNAs or scrambled negative control (shScr). Numbers below each panel indicate fold change after normalization to β-Actin loading control.

(**B**) Flow cytometric analysis of cell proliferation by BrdU incorporation in PF382 cells, following transduction with shCTNNB1 and shFOXO3 constructs or scramble control as indicated. BrdU+ cells were measured after two days of *in vitro* growth by flow cytometry. The graphs report the result of two independent experiments performed in triplicate. Each reported statistical value is compared with scramble control. * *p<0.05,* ** *p<0.01, ns, not significant (Student's t test).*

(**C**) Flow cytometric analysis of apoptotic level by AnnexinV binding and 7AAD exclusion in PF382 cells after transduction with shCTNNB1 and shFOXO3 constructs or scramble control as indicated. AnnezinV+ 7AAD- cells were measured after two days of *in vitro* growth by flow cytometry. The graphs report the result of two independent experiments performed in triplicate. Each reported statistical value is compared with scramble control. ** *p<0.01,* *** *p<0.001, ns, not significant (Student's t test).*

Fig. S11.

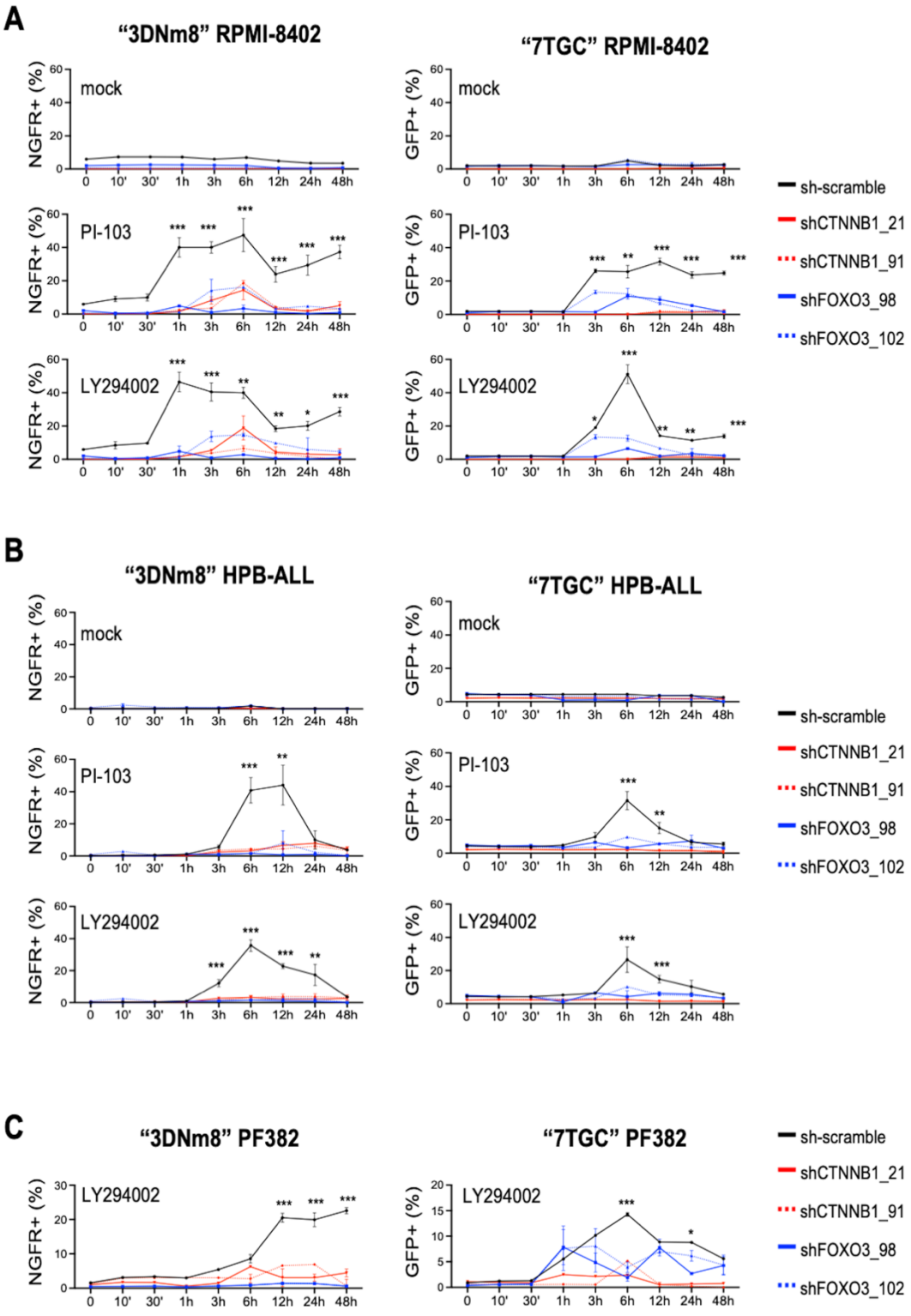
A
"3DNm8" RPMI-8402
"7TGC" RPMI-8402
mock
PI-103
LY294002
NGFR+ (%)
GFP+ (%)
0 10' 30' 1h 3h 6h 12h 24h 48h
sh-scramble
shCTNNB1_21
shCTNNB1_91
shFOXO3_98
shFOXO3_102
B
"3DNm8" HPB-ALL
"7TGC" HPB-ALL
C
"3DNm8" PF382
"7TGC" PF382

Figure S11. β-Catenin modulates the transcriptional activity of FOXO3 induced by inhibition of the PI3K/Akt pathway.

Flow cytometric analysis of abundance of NGFR+ and GFP+ cells in T-ALL cell lines transduced with FOXO or Wnt/β-Catenin lentiviral reporter, respectively. RPMI-8402 (**A**), HPB-ALL (**B**) and PF-382 (**C**) leukemia cells were doubly transduced with 3DNm8 & shRNA/GFP (**A**) or 7TGC & shRNA/NGFR lentiviral constructs. Transduced cells were FACS sorted and cultured *in vitro* with the PI3K inhibitors, PI-103 and LY294002 or mock control. NGFR+ or GFP+ alive cells were measured at the indicated time points by flow cytometry for DRAQ7 exclusion. The graphs report the result of three independent experiments performed in triplicate. **, p<0.05; **, p<0.01; ***, p<0.001 (Two-way ANOVA with Dunnett's test, comparing the sh-scramble control mean with the other values).*

Fig. S12.

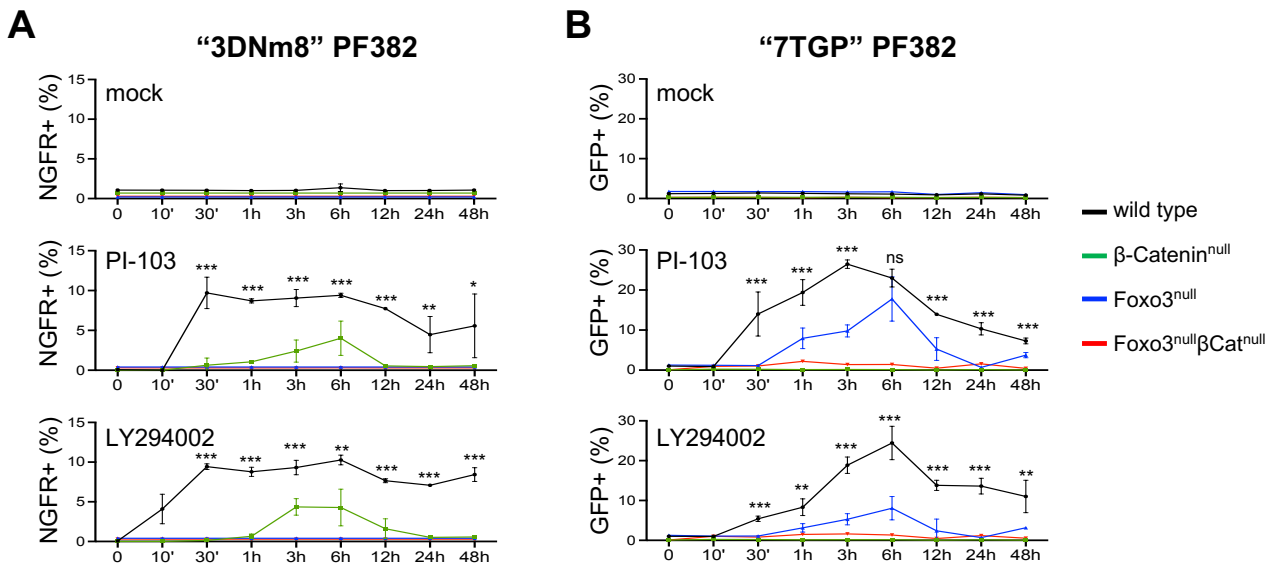

Figure S12. CRISPR/Cas9-mediated knockout of CTNNB1 gene impairs the transcriptional activity of FOXO3 induced by inhibition of the PI3K/Akt pathway.
Flow cytometric analysis of abundance of NGFR+ and GFP+ cells in PF382 cell line with inactivating DNA mutations in CTNNB1 and/or FOXO3 genes, as described in Figure 3, and subsequently transduced with 3DNm8 (**A**) or 7TGC (**B**) lentiviral constructs of FOXO and Wnt/*β*-Catenin activity, respectively. Transduced cells were cultured *in vitro* with the PI3K inhibitors, PI-103 and LY294002 or mock control. NGFR+ or GFP+ alive cells were measured at the indicated time points by flow cytometry for DRAQ7 exclusion. The graphs report the result of three independent experiments performed in triplicate. **, p<0.05; **, p<0.01; ***, p<0.001 (Two-way ANOVA with Dunnett's test, comparing the wild type control mean with the other values).*

Fig. S13.

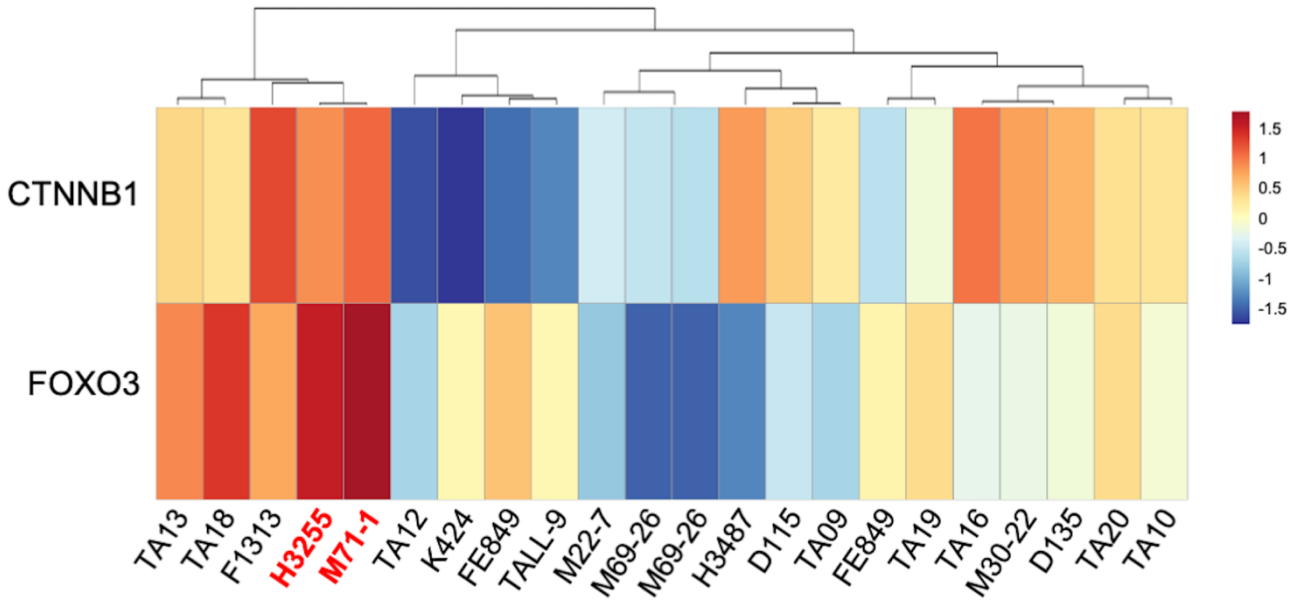

Figure S13. Heatmap and unsupervised hierarchical clustering of 22 PDX T-ALLs based on the transcriptional expression of CTNNB1 and FOXO3 genes.
The heatmap shows the correlation matrix between the different RNA-Seq samples based on the mRNA expression of CTNNB1 and FOXO3 genes in 22 PDX T-ALLs. Darker red color indicates stronger correlation. The PDX RNA-seq data are from the PRoXe repository (NCBI SRA Accession SRP103099). The patient-derived xenografts (PDX), transduced with 7TGC and 3DNm8 lentiviruses and transplanted at limiting dilution into new mice recipients (**Fig. 2E-F**) are highlighted in red.

Fig. S14.

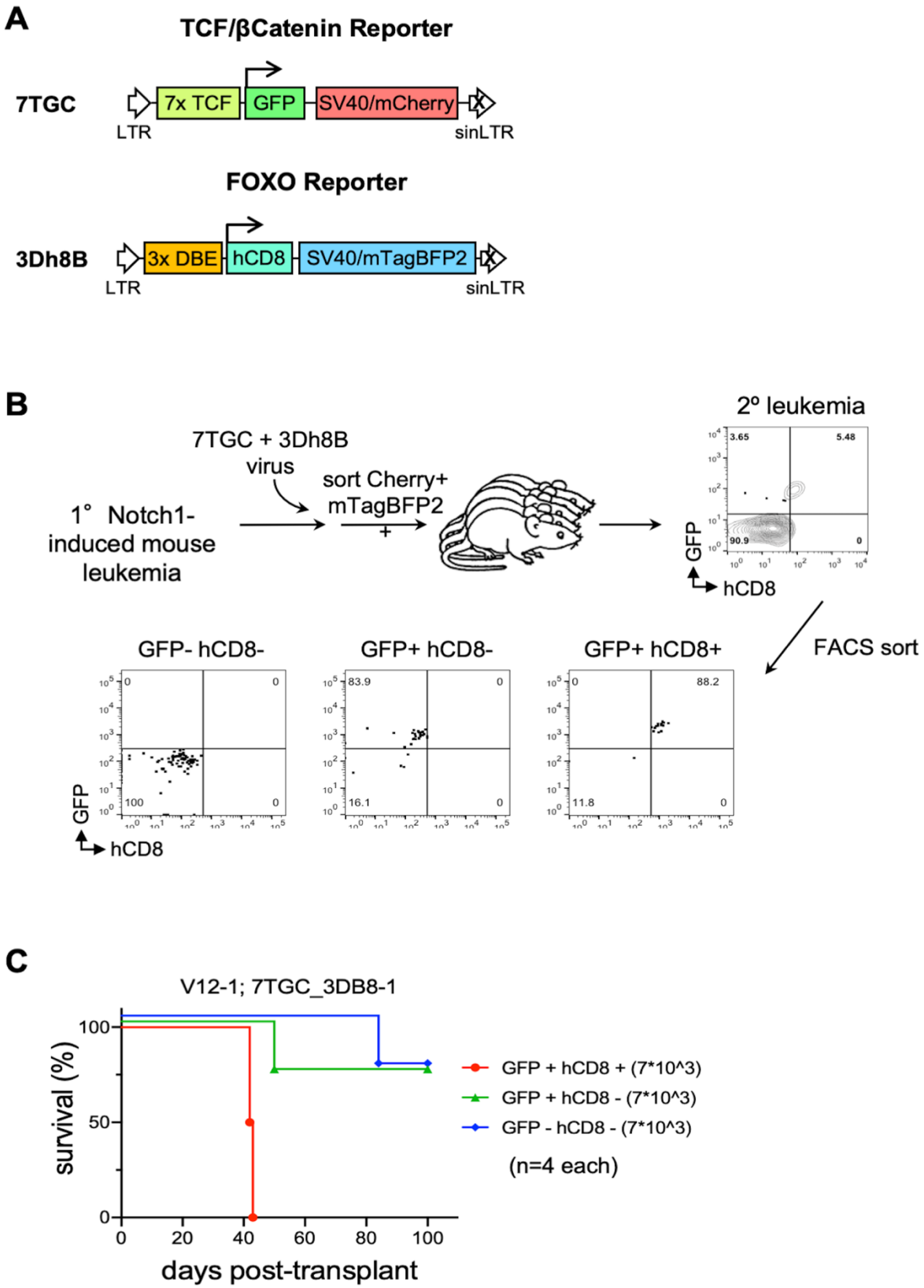
A
TCF/βCatenin Reporter
7TGC
7x TCF
GFP
SV40/mCherry
LTR
sinLTR
FOXO Reporter
3Dh8B
3x DBE
hCD8
SV40/mTagBFP2
LTR
sinLTR
B
1° Notch1-induced mouse leukemia
7TGC + 3Dh8B virus
sort Cherry+ mTagBFP2 +
2° leukemia
3.65
5.48
90.9
0
GFP
hCD8
FACS sort
GFP- hCD8-
GFP+ hCD8-
GFP+ hCD8+
0
0
100
0
83.9
0
16.1
0
0
88.2
11.8
0
GFP
hCD8
C
V12-1; 7TGC_3DB8-1
survival (%)
100
50
0
0
20
40
60
80
100
days post-transplant
GFP + hCD8 + (7*10^3)
GFP + hCD8 - (7*10^3)
GFP - hCD8 - (7*10^3)
(n=4 each)

Figure S14. Leukemia-initiating cell (LIC) activity is enriched within a small subpopulation of mouse Notch1-induced leukemia cells with active *β*-Catenin and FOXO signaling.
(A) Schematic map of the FOXO and TCF/*β*-Catenin reporters, used in primary cells of Notch1-induced mouse leukemia. The integrated FOXO lentiviral reporter (3Dh8B) is composed of 3 DBE elements upstream of a minimal promoter expressing a truncated human CD8 marker (hCD8), followed by a separate SV40 promoter expressing mTagBFP2. The integrated fluorescent TCF/*β*-Catenin lentiviral reporter (7TGC) is composed of 7 TCF/LEF-binding sites upstream of a minimal promoter and GFP, followed by a separate SV40-mCherry cassette.

(B) Schematic diagram of experimental approach. Cells of primary Notch1-induced mouse leukemia were transduced with 7TGC and 3Dh8B lentiviruses, FACS sorted for Cherry and mTagBFP2 expression and then transplanted into secondary recipient mice, all of which subsequently developed leukemia. These secondary 7TGC_3Dh8B-transduced leukemias were then analyzed by flow cytometry for GFP and hCD8 expression. GFP+hCD8+, GFP+hCD8-, GFP-hCD8+ and GFP−hCD8- subsets were then FACS sorted and transplanted into tertiary recipients.

(C) Survival of recipient mice after transplantation with FACS-sorted *β*-Catenin active (GFP+) and/or FOXO active (hCD8+) subsets from 7TGC_3Dh8B-transduced secondary leukemias. Each of the 4 recipient animals was injected with the cell doses as indicated in parentheses.

Fig. S15.

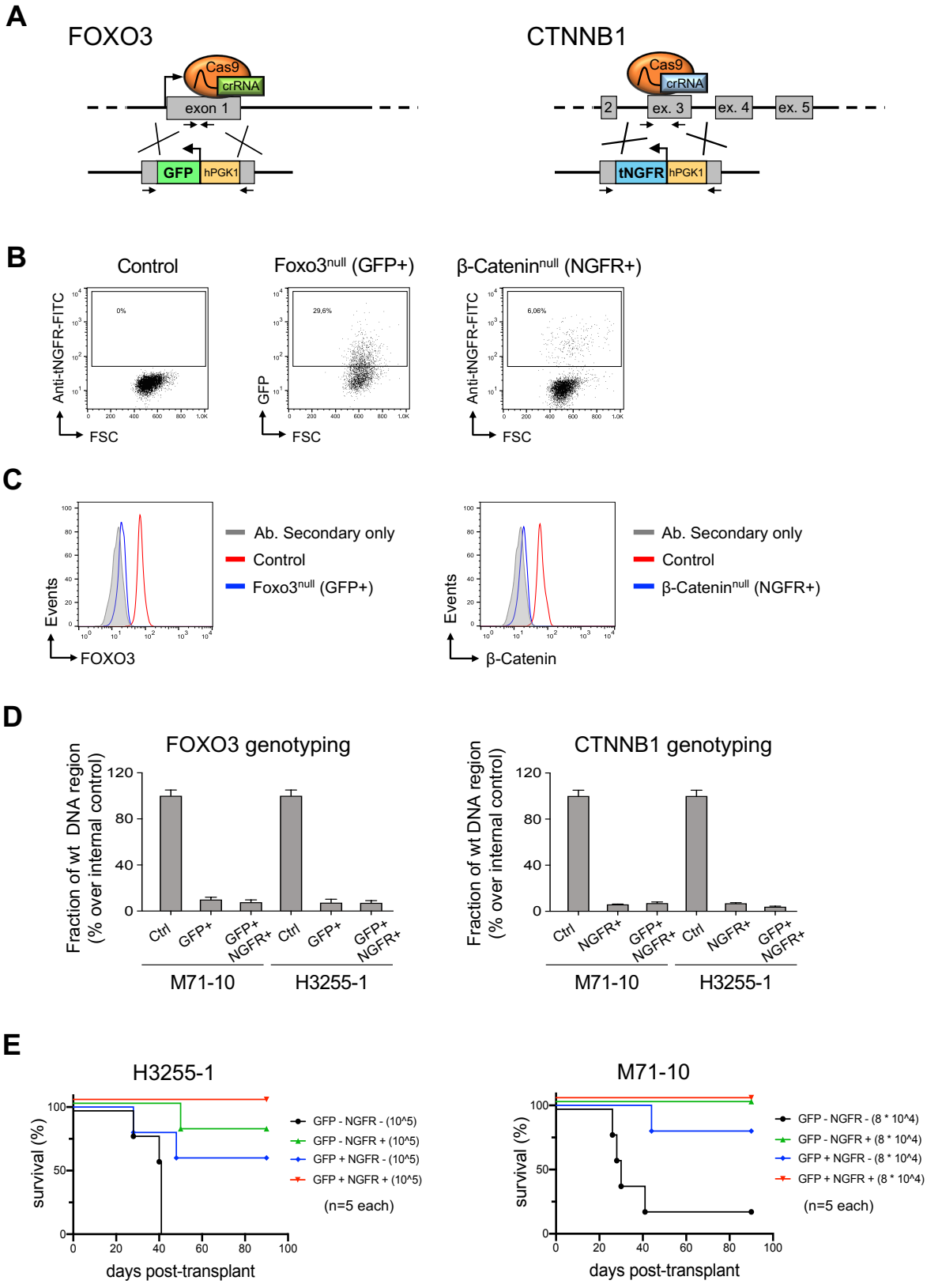
A
FOXO3
Cas9
crRNA
exon 1
GFP
hPGK1
CTNNB1
2
ex. 3
ex. 4
ex. 5
tNGFR
B
Control
Foxo3null (GFP+)
β-Catenin null (NGFR+)
Anti-tNGFR-FITC
GFP
FSC
C
Ab. Secondary only
Control
Foxo3null (GFP+)
β-Catenin null (NGFR+)
Events
FOXO3
β-Catenin
D
FOXO3 genotyping
CTNNB1 genotyping
Fraction of wt DNA region (% over internal control)
Ctrl
GFP+
GFP+ NGFR+
NGFR+
M71-10
H3255-1
E
H3255-1
M71-10
survival (%)
days post-transplant
GFP - NGFR - (10^5)
GFP - NGFR + (10^5)
GFP + NGFR - (10^5)
GFP + NGFR + (10^5)
(n=5 each)
GFP - NGFR - (8 * 10^4)
GFP - NGFR + (8 * 10^4)
GFP + NGFR - (8 * 10^4)
GFP + NGFR + (8 * 10^4)

Figure S15. CRISPR/Cas9-mediated deletion of both FOXO3 and CTNNB1 genes in PDX samples of T-ALL results in a marked decrease in LIC frequency.
(A) Schematic overview of experimental approach. A DNA fragment, including the GFP or truncated NGFR (tNGFR) marker gene under the constitutive hPGK-1 promoter and flanked with two homologous arms, was integrated into the exon 1 of FOXO3 human gene (chr6:108561762-108561829) and exon 3 of CTNNB1 human gene (chr3:41224526-41224753) by CRISPR/Cas9-mediated homologous recombination. The insertion of PGK1-GFP/tNGFR fragment resulted in the disruption of the exon and loss of gene expression. The primer pair used for the ddPCR-based genotyping of DNA insertion are indicated by small arrows.

(B) Flow cytometry plots of GFP or NGFR marker expression in H3255-1 PDX sample following the CRISPR/Cas9-mediated deletion of FOXO3 and CTNNB1 human genes.

(C) Protein expression level of intracellular FOXO3 and *β*-Catenin into the GFP+ and NGFR+ cell fractions of CRISPR/Cas9-treated cells by flow cytometric analysis as indicated.

(D) Genotyping of PGK1/GFP insertion into FOXO3 locus and the PGK1/tNGFR insertion into the CTNNB1 gene by digital droplet PCR (ddPCR). Genomic DNA was purified from CRISPR/Cas9-treated cells after three days of *in vitro* growth. The fraction of PCR-amplified region over an internal untreated region located in the GAPDH locus (chr12:6534373-6534538) is reported in the graph.

(E) Survival of recipient mice after transplantation with FACS-sorted GFP+ (Foxo3^{null}) and/or NGFR+ (*β*-Catenin ^{null}) subsets from CRISPR/Cas9-treated PDX. Each of the 5 recipient animals was injected with the cell doses as indicated in parentheses.

Fig. S16.

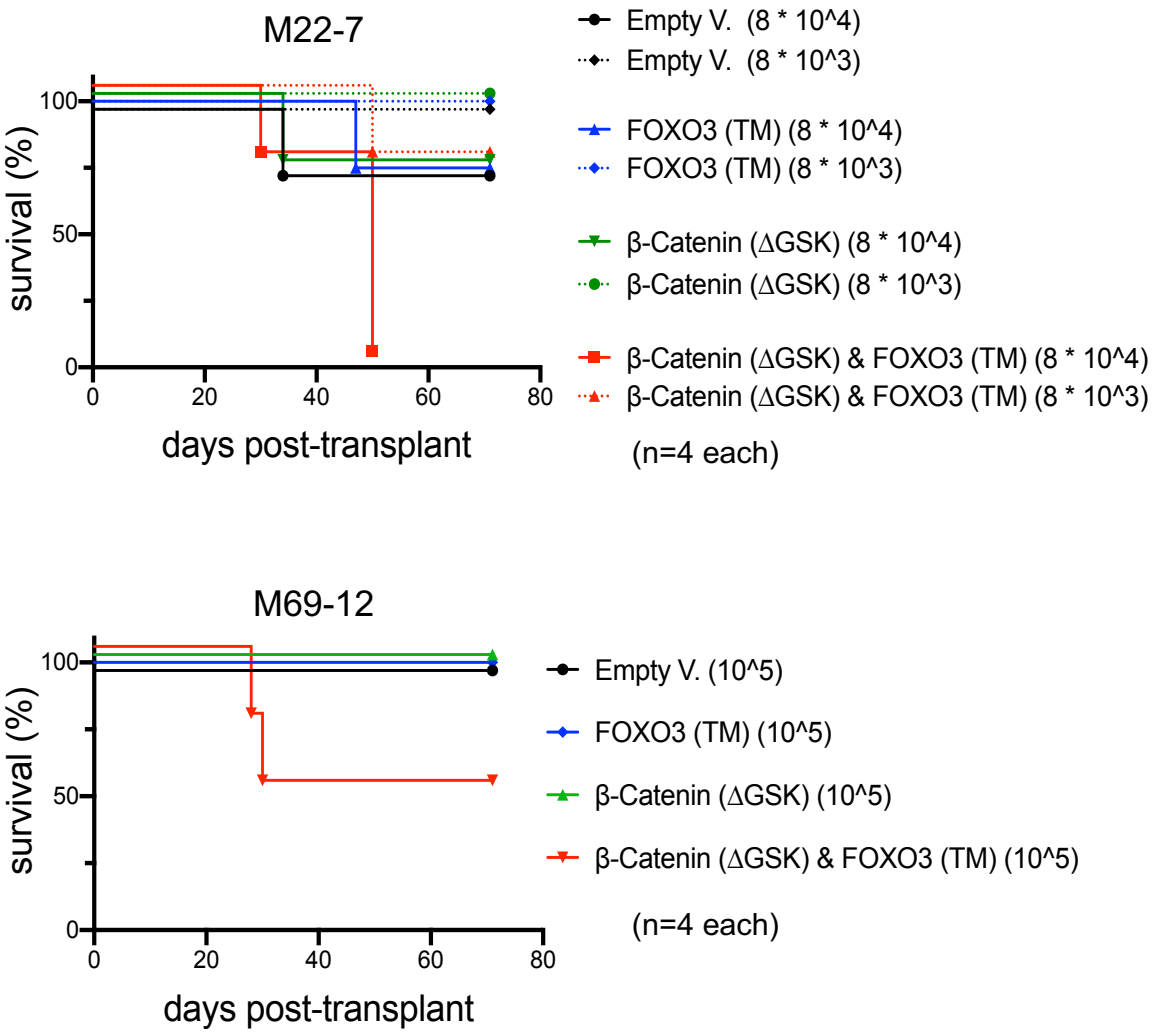

Figure S16. Co-expression of FOXO3 (TM) and *β*-Catenin (ΔGSK) in leukemia cells of two independent PDX clones increased the LIC frequency.
Survival of recipient NSG mice after transduction of FOXO3_TM/mCD8 alone or in combination with β-Catenin_ΔGSK/mCherry in xenograft-expanded human leukemias and subsequently transplantation of FACS-sorted cells into immunocompromised mice. Two separate experiments are depicted using M22-7 and M69-12 independent PDX clones as indicated. The cell doses injected in each of the four recipient animals are indicated in parentheses. The calculated LIC frequency in mCD8+ (FOXO3_TM) Cherry+ (β-Catenin_ΔGSK) cells is 1 in 20,702 (95% CI: 1 in 6,093-70,883) and in the other cell subsets is 1 in 310,286 (95% CI: 1 in 43,959-2,190,158) and 1 in 498,332 (95% CI: 1 in 70,566-3,519,195) for M22-7 sample.

Fig. S17.

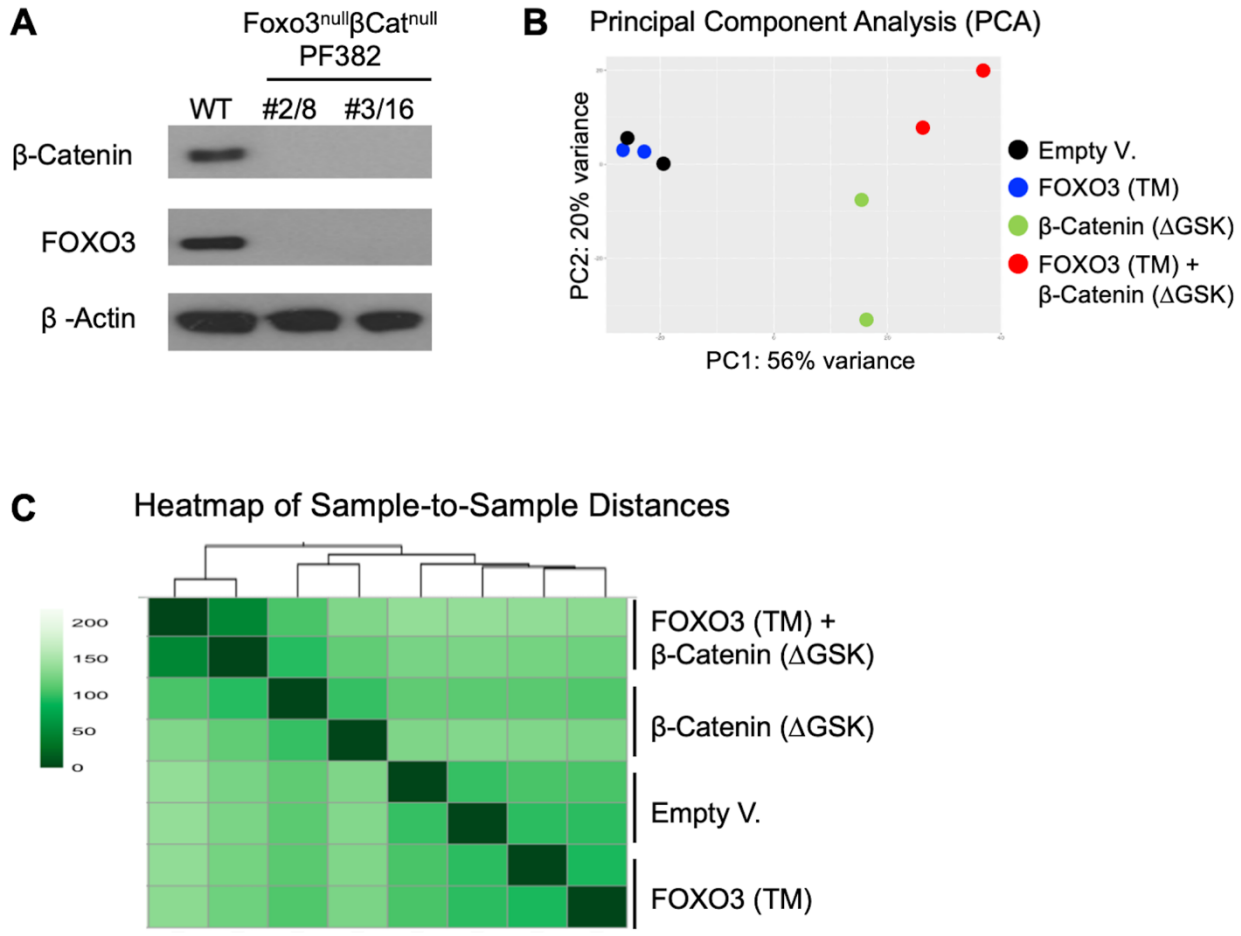

Figure S17. Co-expression of FOXO3 and *β*-Catenin in FOXO3^{null} CTNNB1^{null} PF382 cells defines a distinct gene expression profiling in human T-ALL.
(A) Western blot analysis of FOXO3 and *β*-Catenin protein expression in two independent clones of human FOXO3^{null} CTNNB1^{null} PF382 cell line generated using the CRISPR/Cas9 technology. **(B)** Principal Component analysis (PCA) of RNA-Seq data from FOXO3^{null} CTNNB1^{null} PF382 cells, transduced with lentiviruses for expression of *β*-Catenin (ΔGSK), FOXO3(TM) and/or empty vector as indicated.
(C) The heatmap shows the correlation matrix between the different RNA-Seq samples based on the differential expressed genes. Darker color indicates stronger correlation.

Fig. S18.

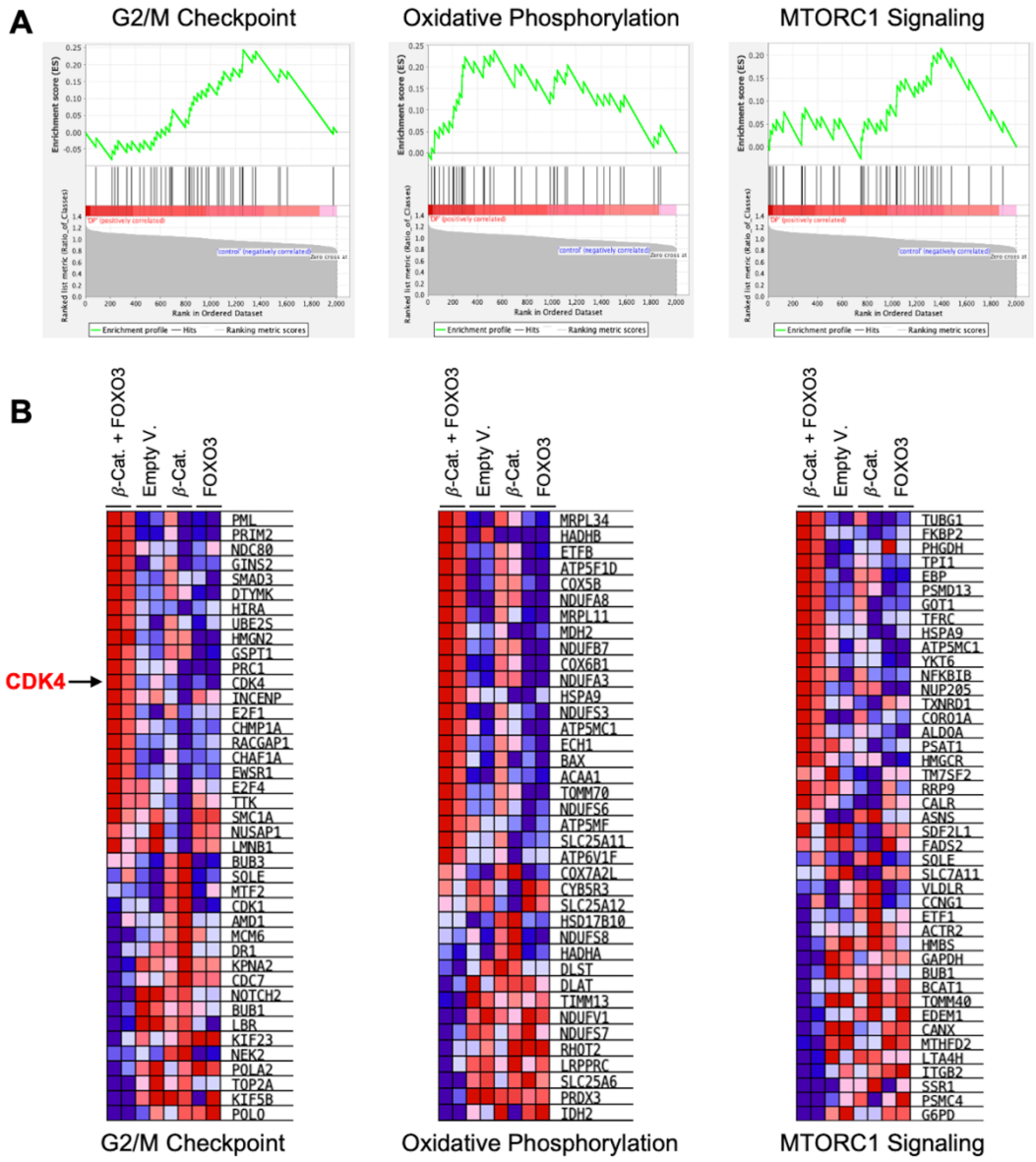

Figure S18. Gene Set Enrichment Analysis (GSEA) of the most relevant pathways in FOXO3^{null} CTNNB1^{null} PF382 cells, doubly transduced with *β*-Catenin(ΔGSK) and FOXO3(TM).

(A) GSEA Enrichment plot (score curves) of the most relevant hallmark gene sets [32] identified in FOXO3^{null} CTNNB1^{null} PF382 cells, doubly transduced with *β*-Catenin(ΔGSK) and FOXO3(TM), reported as "DP" with respect to other samples indicated as "control" in each plot. The green curve corresponds to the enrichment score (ES) curve, as obtained from GSEA software [14,15].

(B) The heatmap of genes contributing the most to the **"**G2/M Checkpoint", "Oxidative Phosphorylation" and "MTORC1 Signaling" enriched gene sets. Darker red color indicates higher expression.

Fig. S19.

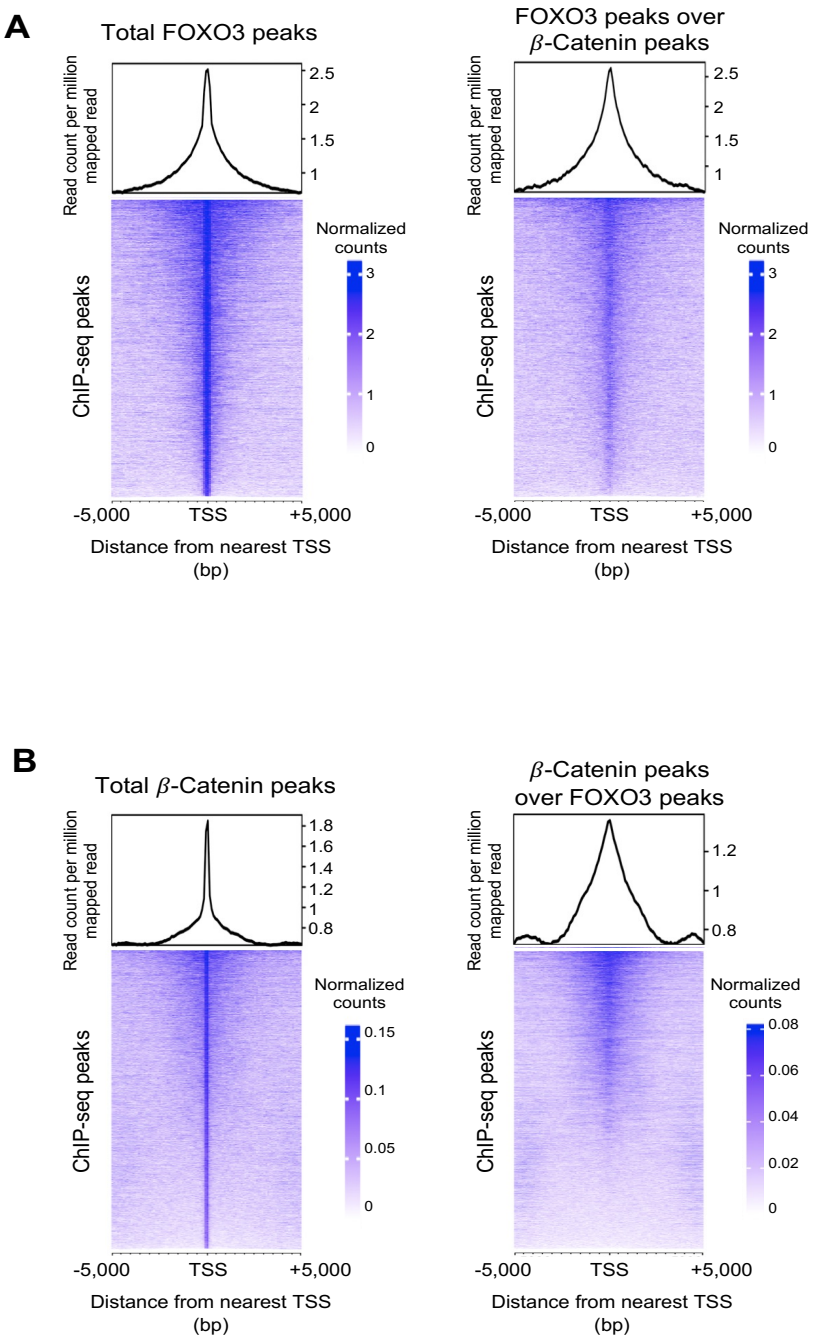

Figure S19. Average plot (top) and heatmap (bottom) of ChIP-Seq reads for FOXO3 and *β*-Catenin around the transcriptional starting site (TSS) in PF382 cell line.
Upper panels show the average profile ± 5 kb around the centered TSS for FOXO3 (**A**) and *β*-Catenin (**B**) binding. Lower panels show read density heatmaps around the detected peak centers for total FOXO3 and *β*-Catenin peaks, as well as the reciprocal FOXO3 (over *β*-Catenin peaks in **A**) and *β*-Catenin (over FOXO3 peaks in **B**) binding patterns in shared regions in PF382 cell line. Scales indicate normalized counts in the ChIP-Seq signal.

Fig. S20.

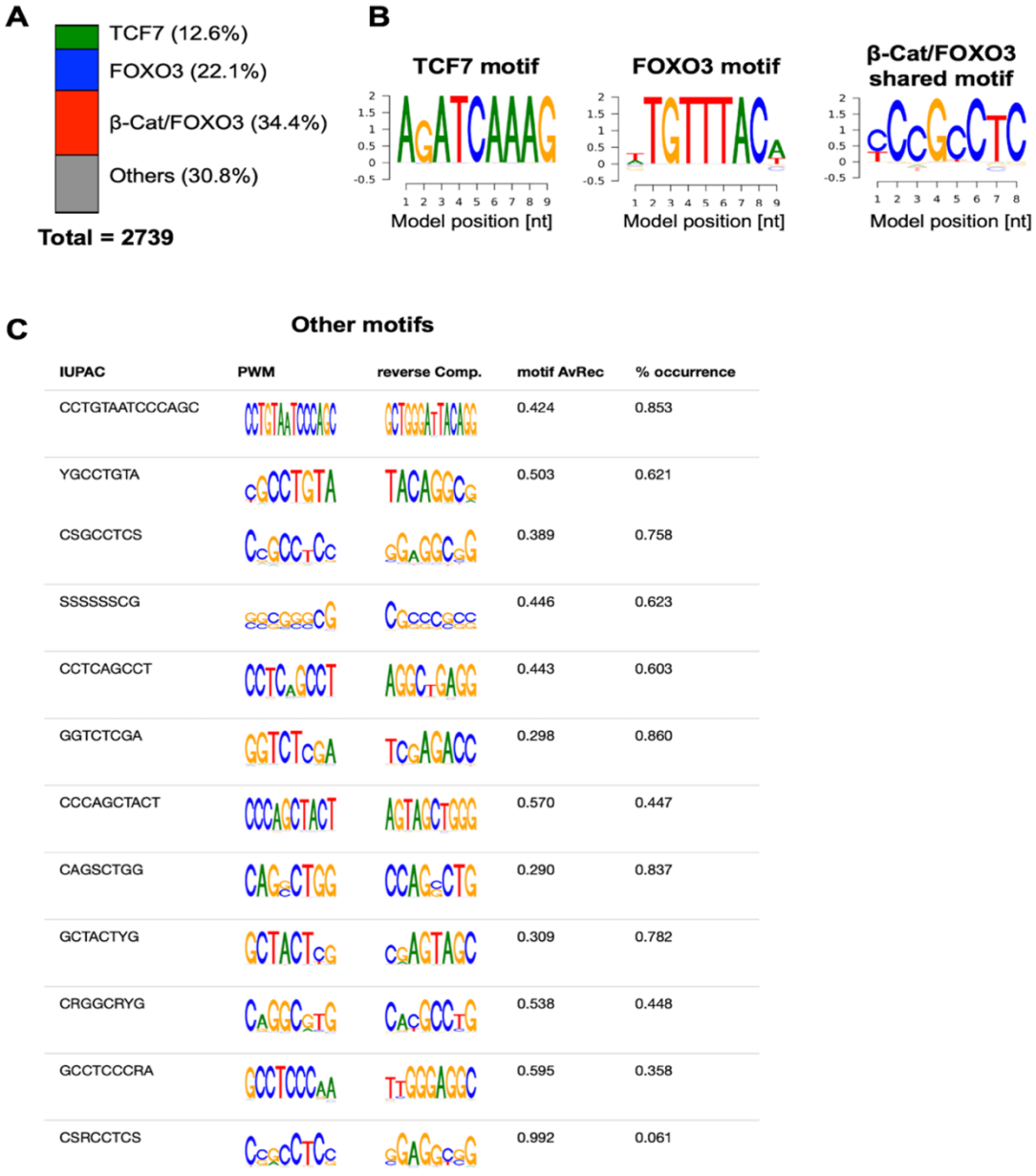

Figure S20. Identification of sequence site motifs in the genomic regions, overlapping FOXO3 and *β*-Catenin ChIP-Seq peaks.

(**A**) Distribution of shared consensus motifs for FOXO3 and *β*-Catenin ChIP-seq signals in the PF382 cell line and publicly available ChIP-Seq datasets (*β*-Catenin, GEO:GSE53927 and FOXO3, GEO:GSE35486).

(**B-C**) Position Weighted Matrix (PWM) logo identified by the BAMM suite platform (https://bammmotif.soedinglab.org/seed_results/423b6b96-fc2c-4ae3-a248-c2ea4a8eed7c/). The most frequent motifs in the analyzed ChIP-seq data include the canonical binding sites for TCF7 and FOXO3 and a new predicted site, shared between FOXO3 and *β*-Catenin.

Fig. S21.

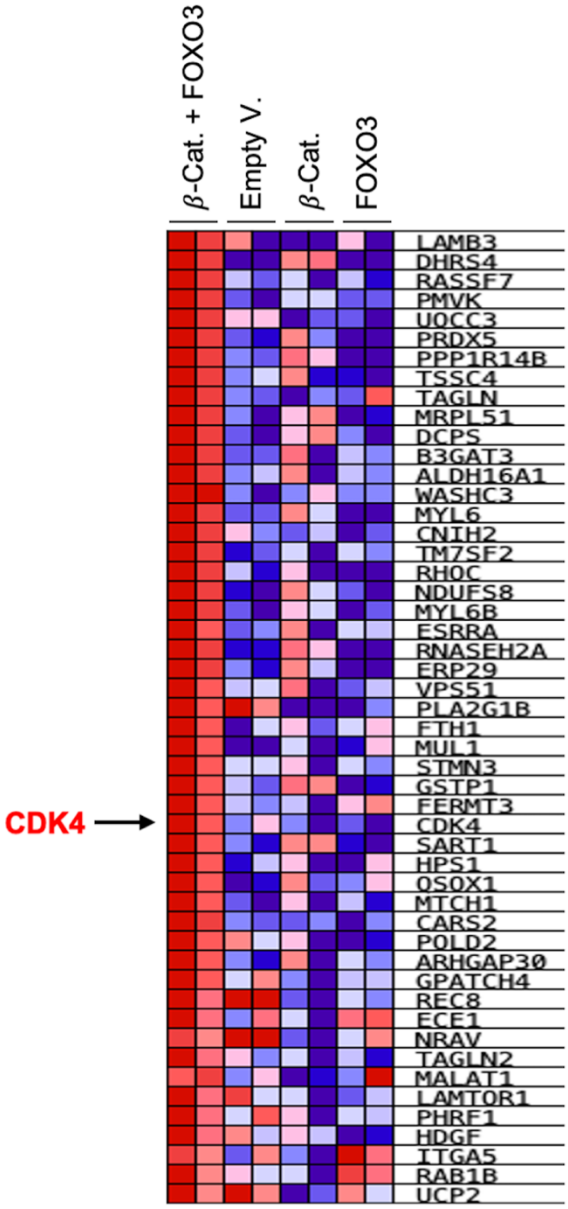

Figure S21. Heatmap of the top 50 genes highlighted by the integrated analysis of ChIP-Seq and RNA-Seq data.

The heatmap shows the correlation matrix between the different RNA-Seq samples based on the top 50 genes, which are mostly expressed in the FOXO3^{null}CTNNB1^{null} PF382 cells co-transduced with *β*-Catenin (ΔGSK) and FOXO3 (TM) lentiviruses as compared to other cell conditions and show shared consensus motifs for *β*-Catenin and FOXO3 within 1Kb around transcription start sites (TSS) (**Fig. 3C**). Darker red color indicates stronger correlation.

Fig. S22.

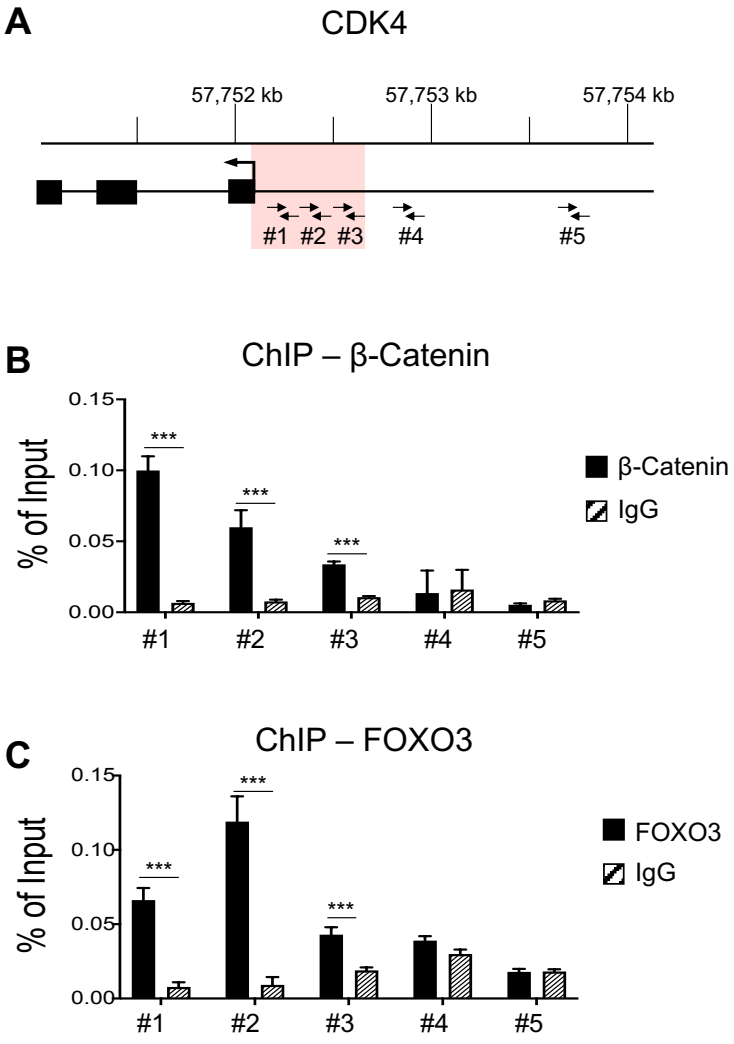

Figure S22. Local chromatin immunoprecipitation (ChIP) assay revealed substantial enrichment of FOXO3 and *β*-Catenin binding in an overlapping region of human CDK4 promoter region in PF382 cell line.

(**A**) Schematic map of human CDK4 promoter region. Primer pairs used for ChIP-qPCR assays are indicated by small arrows. The genomic region identified as overlapping between FOXO3 and *β*-Catenin ChIP-Seq peaks in the CDK4 locus is highlighted in red. Map positions correspond to locus coordinates chr12:57,751,000-57,754,000 (GRCh38).

(**B–C**) ChIP-qPCR analysis. Local ChIP was performed with antibodies against *β*-Catenin (B), FOXO3 (C) or immunoglobulin G (IgG) control in PF382 cell line. Primers pairs spanning the CDK4 promoter region as indicated in (A) were used for qPCR on immunoprecipitated DNA. Values are expressed as a fraction of input DNA controls. Mean values are plotted for assays performed in triplicate. Error bars indicate SD. ***$p < 0.001$ (Student's t test).

Fig. S23.

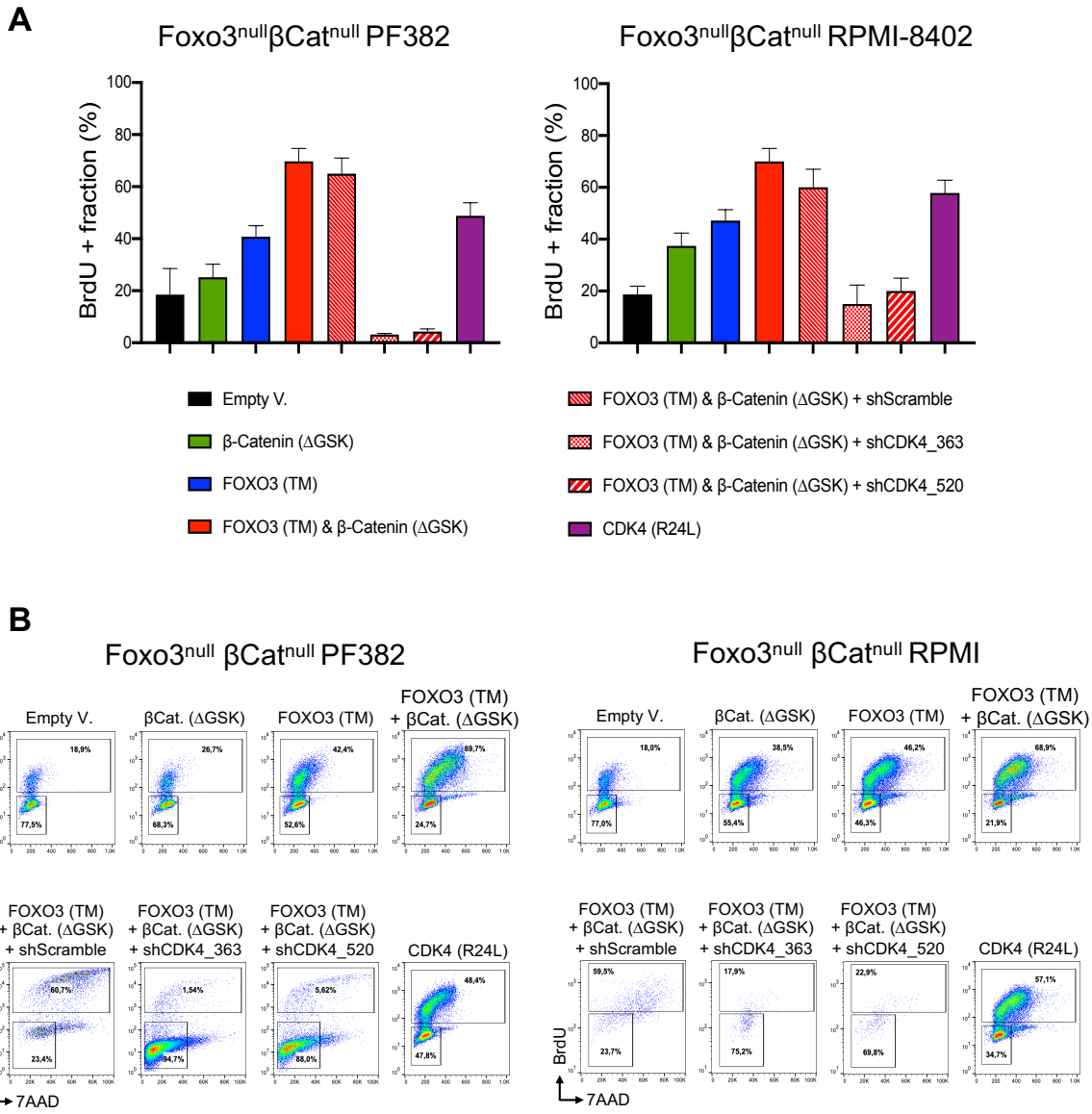

Figure S23. *β*-Catenin, FOXO3 and CDK4 promote the cell proliferation of FOXO3^{null}CTNNB1^{null} PF382 and RPMI-8402 cell lines.

(**A**) Flow cytometric analysis of cell proliferation in FOXO3^{null}CTNNB1^{null} PF382 and RPMI-8402 cell lines by BrdU incorporation after lentiviral transduction of *β*-Catenin(ΔGSK), FOXO3(TM), CDK4 (R24L) and/or empty vector as indicated. The R24L mutation at position 24 in the CDK4 gene results in an amino acid substitution from an Arginine (R) to Leucine (L) and renders the protein resistant to the inhibitory effects of INK4A function[7]. Proliferation of FOXO3^{null}CTNNB1^{null} PF382 and RPMI-8402 cell lines following transduction with *β*-Catenin(ΔGSK), FOXO3(TM) and shCDK4 constructs or scramble control is also reported.

(**B**) Flow cytometry plots of BrdU assay used to generate the bar charts reported above.

Fig. S24.

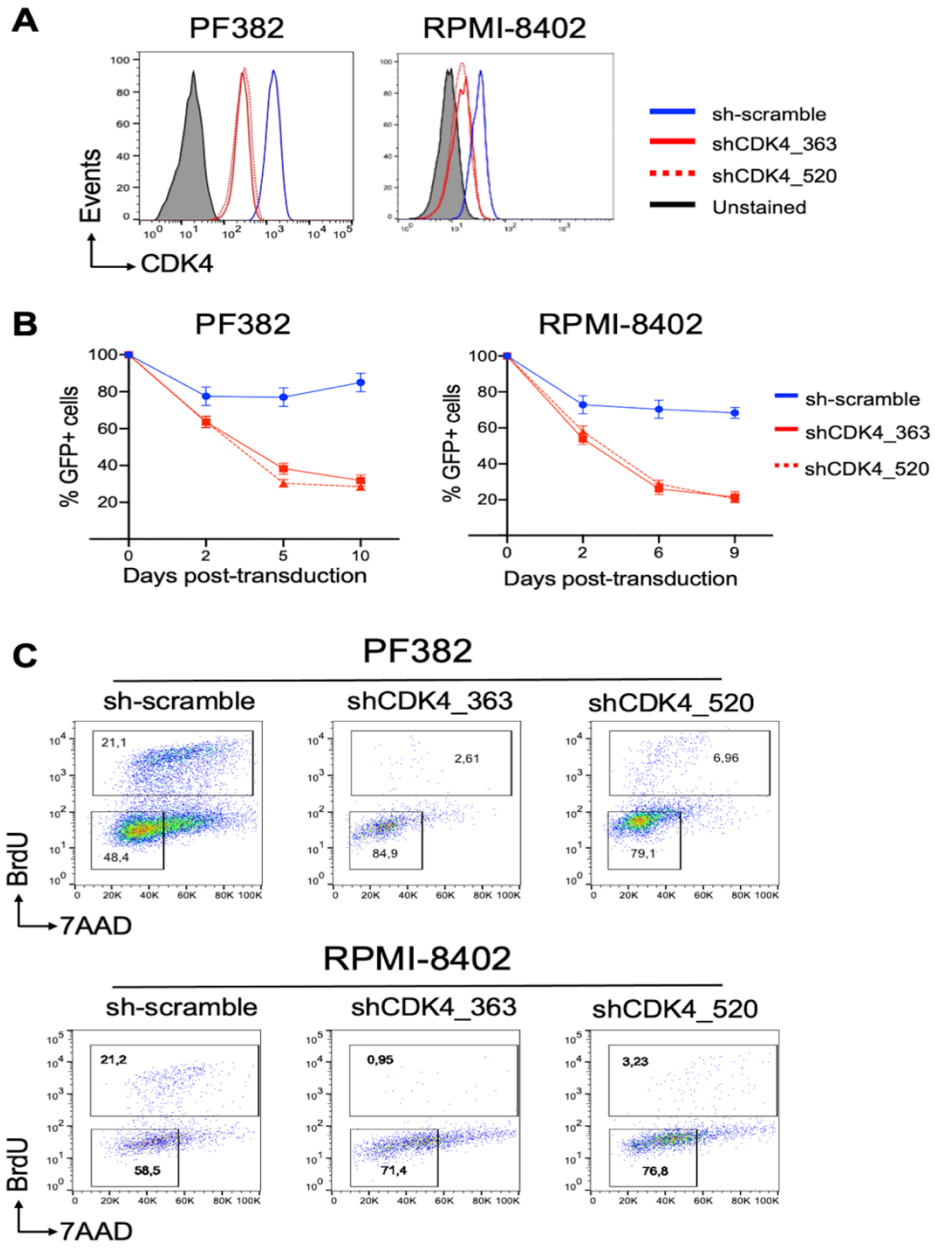

Figure S24. Reduced CDK4 expression inhibits growth and cell proliferation in human T-ALL cells.

(**A**) Protein expression level of intracellular CDK4 by flow cytometric analysis in the PF382 and RPMI-8402 cell lines, transduced by lentivirus encoding shRNAs against CDK4 or scrambled shRNA control.

(**B**) Abundance of shRNA-transduced GFP+ cell fraction, tracked over time in culture by flow cytometry. Means ± SD fraction of the initial transduction value are plotted for experiments performed at least in triplicate.

(**C**) Proliferation of PF382 and RPMI-8402 cell lines following transduction with shCDK4 constructs or scrambled shRNA control as measured by BrdU incorporation. G1/G0 and S populations are gated as shown. The results depicted are representative of two independent experiments.

Fig. S25.

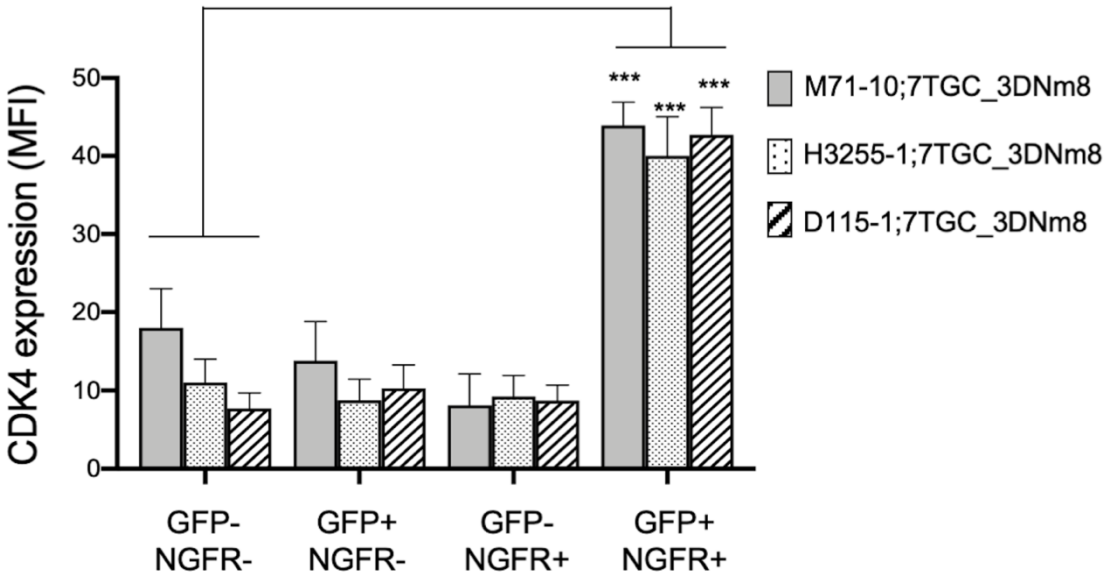

Figure S25. CDK4 is highly expressed in Wnt/*β*-Catenin active (GFP+) and FOXO active (NGFR+) LIC-enriched subsets from 7TGC_3DNm8-transduced xenograft-expanded human leukemias.

Flow cytometric analysis of CDK4 protein levels. Leukemia cells of three independent PDX clones were transduced with FOXO (3DNm8) or Wnt/*β*-Catenin (7TGC) lentiviral reporters and expanded *in vivo* into immunocompromised (NSG) mice. The secondary 7TGC_3DNm8-transduced leukemias were then analyzed for CDK4 expression by intracellular flow cytometry after FACS sorting of GFP+NGFR+, GFP+NGFR-, GFP-NGFR+ and GFP−NGFR- subsets. The mean fluorescence intensity (MFI) of the CDK4 expression level is reported in the vertical axis of the graph. Error bars indicate standard deviation. Results depicted are representative of two different leukemic animals. ***, *P < 0.001 (Student's t test).*

Fig. S26.

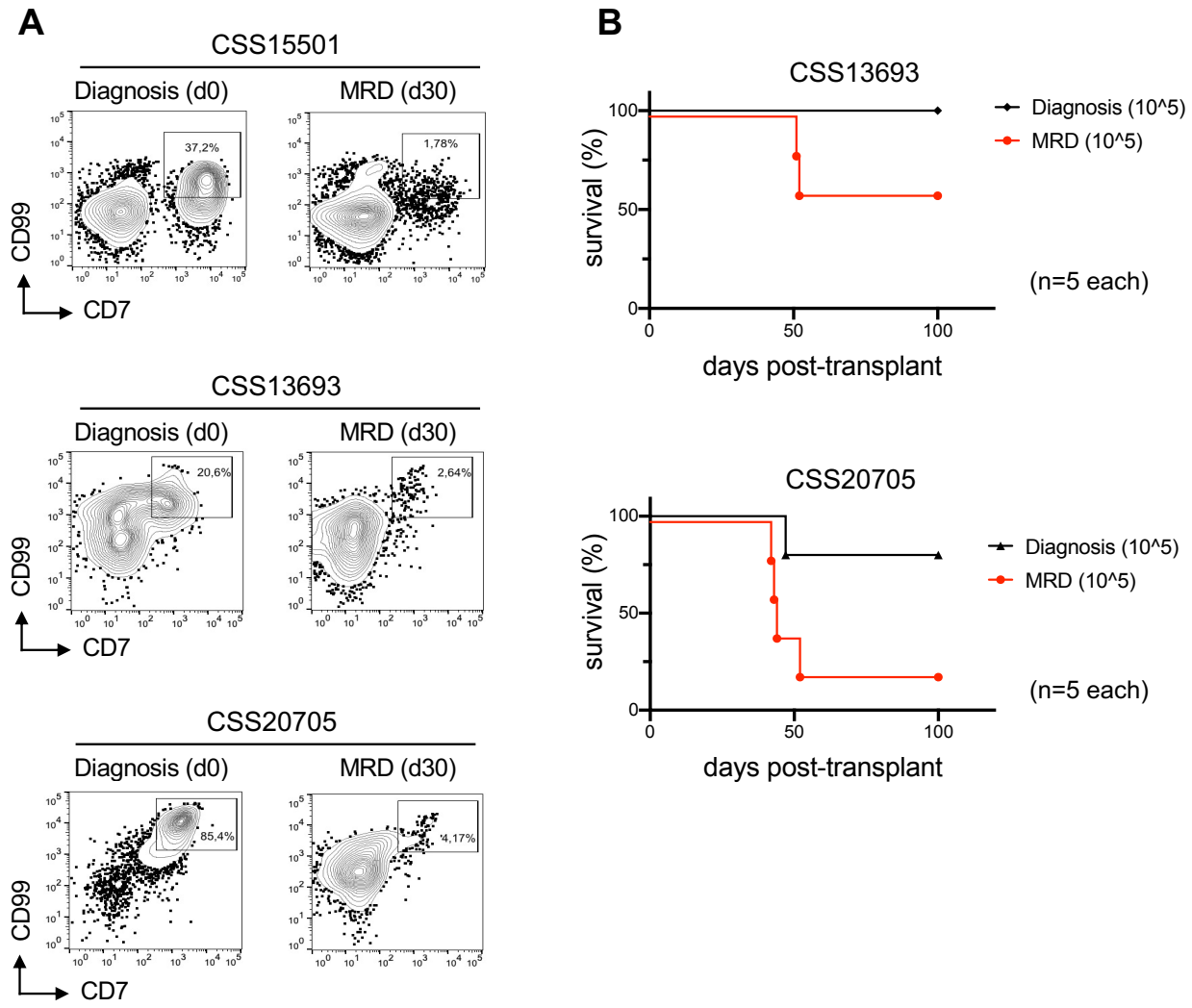

Figure S26. Flow cytometry gate and in vivo engraftment of tumor subpopulations analyzed by scRNA-seq and Abseq assays.

(A) Flow cytometry plots of CSS15501, CSS13693 and CSS20705 samples at the diagnosis (d0) and 30 days after the start of therapy (MRD d30), showing CD99 and CD7 expression for the identification of tumor cells. Viable cells were distinguished by negative staining for DAPI, followed by debris exclusion and singlet gating based on forward and side scatter. Tumor cells were determined in the CD45+CD3- cell fraction and further gated as CD99+CD7+ subset as previously reported [20]. The described gating strategy was used for FACS sorting of tumor cells, subsequently analyzed by scRNA-seq and Abseq assays.

(B) Survival of recipient NSG mice after transplantation with FACS-sorted CD3-CD99+CD7+ cells from CSS13693 and CSS20705 primary samples at the diagnosis (d0) and MRD (d30). Each of the five recipient animals was injected with the cell doses as indicated in parentheses.

Fig. S27.

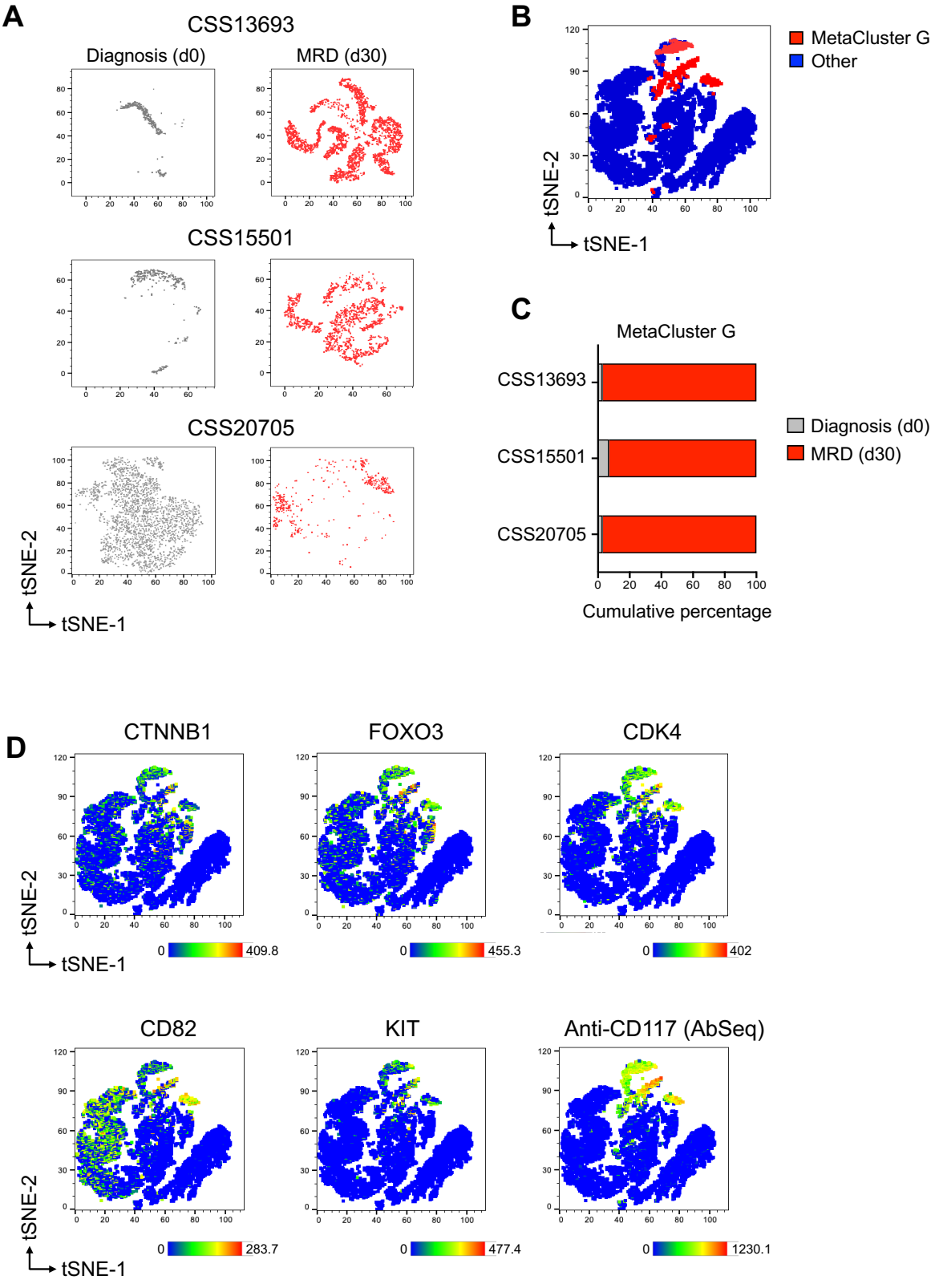
A
CSS13693
Diagnosis (d0)
MRD (d30)
CSS15501
CSS20705
tSNE-2
tSNE-1
B
MetaCluster G
Other
tSNE-2
tSNE-1
C
MetaCluster G
CSS13693
CSS15501
CSS20705
Diagnosis (d0)
MRD (d30)
Cumulative percentage
D
CTNNB1
FOXO3
CDK4
409.8
455.3
402
CD82
KIT
Anti-CD117 (AbSeq)
283.7
477.4
1230.1
tSNE-2
tSNE-1

Figure S27. The assigned "G" MetaCluster (MC-G) shows co-expression of *β*-Catenin, FOXO3 and CDK4 as well as CD117 and CD82 surface markers.
(**A**) tSNE plots based on the single cell RNA-Sequencing (scRNA-Seq) and AbSeq data from 3 primary T-ALL samples, CSS13693, CSS15501 and CSS20705 at the diagnosis (d0) and 30 days after the start of therapy (MRD_d30) without passaging into immunocompromised mice. In the map, leukemia cells at d0 and d30 are colored in grey and red, respectively.
(**B**) Dimensional reduction tSNE plots of scRNA-Seq data from combined analysis of three primary T-ALL patient samples. Leukemia cells, assigned to "G" MetaCluster (MC-G) showing co-expression of *β*-Catenin, FOXO3 and CDK4 genes, are colored in red.
(**C**) Graphical representation of cell percentage in the "G" MetaCluster (MC-G) according to each sample group.
(**D**) tSNE plot of the same case as depicted in Panel A, showing the expression level of FOXO3, CTNNB1, CDK4, CD82 and KIT transcripts and the tag of anti-CD117 oligo-conjugated antibody (AbSeq). Each dot represents an individual cell.

Fig. S28.

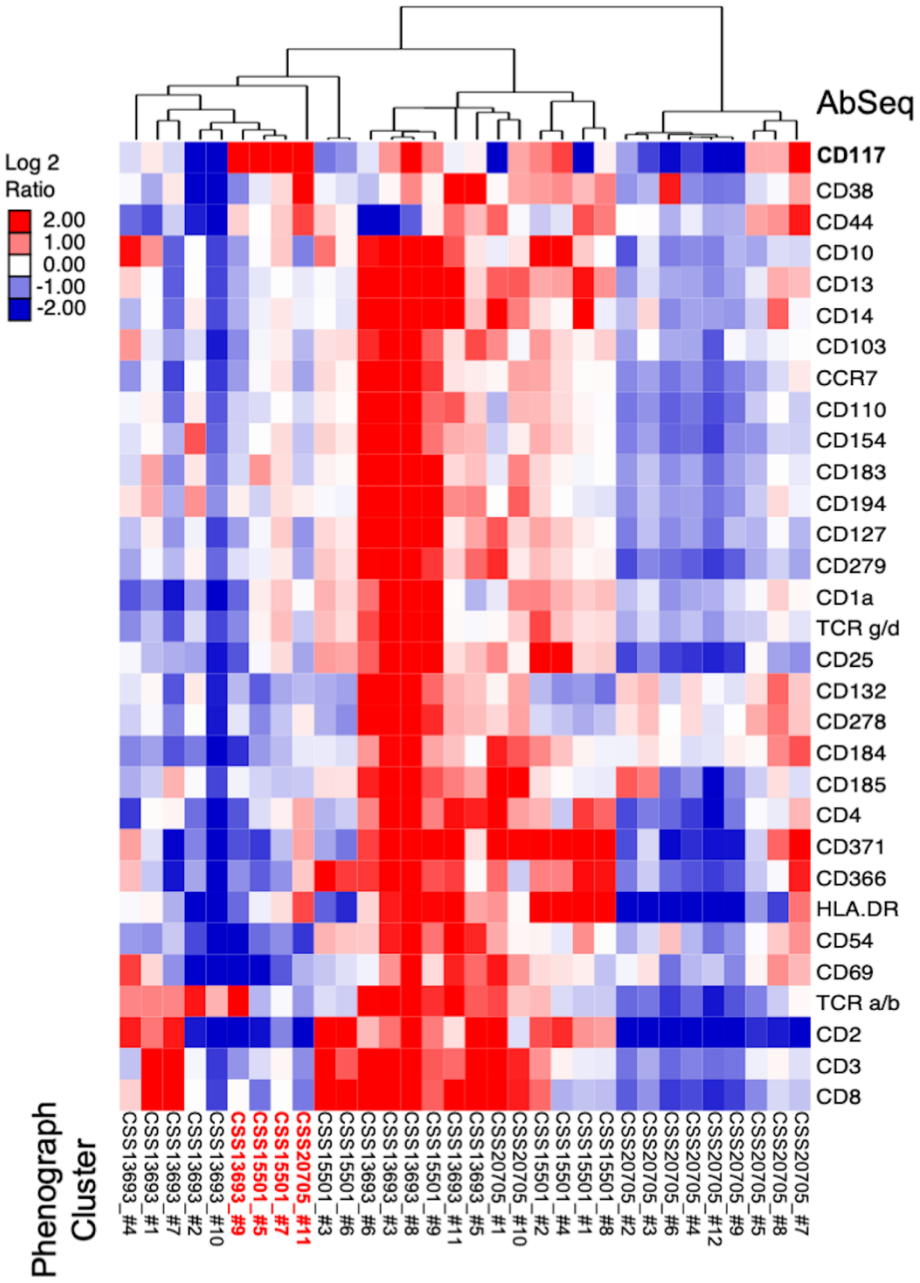

Figure S28. Immunophenotypic profiling of the 32 Phenograph clusters identified in primary T-ALL samples by scRNA-seq assay.
Expression heatmap and hierarchical clustering of all surface markers recognized by 42 oligo-conjugated antibodies (Abseq panel in **Table S9**) in each of the 32 Phenograph clusters.

Fig. S29.

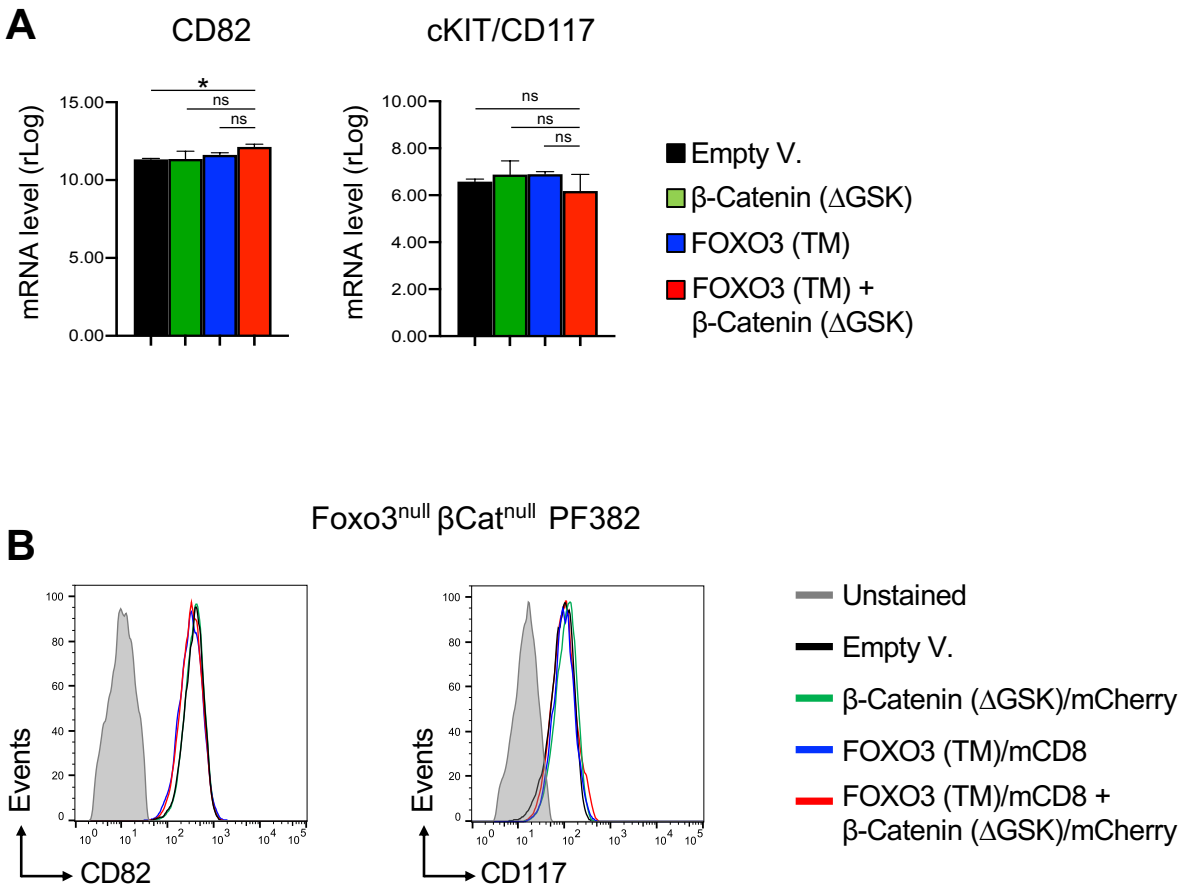

Figure S29. The expression level of CD82 and CD117/KIT cell surface markers is not modulated by FOXO3 and *β*-Catenin.
(**A**) mRNA expression level of CD82 and CD117/KIT transcripts in FOXO3^{null} CTNNB1^{null} PF382 cells with engineered levels of the active FOXO3_TM mutant alone or in combination with the stable ΔGSK isoform of *β*-Catenin. Bars indicate mean ± SD of Rlog values from DESeq2 for each RNA-Seq dataset reported in Figure 3. *$p < 0.05$; ns, not significant (Student's t test).
(**B**) Protein expression level of CD82 and CD117/KIT cell surface markers by flow cytometric analysis in the transduced cells as reported in (A).

Fig. S30

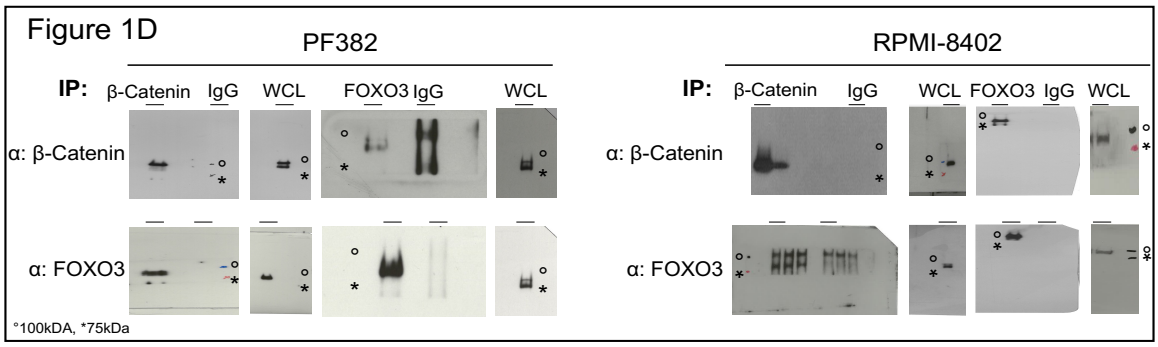
Figure 1D
PF382
RPMI-8402
IP:
β-Catenin
IgG
WCL
FOXO3
α: β-Catenin
α: FOXO3
°100kDA, *75kDa

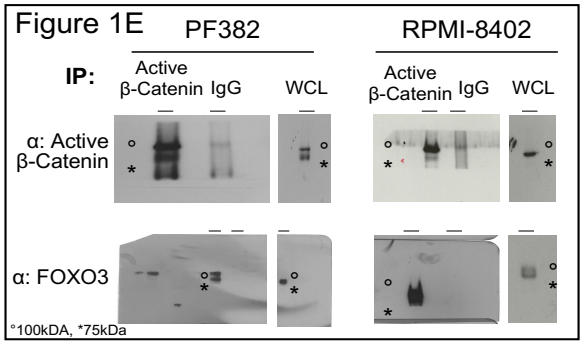
Figure 1E
PF382
RPMI-8402
IP:
Active β-Catenin
IgG
WCL
α: Active β-Catenin
α: FOXO3
°100kDA, *75kDa

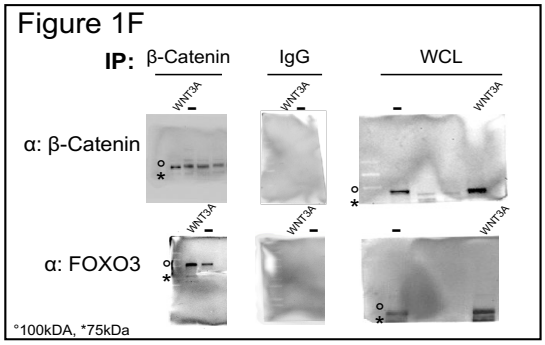
Figure 1F
IP:
β-Catenin
IgG
WCL
WNT3A
α: β-Catenin
α: FOXO3
°100kDA, *75kDa

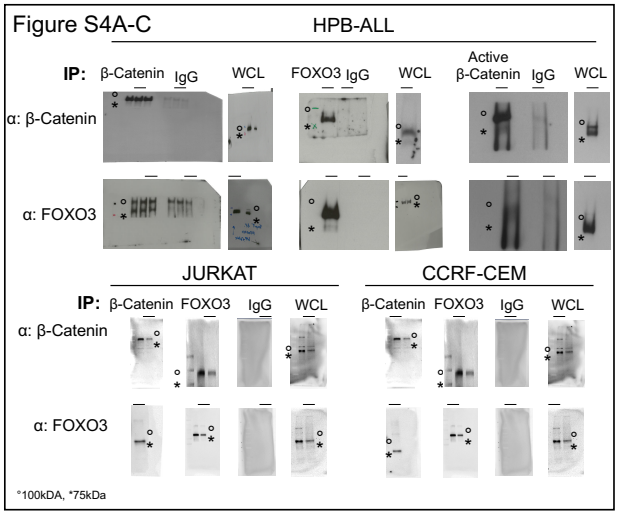
Figure S4A-C
HPB-ALL
IP:
β-Catenin
IgG
WCL
FOXO3
Active β-Catenin
α: β-Catenin
α: FOXO3
JURKAT
CCRF-CEM
°100kDA, *75kDa

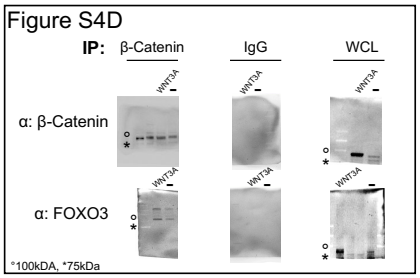
Figure S4D
IP:
β-Catenin
IgG
WCL
WNT3A
α: β-Catenin
α: FOXO3
°100kDA, *75kDa

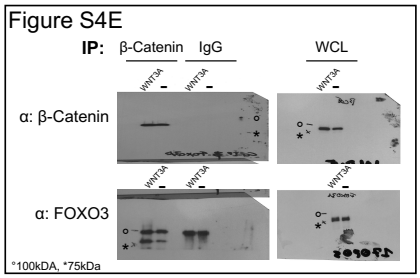
Figure S4E
IP:
β-Catenin
IgG
WCL
WNT3A
α: β-Catenin
α: FOXO3
°100kDA, *75kDa

Fig. S30.

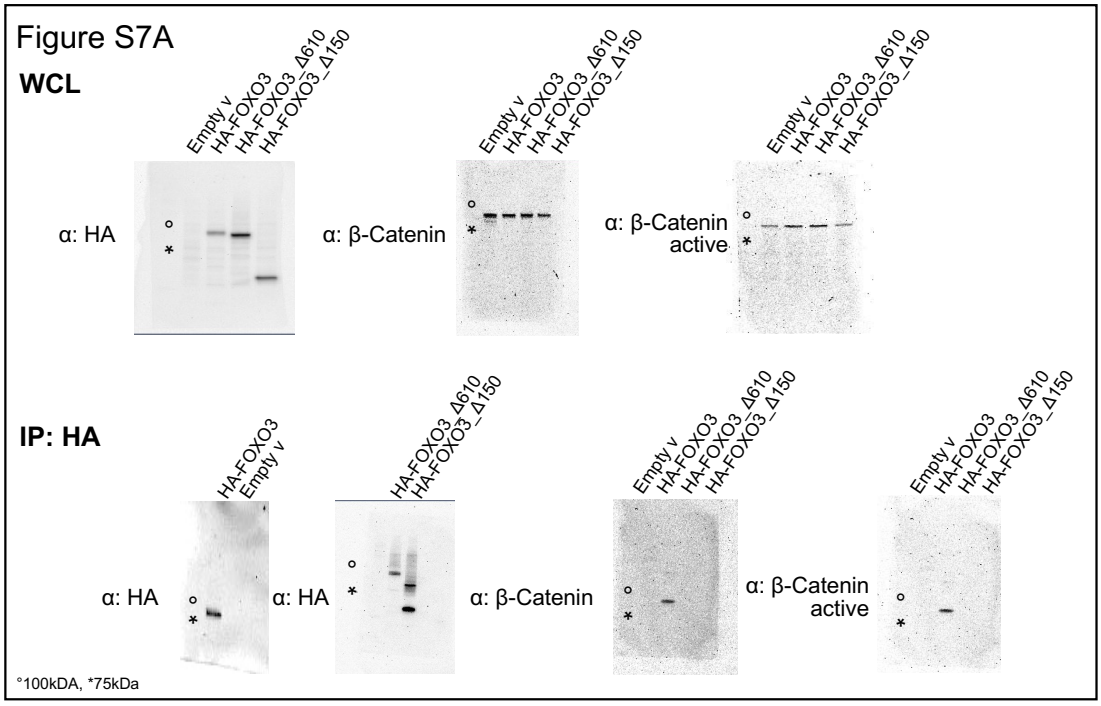

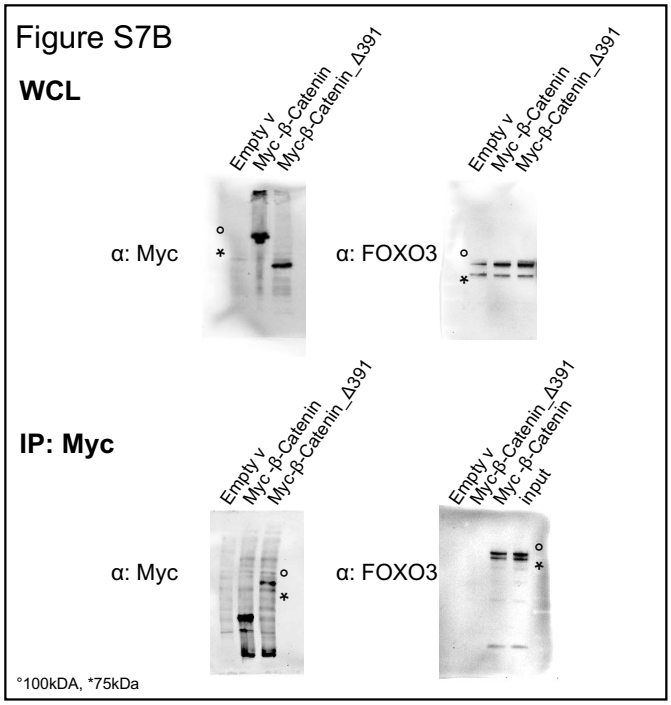

Figure S30. Related to Figures 1, S4 and S7. Uncropped blots of reported Co-Immunoprecipitation (Co-IP) assays